

Old Dominion University

ODU Digital Commons

Electrical & Computer Engineering Theses & Dissertations

Electrical & Computer Engineering

Summer 8-2020

A Novel Non-Enzymatic Glucose Biofuel Cell with Mobile Glucose Sensing

Ankit Baingane

Old Dominion University, abain001@odu.edu

Follow this and additional works at: https://digitalcommons.odu.edu/ece_etds



Part of the [Biomedical Engineering and Bioengineering Commons](#), and the [Electrical and Computer Engineering Commons](#)

Recommended Citation

Baingane, Ankit. "A Novel Non-Enzymatic Glucose Biofuel Cell with Mobile Glucose Sensing" (2020). Doctor of Philosophy (PhD), Dissertation, Electrical & Computer Engineering, Old Dominion University, DOI: 10.25777/2xc4-ba54
https://digitalcommons.odu.edu/ece_etds/220

This Dissertation is brought to you for free and open access by the Electrical & Computer Engineering at ODU Digital Commons. It has been accepted for inclusion in Electrical & Computer Engineering Theses & Dissertations by an authorized administrator of ODU Digital Commons. For more information, please contact digitalcommons@odu.edu.

**A NOVEL NON-ENZYMATIC GLUCOSE BIOFUEL CELL WITH MOBILE
GLUCOSE SENSING**

by

Ankit Baingane

B.E. August 2016, Nagpur University, India

M.S. December 2017, University of Maryland, Baltimore County

A Dissertation Submitted to the Faculty of
Old Dominion University in Partial Fulfillment of the
Requirements for the Degree of

DOCTOR OF PHILOSOPHY

ELECTRICAL AND COMPUTER ENGINEERING

OLD DOMINION UNIVERSITY

August 2020

Approved by:

Gymama Slaughter (Director)

Chungsheng Xin (Member)

Barbara Hargrave (Member)

Shirshak Dhali (Member)

Nancy Xu (Member)

ABSTRACT

A NOVEL NON-ENZYMATIC GLUCOSE BIOFUEL CELL WITH MOBILE GLUCOSE SENSING

Ankit Baingane
Old Dominion University, 2020
Director: Dr. Gymama Slaughter

Herein, we report a novel non-enzymatic glucose biofuel cell with mobile glucose sensing. We characterized the power generation and biosensing capabilities in presence of glucose analyte. This system was developed using a non-enzymatic glucose biofuel cell consisting of colloidal platinum coated gold microwire (Au-co-Pt) employed as an anode and the cathode which was constructed using a Gas diffusion electrode (GDE) with a platinum catalyst. The non-enzymatic glucose biofuel cell produced a maximum open circuit voltage of 0.54 V and delivered and a maximum short circuit current density of 1.6 mA/cm² with a peak power density of 0.226 mW/cm² at a concentration of 1 M glucose. The non-enzymatic glucose biofuel cell produced an open circuit voltage of 0.38 V and delivered and a short circuit current density of 0.225 mA/cm² with a peak power density of 0.022 mW/cm² at a concentration of 5 mM glucose. These findings showed that glucose biofuel cells can be further investigated in the development of a self-powered glucose biosensor. When used as self-powered glucose sensor, the system showed a good sensitivity of 0.616 $\mu\text{A mM}^{-1}$ and linear dependence with a correlation coefficient of 0.995 in the glucose concentration range of 2 mM to 50 mM.

The system was further characterized by testing the performance of the system at various temperature, pH and amidst various interfering and competing chemical species such as uric acid, ascorbic acid, fructose, maltose and galactose. A charge pump circuit consisting of a blinking LED was connected to the biofuel cell to amplify the input voltage to power small electronic devices. The

blinking frequency of the LED corresponds to the glucose concentration. An android mobile phone camera application was used to measure this LED blinking frequency which was in turn converted into the glucose concentration readings using image processing in MATLAB. The user was notified via text message and an email.

Copyright, 2020, by Ankit Baingane, All Rights Reserved.

This thesis is dedicated to my parents Ratna and Bhanudas Baingane, my brother Aditya, and all my friends & family.

ACKNOWLEDGMENTS

Foremost, I would like to thank my advisor, Dr. Gymama Slaughter, for her patience and guidance throughout the project. She has been a true mentor to me, and I couldn't have asked for anyone better. Her mentorship was paramount in helping me set long-term career goals. I would also like to thank Dr. Shankar Narayanan, Dr. Meimei Lai, Dr. Thakshila Lingaye, Dr. Faruk Hossain and Dr. Ahmad Qamar for giving me an opportunity to work with them. Their guidance helped me gain a wider breadth of experience during my PhD. I would also like to thank my committee members Dr. Barbara Hargrave, Dr. Nancy Xu, Dr. Chenshung Xin and Dr. Shirshak Dhali for their encouragement and insightful comments. Most importantly, I would like to thank my exceptional family and my girlfriend Madison Rose for their constant support, encouragement and unwavering love that has allowed me to be ambitious and achieve my goals. Lastly, I thank my lab-mate Peyton Miesse and Dominic Nnanyelugoh and my friends Kunal Bendey, Prasad Akmar, Saikat Bainerjee and Kapeel Sable for providing humor and entertainment, but most importantly just being there for me.

TABLE OF CONTENTS

	Page
LIST OF TABLES.....	ix
LIST OF FIGURES	x
Chapter	
I. INTRODUCTION	1
BACKGROUND	1
PROBLEM STATEMENT	11
DISSERTATION CONTRIBUTION	12
SCOPE OF DISSERTATION	12
II. BIOFUEL CELL	14
FUEL CELL	14
BIOFUEL CELL	17
III. GLUCOSE BIOSENSOR	26
GLUCOSE MONITORING IN BLOOD	27
GLUCOSE MONITORING IN ALTERNATIVE PHYSIOLOGICAL FLUIDS	31
IV. CHARGE PUMP CIRCUIT	35
CHARGE PUMP CIRCUIT	35
S882Z INTEGRATED CIRCUIT	40
V. ELECTROCHEMICAL CHARACTERIZATION	43
CYCLIC VOLTAMMETRY (CV)	43
CHRONOAMPEROMETRY (CA)	47
CURRENT-VOLTAGE CHARACTERISTICS (IV)	49
pH AND TEMPERATURE CHARACTERISTICS	51

Chapter	Page
VI. MATERIALS AND METHODS	53
MATERIALS	53
ELECTRODE FABRICATION AND DESIGN	53
CHARGE PUMP CIRCUIT FABRICATION	55
ESP8266, MATLAB AND ANDROID APPLICATION	57
VII. RESULTS	62
CYCLIC VOLTAMMETRY (CV)	64
CURRENT-VOLTAGE CHARACTERISTICS (IV)	67
pH AND TEMPERATURE	70
CHRONOAMPEROMETRY (CA)	71
SELFPOWERED GLUCOSE BIOSENSING	75
MATLAB IMAGE PROCESSING FROM ANDROID APPLICATION DATA	77
ESP DATA PROCESSING	78
INTERFERENCE STUDY	81
VIII. CONCLUSION	84
FUTURE WORKS	85
REFERENCES	87
APPENDIX A	103
APPENDIX B	106
VITA	110

LIST OF TABLES

Table	Page
1. Normal blood glucose levels for non-diabetic and diabetic people.....	1
2. Glucose concentration level in different physiological fluids for healthy and diabetic Patients in mM.....	30

LIST OF FIGURES

Figure	Page
1. Example of most commonly available methods for individual with diabetes to monitor and maintain normal blood glucose levels	5
2. A continuous glucose monitoring system with implanted sensor and data reader.....	6
3. Schematic of a self-powered continuous glucose monitoring system with wireless data access and monitoring.	11
4. Hydrocarbon Fuel Cell Representation	15
5. Biofuel cell schematic showing its major components and basic operation. In this example, the anodic electron transfer occurs through a mediator while at the cathode it occurs directly through a biological catalyst.....	18
6. Schematic representation of Enzymatic biofuel Cell	20
7. Schematic reference of power range that some of the alternative energy production methods provide	22
8. A model of a non-enzymatic biofuel cell	24
9. Conversion of glucose to gluconic acid using glucose oxidase.	28
10. Illustration of a glucometer and continuous glucose monitor (CGM)	29
11. Schematic of the microneedle glucose-sensing patch on the forearm	32
12. A) Flexible glucose sensor. B) Glucose sensor integrated into a wearable wristband for noninvasive sensing in sweat.	33
13. Two-step charge discharge cycle.	36
14. This reconfiguring of the basic boost-converter charge pump results in a circuit which converts a positive rail to a negative one, which is frequently needed for biasing or providing an offset voltage.	38
15. Schematics of charge pump circuit designed in Eagle.	41
16. Internal operation of charge pump IC.	42
17. CV excitation signal showing a typical reduction occurring from (a) to (d) and an oxidation occurring from (d) to (g).....	44
18. Voltammogram of a Single electron oxidation-reduction.	45
19. Resistor i-v characteristic curve.	50
20. Fabricated Au-co-Pt anode on left and GDE cathode on the right.	54
21. Sawtooth frequency obtained from charge pump circuit.	56
22. An ESP8266 Wi-Fi module.	58

Figure	Page
23. Sample code for ESP8266 programming which takes the analog values coming from charge pump and plots it versus time.	59
24. Assembled biofuel cell setup with voltage measurement.	62
25. Scanning electron microscopy (SEM) images of (A) Braided Au microwire, (B) high-resolution SEM image of Au-co-Pt abiotic anode and (C) Au-co-Pt abiotic anode ...	63
26. Cyclic voltammetry performed on the Au-co-Pt showing linear increase in current with increase in glucose concentration.	64
27. Internal layers of GDE electrode.....	65
28. Cyclic voltammetry performed on the GDE cathode showing linear increase in current with increase in purged oxygen.	66
29. Polarization curve obtained from the non-enzymatic biofuel cell from glucose concentration of 1mM to 1M.	67
30. Power curve obtained from the non-enzymatic biofuel cell from glucose concentration of 1mM to 1M.	68
31. Power-concentration curve from 1mM to 50mM glucose	69
32. Effect of pH on the frequency of the non-enzymatic glucose biosensing system operating in 5 mM glucose at 37 °C.	70
33. Effect of temperature on the frequency of the non-enzymatic glucose biosensing system operating on 5 mM glucose at a pH of 7.4.....	70
34. Amperometry response of the Au-co-Pt electrode to successive addition of 2 mM glucose in 0.1 M PBS solution after every 50 seconds interval.	71
35. Calibration curve derived from the linear response of the sensor to change in glucose concentration.	72
36. IC circuit with glucose biofuel cell as power source	73
37. The construction of the self-powered glucose biosensor via a charge pump integrated circuit and a capacitor functioning as a transducer.	74
38. Charge pump circuit with LED blinking.	75
39. A model of a novel self-powered glucose monitoring biosystem with data acquisition using mobile camera.	76
40. Received text message and email by the user containing information about their blood glucose level.	77
41. A model of miniaturized continuous glucose monitoring system with remote access and monitoring using E-oscilloscope (ESP8266)	78

Figure	Page
42. Capacitor charge/discharge rate obtained from glucose biosensing system operating in the absence (blue curve) and in the presence of 5 mM glucose (black curve) using the e-oscilloscope program.....	79
43. Adafuit live feed of the capacitor charge/discharge rate obtained from glucose biosensing system operating in the presence of 5 mM glucose using the e-oscilloscope program.....	80
44. Calibration curve of hybrid glucose biosensing system operating in various glucose concentration using the e-oscilloscope.	80
45. The charge/discharge frequency of the capacitor in the presence of 5 mM glucose and 0.3 mM interfering species	82
46. The charge/discharge frequency of the capacitor in the presence of the respective interfering analyte independent of glucose	83
47. Stability study performed for 20 days at 10 mM glucose concentration.	84
48. Ideal charge pump circuit	103
49. Output voltage obtained across different load resistances of 1, 10 and 100 K Ohms	104
50. Output waveforms obtained at different nodes and stages	105
51. Power curve obtained from MATLAB simulation	107
52. Polarization curve obtained from the MATLAB simulation	108
53. Calibration curve obtained from MATLAB simulation	109

CHAPTER 1

INTRODUCTION

Background

Blood glucose is the main type of sugar found in the blood and is the main source of energy. Glucose comes from the food that an individual eats and is also made in the liver and muscles. Blood carries glucose to all the body's cells to use for energy. The pancreas - an organ, located between the stomach and spine, helps with digestion and releases a hormone called insulin into the blood [1]. Insulin helps the blood carry glucose to all the body's cells. Sometimes an individual's body does not make enough insulin, or the insulin does not work the way it should [2,3]. Glucose then stays in the blood and does not reach the cells. If blood glucose levels get too high, it can cause the disease, diabetes, or prediabetes. Over time, having too much glucose in the blood can cause health problems. Table I represents normal levels of blood glucose for non-diabetic and diabetic individuals.

Table I. Normal blood glucose levels for non-diabetic and diabetic people

Non-diabetic people		Diabetic people	
Test	Blood glucose (mg/dL)	Test	Blood glucose(mg/dL)
Normal	79.2-110	Pre-meal	90-130
Fasting	70-100	Post-meal	< 180

Prediabetes is when the amount of glucose in the blood is above normal yet not high enough to be called diabetes [3]. With prediabetes, the chances of getting type 2 diabetes, heart disease, and

stroke are higher. With some weight loss and moderate physical activity, an individual can delay or prevent type 2 diabetes. The typical signs and symptoms of diabetes are:

- being very thirsty
- urinating often
- feeling very hungry
- feeling very tired
- losing weight without trying
- sores that heal slowly
- dry, itchy skin
- feelings of pins and needles in your feet
- losing feeling in your feet
- blurry eyesight

However, some people with diabetes do not have any of these signs or symptoms. There are three main types of diabetes: type 1, type 2, and gestational diabetes. People can develop diabetes at any age.

Type 1 diabetes

Type 1 diabetes, which used to be called juvenile diabetes, develops most often in young people; however, type 1 diabetes can also develop in adults [1,2]. In type 1 diabetes, the body no longer makes insulin or enough insulin because the body's immune system, which normally protects the body from infection by getting rid of bacteria, viruses, and other harmful substances, has attacked and destroyed the beta cells that make insulin [3]. This type of diabetes is less common and mostly diagnosed in young adults and children and accounts for 5% of the total diabetes cases [1,3].

Treatment for type 1 diabetes includes:

- taking injections of insulin

- sometimes taking medicines by mouth
- making healthy food choices
- being physically active
- controlling blood pressure levels
- controlling cholesterol levels

Type 2 diabetes

Type 2 diabetes also known as adult-onset diabetes, can affect people at any age, even children. However, type 2 diabetes develops most often in middle aged and older people [1,2,3,4,5]. People who are overweight and inactive are also more likely to develop type 2 diabetes. Type 2 diabetes usually begins with insulin resistance - a condition that occurs when fat, muscle, and liver cells do not use insulin to carry glucose into the body's cells to use for energy. As a result, the body needs more insulin to help glucose enter cells. At first, the pancreas keeps up with the added demand by making more insulin. Over time, the pancreas does not make enough insulin when blood sugar levels increase, such as after meals. If the pancreas can no longer make enough insulin, the individual will need to get treated for type 2 diabetes. Type 2 is the most common form of diabetes accounting for 90 – 95% of the total diabetes cases [1]. Treatment for type 2 diabetes includes:

- using medication
- making healthy food choices
- being physically active
- controlling blood pressure levels
- controlling cholesterol levels

Gestational diabetes

Gestational diabetes can develop when a woman is pregnant. Pregnant women make hormones that can lead to insulin resistance [3,4,5]. All women have insulin resistance late in their

pregnancy. If the pancreas does not make enough insulin during pregnancy, a woman develops gestational diabetes. Overweight or obese women have a higher chance of gestational diabetes. Also, gaining too much weight during pregnancy may increase your likelihood of developing gestational diabetes. Gestational diabetes usually goes away after the baby is born. However, a woman who has had gestational diabetes is more likely to develop type 2 diabetes later in life. Babies born to mothers who had gestational diabetes are also more likely to develop obesity and type 2 diabetes. The prevalence of gestational diabetes was as high as 9.2% according to CDC report from 2014 [6].

Other diabetes

Other forms of diabetes include congenital diabetes, cystic fibrosis-related diabetes, steroid diabetes, and several forms of monogenic diabetes are also common. Congenital diabetes is a result of genetic defects of insulin secretion and steroid diabetes is induced by high doses of glucocorticoids. These other types of diabetes accounts for 1 – 5% of the total diabetes cases [4,5,6].

According to a 2014 report, from the Centers for Disease Control (CDC), 29.1 million people or 9.3% of the population suffer from diabetes in the United States (US) alone, and the cost incurred to keep diabetes under control was 245 billion US dollars [6]. Over time, diabetes can lead to serious problems with blood vessels, the heart, nerves, kidneys, the mouth, eyes, and feet. These problems can lead to an amputation of a limb. The most serious problem caused by diabetes is heart disease. When a person has diabetes, they are more than twice as likely as people without diabetes to have heart disease or a stroke. With diabetes, the person may not have the usual signs or symptoms of a heart attack.

Continuously checking and recording blood glucose levels can help monitor and better manage diabetes. If the blood has too much or too little glucose, the person may need a change in diet, physical activity, or medication to have a stress-free and healthy lifestyle.

The most commonly available methods for an individual with diabetes to monitor and maintain normal blood glucose levels are:

- Finger prick test using a test strip and a glucometer
- Continuous glucose monitoring (CGM) system

The finger prick test involves pricking the finger using a lancet and extracting the blood drop with a disposable glucose test strip, which is then placed in the glucometer to measure the blood glucose level as shown in Figure 1.



Figure 1. Example of most commonly available methods for individual with diabetes to monitor and maintain normal blood glucose levels [8]

The disposable test strip consists of a glucose selective enzyme such as glucose oxidase. The glucose selective enzyme oxidizes the glucose in the blood to produce gluconic acid and release electrons. These released electrons are proportional to the glucose concentration, which is converted into variable voltages using analog to digital converters. The meter then displays the level in the units of mg/dl or mmol/l. The test strips used in glucometer are expensive. The consumer cost for each glucose strip ranged from about \$0.35 to \$1.00. Manufacturers often provide meters at little to no

cost to create a demand for the use of the profitable test strips. Individuals with type 1 diabetes may test as often as 4 to 10 times a day due to the dynamics of insulin adjustment, whereas with type 2 typically, tests are less frequent, especially when insulin is not part of treatment [7,8]. These strips are also affected by external factors like humidity, temperature, and altitude. For different batches of the test strips, the glucometer requires recalibration. Additionally, the blood glucose reading can drift by as large as 4 mmol/dL or 72 mg/dL which can prove to be fatal in blood glucose monitoring [7,8,9]. Therefore, close monitoring of blood glucose levels may involve pricking the finger multiple times a day, which may prove painful and tedious.

To reduce finger pricking frequency, continuous glucose monitoring systems (CGMs) were developed. A continuous glucose monitoring system (CGM) can consist of a disposable sensor placed under the skin, a transmitter connected to the sensor and a reader that receives and displays the measurements [10,11,12] as shown in Figure 2.



Figure 2. A continuous glucose monitoring system with implanted sensor and data reader. [12]

The sensor can be used for several days before it needs to be replaced [11-13]. The devices provide real-time measurements and reduce the need for finger prick testing. A drawback is that the meters are not as accurate because they read the glucose levels in the interstitial fluid which lags the

levels in the blood. Also, CGMs are powered by an external power source such as a battery, thereby rendering the device bulky. CGM devices often requires recalibration every 12 hours after the first day.

A lot of research has been conducted to improve the quality and efficiency of CGMs. Companies like Medtronic and Dexcom are at the forefront of glucose monitoring research as it is a very valuable market for them, but the CGM devices developed by both Medtronic and Dexcom, have a bulky receiver, often making them cumbersome to carry. This is mainly because these systems are powered by external power sources such as batteries and are very difficult to miniaturize. Also, one must calibrate the receiver for accurate blood glucose measurements which takes nearly 2 hours and demonstrates a maximum lifetime of just one week [11-13]. Although these devices show promising results, the quest to maintain normal blood glucose levels and improving quality of life for individuals with diabetes remains a challenge. It is imperative that there is a closed loop system that would be minimally invasive, flexible, and easy to use and where the data is easily accessible to the end user and service providers. To solve this problem, a lot of research has been done on making these monitoring devices as non-invasive and small as possible and the development of miniaturized alternative power sources to batteries.

Whenever a need for small and portable power source arises, alternative fuel sources other than batteries are needed. Alternative fuel source offers flexibility when energy needs cannot be met by traditional means due to location, emergency power loss and lack of space. The market for rechargeable batteries is projected to grow at a rate of 7% per year through 2027 [14]. Despite their many advantages, batteries are hindered by the limited lifetime of the materials used to construct the battery. In addition, many batteries use hazardous chemicals that can potentially leak, can cause poisoning if not disposed of properly or even explode [15]. Also, batteries are limited by size as they cannot be miniaturized after a certain point due to limitations in achieved power densities. Therefore,

there is a high demand for alternate power sources that can compete with current battery technologies.

The first conventional fuel cell was introduced by Neidrach and Grubb from General Electric for NASA [16]. The fuel cell consisted of platinum as a noble metal electrocatalyst, which oxidizes hydrogen and reduces oxygen. Oxidation of hydrogen produces protons and electrons which moved through the electrolyte and then the external circuit. This flow of electrons in the system results in the generation of electricity. Oxygen is reduced at the cathode when the electron in the system recombines with the oxygen present in the system. This reaction produce water as a byproduct. A platinum metal catalyst is used because of its efficiency for oxidizing hydrogen. However, in large-scale applications, the use of platinum in fuel cells is limited due to its expensive and nonrenewable nature. In addition, hydrogen fuel is susceptible to carbon contamination and a continuous supply of hydrogen fuel is needed to generate electrical power continuously. These complicate the oxidation process due to carbon monoxide poisoning of the electrocatalyst. The high cost of noble metal electrocatalyst, carbon monoxide poisoning and need for continuous supply of hydrogen results in the unsustainability of hydrogen fuel cells as an ideal power source for implantable bioelectronic devices. The glucose biofuel cell has been looked upon as an alternative to powering implantable bioelectronic devices.

The main motivation for the extensive research in the field of glucose biofuel cell technology is attributed to the search for an alternative sustainable fuel source that is cost-effective and can meet increasing global energy demands and recent advancements in microelectronics [17]. Many researchers are working to use glucose biofuel cells in powering implantable bioelectronic devices. Conventional fuel cell assembly consists of an anode, a cathode and an electrolyte and relies on the conversion of the chemical energy into electrical energy. In a fuel cell, mainly two types of reactions occur: 1) oxidation and 2) reduction reaction. The complete reaction is called a redox reaction. The

oxidation reaction occurs at the anode, and the reduction reaction occurs at the cathode. When the fuel is oxidized due to the redox reaction, electrons are released in the electrolyte, which then travels through an external circuit to the cathode producing electricity. In traditional batteries, two or more solid reactants undergo a chemical reaction which converts chemical energy into electrical energy by consuming one of the reactants. When the disposable reactant is completely consumed, the battery cannot produce any more electrical energy. Once the battery is discharged i.e., the reactant is completely consumed, the battery either must be recharged in case of rechargeable batteries or replaced (traditional batteries). In the case of a glucose fuel cell, the electrical energy is produced due to the chemical reaction occurring between liquid and/or gaseous reactants as long as there is a continuous supply of glucose and the enzymes remain active, in the case of an enzymatic biofuel cell. Glucose is a simple sugar which is mainly produced by plants and algae using water and carbon dioxide from the atmosphere in the presence of sunlight. During this reaction, oxygen is produced as a byproduct and released in the atmosphere. Along with carbon dioxide and sunlight, the reaction also involves Adenosine Triphosphate (ATP) and Nicotinamide Adenine Dinucleotide Phosphate (NADPH) [18]. Scientists have found that this produced glucose can be used as a fuel in glucose biofuel cells since one molecule of glucose upon complete oxidation to CO_2 , generates 24 electrons to produce electrical energy. This glucose fuel is then oxidized into gluconolactone in the presence of oxygen, releasing electrons which in turn reduces the oxygen to produce electricity. Glucose biofuel cell can be differentiated from any other electrochemical energy sources based on the anodic catalysts used for the oxidation of the fuel. A major advantage of glucose biofuel cells over conventional fuel cells is that it employs cheap and environmentally friendly fuel and materials. This makes glucose biofuel cells a great alternative to conventional fuel cells. Also, glucose biofuel cells have high conversion efficiency at ambient temperatures and pH conditions. This electrical energy produced by glucose biofuel cells can be potentially used to power small bioelectronic devices like

pacemakers and continuous glucose monitors. Therefore, great interest has been shown in the field of developing a highly efficient glucose biofuel cell that can generate large amount of electrical energy to power small devices. These glucose biofuel cells can also be employed as a self-powered glucose biosensing system with the addition of a sensing circuit.

As mentioned above, diabetes is one of the most common and debilitating diseases in the world, and it happens due to increased levels of glucose in the blood. Elevated concentrations of glucose in the body are considered one of the important parameters that represent the different states of disorder [19,20]. Continuous glucose monitoring is the best way to minimize the complications arising from increased glucose levels in the body. Implantable glucose biosensors that have 3 electrochemical sensors have continued to attract significant attention because of their unique advantages, such as ease of fabrication, rapid response time, low limit of detection, high selectivity, and sensitivity [20-21, 25]. Electrochemical sensors can convert chemical or biological information rapidly, ranging from the concentration of a specific analyte to the total composition analysis, into an electrical signal [22-24].

Most of the biosensors aimed at detection of various analytes consist of an array of electrodes immobilized with enzymes, aptamers, or antibodies [20,23]. It has been observed that, the enzymes denature after some time of continuous use and their performance is widely affected by the surrounding pH and temperature. Also, the enzyme immobilization process must be performed in a controlled environment. To improve on these limitations, materials like carbon nanotubes [20,21], metal oxides [22,23], nano-structured conducting polymers [24-26], graphene [27], etc., have been considered as an alternative. Moreover, interest has been shown in the utilization of noble metals such as gold, platinum, and silver nanoparticles/ nano features in general because of their unique electrochemical properties [28,30]. These nanoparticles improve the direct electron transfer, signal transduction, and efficiency of the sensor. Platinum nanoparticles have been shown to have the

capacity to directly electro-oxidize glucose even in the absence of enzymes and mediators [30]. The large surface area and good biocompatibility of nanoparticles makes nanoparticles and nanocomposites attractive for the construction of biosensor [30,31].

Gas diffusion electrodes (GDE) are electrodes with a conjunction of a solid, liquid and gaseous interface, and an electrical conducting catalyst supporting an electrochemical reaction between the liquid and the gaseous phase [38-42]. GDEs are typically used in fuel cells, where oxygen and hydrogen react at the gas diffusion electrodes, to form water, while converting the chemical energy into electrical energy. Usually the GDEs are porous and the catalyst is fixed in a porous foil, so that the liquid and the gas can interact. Besides these characteristics, the gas diffusion electrode must, of course, offer optimal electric conductivity, in order to enable electron transport with low ohmic resistance [33-36].

Problem statement

The goal of this work is to develop a self-powered continuous glucose monitoring system with wireless data access and monitoring capabilities. The developed system will not need a battery and will work under physiological conditions. The system is designed to exhibit high sensitivity and selectivity towards glucose analyte and have a wide linear range. It is also able to act as a power source for small electronic devices if the need arises. The data obtained can be forwarded to doctors or health care providers, so that they can have a detailed record of the user's health and act when any kind of anomalies are observed. The fabricated system is equipped with a wireless data access and monitoring system.

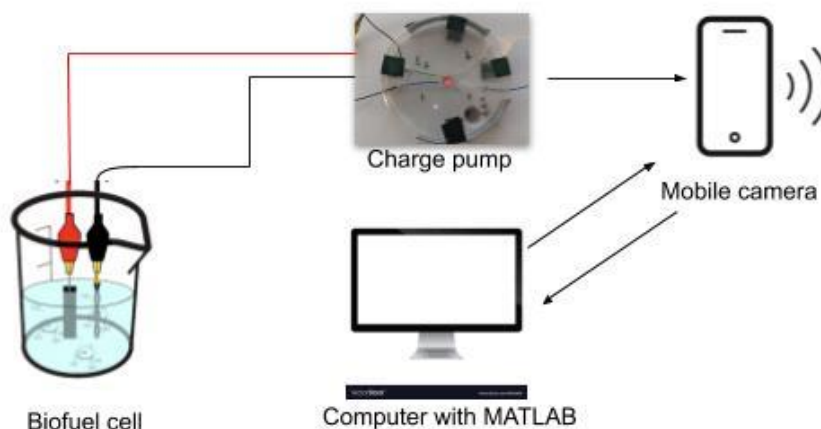


Figure 3. Schematic of a self-powered continuous glucose monitoring system with wireless data access and monitoring

Dissertation contribution

In this dissertation, we developed a novel non-enzymatic glucose biofuel cell consisting of an anode made up of gold microwire electrodeposited with colloidal platinum and a cathode made up of a platinum catalyst layer on carbon cloth GDE substrate. The power output of the biofuel cell is directly proportional to the glucose concentration level. This biofuel can then be used to power a small charge pump circuit. The charge pump circuit consists of a blinking LED whose blinking frequency is directly proportional to the power produced by a biofuel cell. By incorporating the charge pump circuit, a complete glucose biosensing system was realized. An android application was developed, which uses a mobile camera to measure the blinking frequency using image processing in MATLAB and converts it into glucose concentration. Then a text message is sent to the user containing their body glucose level.

We also performed cyclic voltammetry characterization of the non-enzymatic biofuel cell in the absence and presence of glucose and purged oxygen. Current-Voltage characteristics (IV) tests were carried out to study the power characteristics of the glucose biofuel cell. The performance of

the glucose biofuel cell was verified at different pH and temperature conditions to find the optimal working conditions for the glucose biofuel cell along with interference characterization. Amperometry was also carried out to further study the performance of the biosensor.

Scope of dissertation

The purpose of chapter 2 is to provide background to the thesis and introduce the reader to the electrical and bioelectrical concepts that govern the workings of a basic fuel cell and biofuel cells. The chapter also sheds light on the types of electron transfer methods used in biofuel cells, which constitutes how current flow in a biosensing system occurs.

Chapter 3 focuses on the glucose biosensor in general. This chapter sheds a light on different types and generations of glucose biosensors. It also explains continuous glucose monitoring systems and the current trends in research and development.

Chapter 4 focuses on the charge pump circuit and its operating principle. This chapter provides a detailed explanation of the S882Z charge pump IC and general operation.

Chapter 5 focuses on the different electrochemical characterization methods used.

Chapter 6 focuses on the discussion of the fabricated non-enzymatic glucose biosensing system. The manufacturing methods, materials used in the preparation of the bioelectrodes and charge pump circuit are explained. It also reviews the ESP8266 microcontroller, MATLAB and the developed android application.

Chapter 7 describes all the experimental data, the characterization methods, interference studies and results obtained by the self-powered glucose monitoring system.

Chapter 8 summarizes the studies performed. The result and path forward of the novel glucose biosensing system are also discussed.

CHAPTER 2

BIOFUEL CELL

Fuel cell

Fuel cells are electrochemical devices that convert chemical energy in fuels into electrical energy, thereby promising power generation with high efficiency and low environmental impact [43]. Because the intermediate steps of producing heat and mechanical work of most conventional power generation methods are avoided, fuel cells are not limited by thermodynamic limitations of heat engines such as the Carnot efficiency. In addition, because combustion is avoided, fuel cells produce power with minimal pollutants. However, unlike batteries the reductant and oxidant in fuel cells must be continuously replenished to allow continuous operation. Fuel cells bear significant resemblance to electrolyzers [43,44]. In fact, some fuel cells operate in reverse as electrolyzers, yielding a reversible fuel cell that can be used for energy storage. Though fuel cells could, in principle, process a wide variety of fuels and oxidants, of most interest today are those fuel cells that use common fuels (or their derivatives) or hydrogen as a reductant, and ambient air as the oxidant. A hydrocarbon fuel cell is illustrated in 4. This system is characterized by a non-polluting and silent technology.

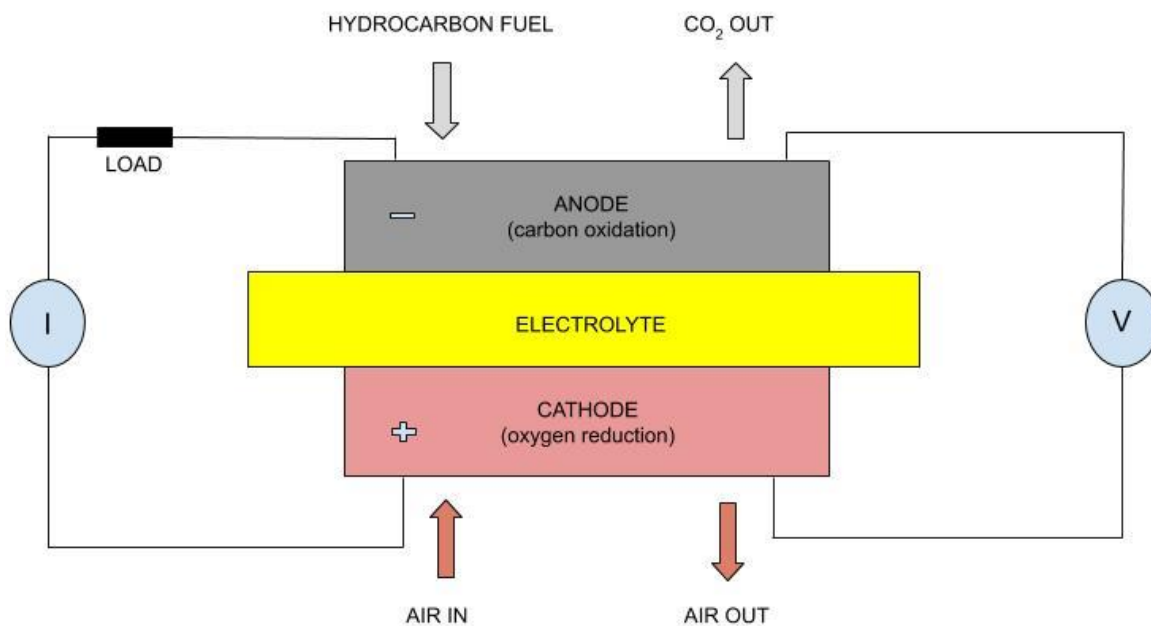


Figure 4. Hydrocarbon Fuel Cell Representation

In general, traditional fuel cells use noble metal catalysts to generate electrons from fuel oxidation (typical fuels are hydrogen or small organic molecules such as methanol, ethanol, etc.). After the oxidation step, an external circuit transfers the electrons to the cathode side where the electrons react with an oxidant molecule (usually oxygen) and generate electrical work as well as water and heat.

Fuel cells can vary from tiny devices producing only a few watts of electricity, right up to large power plants producing megawatts of power. All fuel cells are based around a central design using two electrodes separated by a solid or liquid electrolyte that carries electrically charged particles between them [43]. A catalyst is often used to speed up the reactions at the electrodes. Fuel cell types are generally classified according to the nature of the electrolyte they use. Each type requires materials and fuels that are suitable for different applications [44].

Basic Fuel cells can be differentiated into various types, depending on the type of electrolyte and operation temperature. Proton exchange membrane fuel cells (PEMFC), Direct methanol fuel

cells (DMFC), Phosphoric acid fuel cells (PAFC), Alkaline fuel cells (AFC) and Solid oxide fuel cells (SOFC) are some of the main types of fuel cells produced [45]. Fuel cell technology offers considerable advantages over other processes, such as high conversion efficiency and generation of substantial power density. Although fuel cells yield good results, some factors limit their large-scale application: high cost and future scarcity of noble metal catalysts (e.g., platinum) employed as a base catalyst in many fuel cell devices, issues regarding electrode passivation, and inability to oxidize some of the byproducts generated. Furthermore, hydrogen production, purification, and storage also pose major technical challenges.

In laboratory and commercial settings, acids, alcohol, oxides and hydrogen are used as the fuel source. In the case of portable and implantable electronics, the fuel needs to be readily available inside human body. A standard fuel cell cannot be applied in this situation. To solve this problem, biofuel cells (BFCs) can be looked upon as the ideal power source for portable and implantable electronics. On average there is >100 W of power contained as chemical energy in human body. Biofuel cells transform chemical energy into electrical energy from molecules presents in a living organism. The difference between biofuel cells and batteries is that in BFCs the concentration of the reactants is continually re-established by the body fluids. The constant presence and availability of the fuel directly from the body makes external recharging mechanisms or replacement unnecessary and provides a theoretical capability for operating indefinitely, as long as there is a constant supply of fuel.

Biofuel cell

Biofuel cells are structurally and functionally similar to conventional fuel cells as seen in Figure 5, but their catalysts are biological entities such as enzymes, microbes, and organelles [46]. Biofuel cells can be abiotic, enzymatic, microbial, or mammalian type depending on the catalysts used for the oxidation and reduction reactions. The development and fabrication of biofuel cells depend on multidisciplinary research that requires conceptual understanding of the metabolic pathways of microorganisms, catalysts, material sciences, fabrication, and bioelectronics [47,48]. Presently, researchers are focusing on the development of biofuel cells that can be implanted in living organisms to power medical devices and biosensors. Moreover, biofuel cells can also be a better alternative to batteries and conventional fuel cells.

Using biological catalysts gives biofuel cells some unique properties: room temperature operation, catalyst-fuel specificity, membrane-less (no separation between the anode and cathode), and finally, there are a wide range of possible fuels owing to the multitude of biological catalysts that can be used. Biofuel cell fuels (commonly referred to as substrates) include alcohols, sugars, wastewater, and biological fluids such as blood, sweat, and tears. The abundance and sustainable nature of these fuels make biofuel cells a renewable energy option, although it has recently been shown that biofuel cells can even operate using JP-8 aircraft fuel [48]. The choice of electrodes and biocatalysts are the main factors that affect the power generation of a biofuel cell.

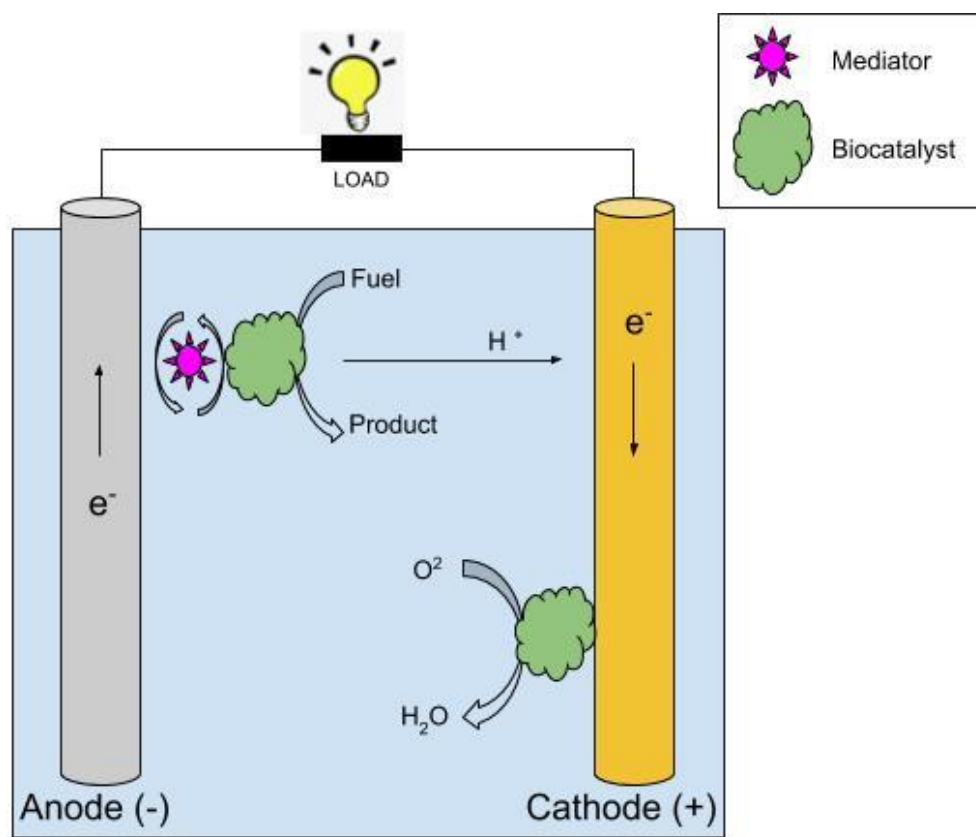


Figure 5. Biofuel cell schematic showing its major components and basic operation. In this example, the anodic electron transfer occurs through a mediator while at the cathode it occurs directly through a biological catalyst.

Enzymatic biofuel cells consist of enzyme catalysts that have been isolated from a biological source and placed on either the anode, cathode, or both electrodes. Because the enzymes have been removed from their natural environment, they can communicate with mediators or electrodes directly, so they typically have higher power density than microbial or organelle biofuel cells. However, removing the enzymes from their native environment also lowers their stability [49]. Microbial biofuel cells, on the other hand, employ microbial catalysts that are grown directly on the electrodes and remain intact during operation. This greatly increases catalyst lifetime [50,51] but insulates enzymatic reaction sites, making electron transfer to the electrodes more difficult. Regarding the third type of biofuel cell

utilizing organelles, they are in their infancy compared to their enzymatic and microbial counterparts. As a result, they have neither the power output of enzymatic biofuel cells nor the stability of microbial biofuel cells. Organelles, such as mitochondria, can be isolated from living cells and immobilized directly on an electrode [52]. Mitochondria contain a series of membrane-bound enzymes that form an electron transport chain that can communicate directly with an electrode. Because the enzymes are membrane-bound, they are theoretically more stable than those found in an enzymatic biofuel cell, and because the mitochondria are not surrounded by cellular walls, they should be capable of faster electron transfer than a microbial fuel cell. There is a wealth of research for each of these biofuel cell classes, but the focus from this point forward will be on enzymatic biofuel cells.

In enzymatic biofuel cell (EBFC), isolated enzymes are used for oxidation and reduction reactions at the anode and cathode, respectively [53-56]. The interest in EBFCs has increased due to implantable medical devices and biosensors for physiological substances. Besides the health-care applications, enzyme-based biofuel cells have also been used to power various portable and low-power devices. Because of their specificity and selectivity, enzymes are preferred biocatalysts where mixed fuel or reactants are to be used. Practically, the lifetime of EBFCs is limited and researchers have focused on different possible solutions for long-term operational stability of EBFCs. These possibilities include enzyme immobilization, genetic engineering of enzymes, and process development to replenish the enzyme level at the electrodes. The operation of an EBFC resembles the functioning of a conventional fuel cell [54,55]. A biofuel cell generates electricity from carbohydrates (sugar) utilizing enzymes as the catalysts through the principles of power generation present in living organisms. The EBFC incorporates an anode consisting of carbohydrate-digesting enzymes and a mediator and a cathode comprising oxygen-reducing enzymes and a mediator on either side of a separator membrane. The anode extracts electrons and hydrogen ions from the sugar (glucose) through enzymatic oxidation. At the cathode, the hydrogen ions and electrons combine with oxygen and produce water as seen in Figure 6.

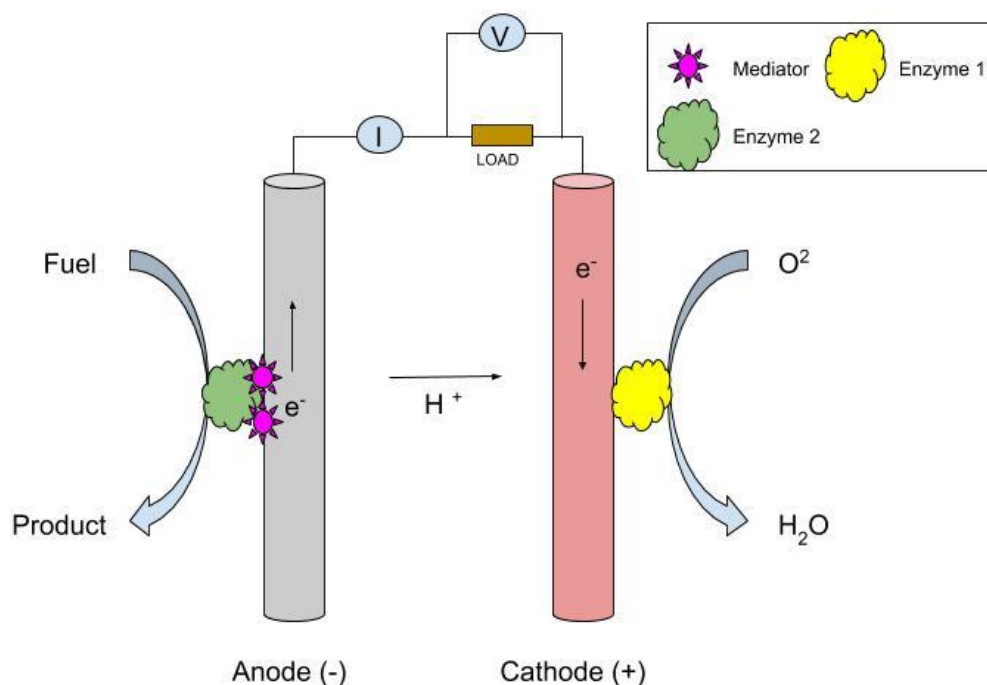


Figure 6. Schematic representation of enzymatic biofuel cell.

Due to the selective reactivity of the enzymes at each electrode, no cross-reaction occurs between the anode and the cathode. In general, the EBFC could be classified into many types based on fuel containment, fuel and catalyst sources, origin of the catalytic enzymes, and method of electron transfer between the reaction site and the electrode [55,56]. Similarly, the enzymes generally used in biofuel cells can also be divided into three groups depending on the location of the enzyme active centers and type of electron transfer between the enzyme and the electrode. These groups are:

- (1) enzymes having nicotinamide adenine dinucleotide (NADH/NAD⁺) or nicotinamide adenine dinucleotide phosphate (NADPH/NADP⁺) redox centers (these redox centers are weakly bound to the enzyme protein),
- (2) enzymes having redox centers at near surface or peripheral locations, and
- (3) enzymes having strongly bound redox centers or enzymes where redox centers are located

deep in the protein or glycoprotein shell.

The enzymes described in points (1) and (2) carry out DET between the electrode surface and enzyme active centers, while enzymes in group (3) are not able to perform the DET with the electrode surface. Therefore, electron transfer to the electrode surface can be achieved by the use of electron transfer mediators. These mediator molecules (either electron donor or acceptor) can be accepted by the redox enzymes used in biofuel cells, and therefore, MET-based EBFCs were focused on by different research groups worldwide [56].

An oxidoreductase enzyme can oxidize carbohydrates, alcohols, lactate, or even amino acids, and transfer electrons from the fuel to the electrode surface. Depending on the fuels mentioned above, it is possible to prepare anode-based electrodes by immobilizing different types of enzymes. For sure, glucose oxidase has been the most often employed enzyme since the first description of a biofuel cell. Its *in vivo* application is desirable because of different human physiological fluids, such as blood, plasma, saliva, and tears, that contain sugar (glucose). Scientists are also testing other enzymes, depending on the target fuel. As for enzyme-based cathodes, laccase or bilirubin oxidase usually perform the oxygen reduction reaction.

The difference between the thermodynamic potential of the cathode and the anode (ΔE_{c-Ea}) expresses the cell voltage, but this value can decrease by several orders of magnitude due to overvoltage ($\Delta\eta$). $\Delta\eta$ results from (i) slow electron transfer occurring at both electrode sides; (ii) ohmic drop ($\Sigma\Omega$), associated with all the resistances in the system (film diffusion, membrane, supporting electrolyte); and (iii) electrode wear out ($\Delta\xi$), a parameter that reflects electrode degradation described in Equation 1:

$$E_{\text{cell}} = \Delta E_{c-Ea} - \Delta\eta - \Sigma\Omega - \Delta\xi \quad (1)$$

This provides important information that can be applied to any enzymatic electrode. Maximizing the so-called thermodynamic potential window ($E_c - E_a$) yields better biofuel cell

performance [57]. Therefore, enzymatic biofuel cell researchers aim to prepare/achieve bioelectrodes that facilitate the catalyzed reactions, to increase the open cell voltage (OCV). Moreover, these researchers target better cell design and prototypes that can reduce the overall resistances, making the electric current flow more easily through the system. To produce commercial devices, it is also necessary to keep $\Delta\epsilon$ as low as possible.

Another crucial parameter associated with the performance of any fuel cell is the power density that this system provides. This parameter reflects the electron generation rate in the enzyme-catalyzed reactions. Unlike traditional fuel cells, which afford power densities of the order of milli to kilowatts, enzymatic biofuel cells generate power densities in the order of micro to a few milliwatts, which is sufficient for applications in portable low-powered electronic devices. The representative scheme in Figure 7 shows the power range of some of the alternative methods of energy production [58].

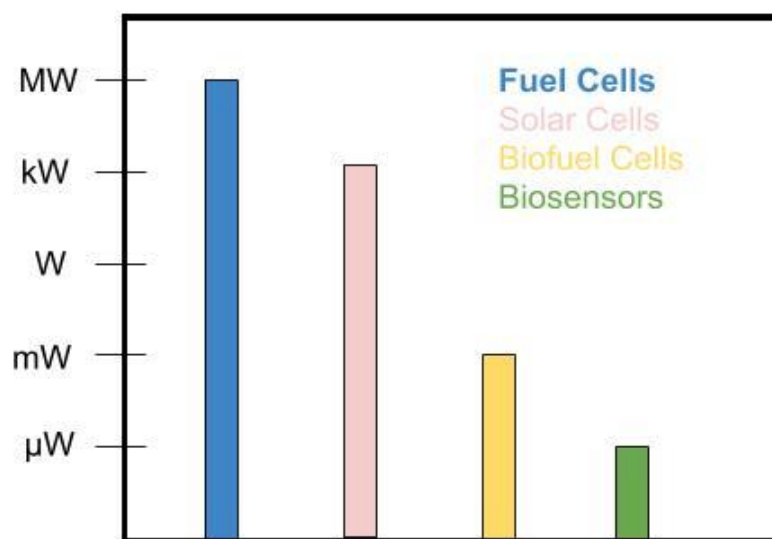


Figure 7. Schematic reference of power range that some of the alternative energy production methods provide

Despite the various advantages and possible applications of enzymatic biofuel cells, to achieve an efficient practical device, it is necessary to consider some crucial factors when developing this type of system. The first major challenge is the fact that enzymes are proteins; therefore, these biomolecules display a weak three-dimensional structure that must be maintained to ensure that its catalytic activity is retained. Although enzymes are highly specific and efficient catalysts, they have a limited lifetime in solution. Hence, their use in biofuel cells requires a critical step: immobilizing the enzyme onto an electrode surface. Achieving electrical contact between the enzyme and the electrode is also fundamental because this is one of the most important processes in the field of bioelectrochemistry. Achieving a high electron transfer rate from the active site of an immobilized enzyme to the electrode surface is probably the most critical point when constructing an enzymatic biofuel cell. Most research analyzing glucose in blood or serum focuses on enzymatic amperometric sensors owing to their simple design and performance. Amperometric enzyme biosensors rely on the measurement of current on the application of a potential between working and reference electrodes. The magnitude of this current depends on the concentration of a redox-active reagent or product in an enzymatic reaction.

Amperometric enzymes based glucose biosensors suffer from complex and complicated enzyme immobilization strategies, critical operating conditions (temperature and pH), high cost and instability of the enzyme over a long period of time [59]. The activity of enzymes is very largely affected by the temperature, pH, humidity, and the presence of toxic chemicals [60]. To address these limitations, enzyme-free sensors, as seen in Figure 8, have been investigated to improve the electrocatalytic activity and selectivity toward the oxidation of glucose. Non-enzymatic biofuel cells use abiotic catalysts like platinum or other noble metals to carry out the electrooxidation of biofuel. Inert metals (Pt, Au, and Ni) metal alloys containing Pt, Au, Pb, Ir, Ru, Cu, and Pd and metal-dispersed carbon nanotubes (CNTs) frameworks in which Pt, Pb, Pd, or Au are mixed with CNTs to form nanocomposites have been explored for glucose catalysis [59,60].

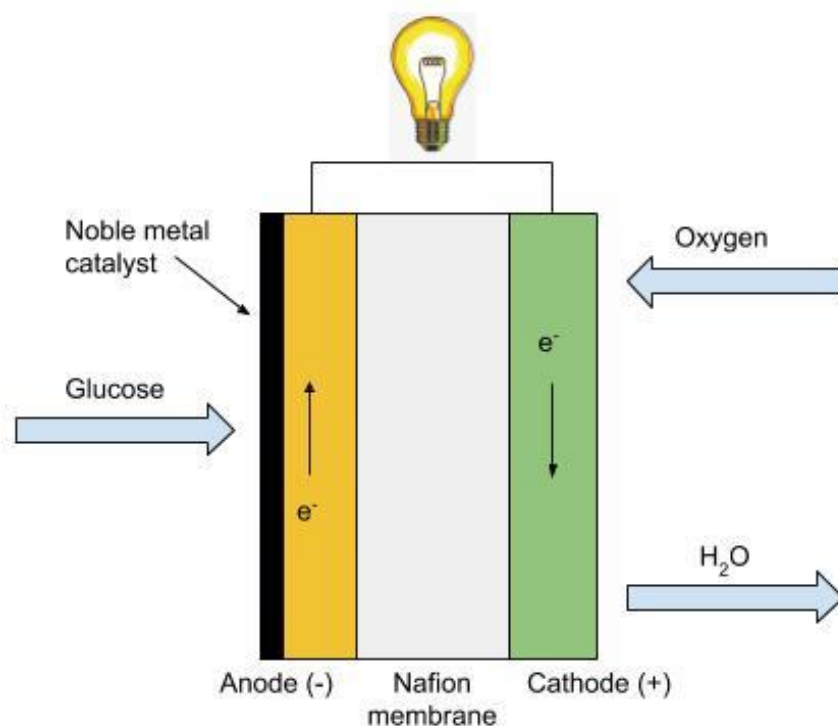


Figure 8. A model of a non-enzymatic biofuel cell

An abiotic glucose fuel cell converts the chemical energy of glucose and oxygen into electric power using noble metals as the catalysts. The general electrode reactions of an abiotic biofuel cell involve oxidation of glucose to gluconic acid at a platinum-based anode catalyst, and oxygen is reduced to water at the cathode. Released protons travel from the anode to the cathode through a proton-conducting membrane or electrolyte and generate electric power. The biofuel may be glucose, methanol, and ethanol [59]. Glucose is used more commonly as biofuel. Though in recent decades much attention has been paid to enzymatic, microbial, and whole cell/organism-based bio-fuel cells for implantable devices, abiotic biofuel cells also possess some advantages over biotic biofuel cells. Though the use of noble catalysts results in a more expensive biofuel cell system, abiotic biofuel cells promise tolerance to high temperatures during steam sterilization or a wide range of pH values. An abiotic cells also promise for long-term stability at operative and physiological conditions. Moreover, abiotic biofuel cells may also perform better at physiological concentrations of glucose [60]. Abiotic glucose fuel cell exhibits

higher stability and a longer life span as compared to EBFC.

Due to increasing research and development in the field of biofuel cells, abiotic fuel cells can be seen as an alternative to conventional fuel cells based on metal catalysts. These devices constitute a system that can directly transform chemical energy into electricity through reactions involving biochemical steps, or even a system in which the activity of the cell (or part of it) stems from the action of biocatalysts. The connection between biology and electricity and the concept of a biofuel cell have been known since 1911, when MC Potter noted that a culture of the bacterium *E. coli* produced electricity in half-cell studies employing platinum electrodes [61]. During the height of the Space race, the interest in this technology increased. The United States space program decided to use the biofuel cell in two entirely different ways. The first was to treat the waste originating from the spacecraft, and the second was to obtain electricity from the treated waste using the reactions involving the biofuel cell. Motivated by the possible in vivo application of this device, Yahiro *et al.* were the first to describe a biofuel cell that used isolated enzymes on the surface of an electrode and to show that it was possible to produce electricity using the enzyme glucose oxidase (GOx) [62]. The main advantages of the biological fuel cells are as follows:

1. The use of clean and renewable catalysts (enzymes or microorganisms),
2. The ability to operate at mild temperatures (20-40 °C) and physiological pH conditions,
3. The possibility to use several fuels because enzymes and microorganisms offer diversity and specificity,
4. Scaling up the use of biocatalysts tends to reduce production costs, which is not possible for non-renewable metallic catalysts.

All these advantages point to an economically viable process, as judged from the growing research in this field all over the world.

CHAPTER 3

GLUCOSE BIOSENSOR

A biosensor is an analytical device, used for the detection of a chemical substance, that combines a biological component with a physicochemical detector. A biosensor consists of an active region that is modified with the enzyme for the detection of the chemical constituent of interest. A transducer converts the chemical signal resulting from the interaction of the analyte with the biological element, into an electrical signal that is processed using a signal processing unit into a readable form [63, 65]. The active region can incorporate biorecognition elements such as receptors, enzymes, antibodies, nucleic acids, microorganisms, and lectins [63,64,65]. A glucose biosensor is a device that senses the concentration of glucose in a complex mixture. A blood glucose sensor measures the concentration of glucose in the blood by breaking down the glucose molecules to produce electrons with the help of a glucose selective enzyme. On complete oxidation of glucose, the current generated correlates to the glucose concentration. Thus, the biorecognition enzyme element is immobilized on a transducer, which in turn transduces the chemical signal into an electrical signal that can be read by a read-out circuit. Since the enzymes act as catalysts, they are not consumed in the oxidation reaction of glucose, thereby making them reusable. Also, the enzymes provide an alternate route for the glucose oxidation reaction with a lower activation energy, which allows the reaction to be thermodynamically favorable. The chemical constituent of interest in this study, is the glucose analyte and it is detected commonly via amperometric detection principle.

A plethora of glucose biosensors have been developed to provide diagnostic information regarding a patient's health status. As a cure for diabetes is yet to be developed, managing the life impeding conditions of this disease is currently the most successful means for its control. Monitoring glucose levels in blood, as a biomarker, has proven to prolong life expectancy by enabling diabetics to

manage episodes of hypo or hyperglycemia, hence providing better control over their condition and preventing some of the debilitating side effects [66,67]. In addition, glucose monitoring can be used to optimize patient treatment strategies, and provide insight into the effect of medications, exercise and diet on the patient [68]. Although blood-glucose monitoring is the gold standard medium for glucose sampling, measurements carried out in this fluid are invasive [66,69].

Glucose monitoring in blood

Blood-glucose concentrations are typically in the range of 4.9–6.9 mM for healthy patients, increasing to up to 40 mM in diabetics after glucose intake [66–72]. The first generation of glucose biosensors proposed by Clark and Lyons at the Children’s Hospital in Cincinnati in 1962 [73]. These sensors were based on an electrochemical approach, which used the enzyme glucose oxidase (GOx) [68]. Electrochemical sensors were chosen for blood-glucose measurements due to their high sensitivity, on the order of μM to mM, good reproducibility and ease of fabrication at relatively low cost [66]. GOx was employed as the enzyme for the sensor, due to its high selectivity for glucose, high tolerance towards extreme changes in pH, temperature and ionic strength in comparison with other enzymes such as hexokinase and glucose-1- dehydrogenase [74–77]. A thin layer of the GOx enzyme was placed on a platinum electrode via a semipermeable dialysis membrane to fabricate the sensor. This sensor measured the decrease in oxygen concentration and the liberation of hydrogen peroxide, which was proportional to the glucose concentration. GOx catalyzes the oxidation of glucose to gluconolactone in the presence of oxygen, while producing hydrogen peroxide (H_2O_2) and water as by-products as seen in Figure 9 [66]. Gluconolactone further undergoes a reaction with water to produce the carboxylic acid product, gluconic acid. GOx requires a redox cofactor to carry out this oxidation process, where flavin adenine dinucleotide (FAD^+) is employed. FAD^+ is an electron acceptor which becomes reduced to FADH_2 during the redox reaction [78]. Subsequent reaction with oxygen to

produce H_2O_2 regenerates the FAD^+ cofactor. This reaction occurs at the anode, where the number of transferred electrons can be correlated to the amount of H_2O_2 produced and, hence, the concentration of glucose.

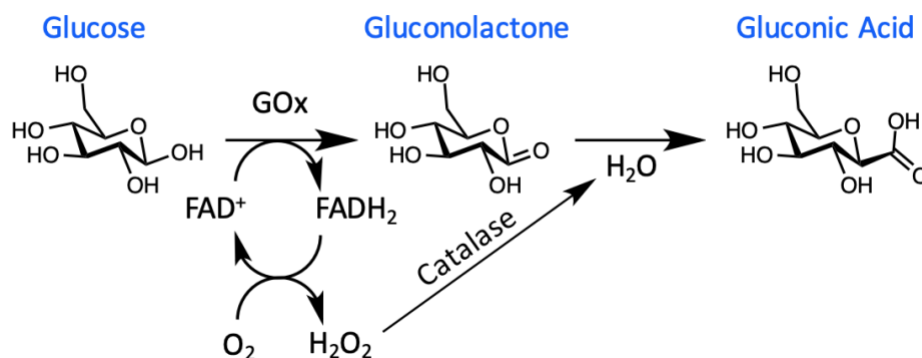


Figure 9. Conversion of glucose to gluconic acid using glucose oxidase.

The main obstacle to overcome with this approach is the interference of other electroactive species present in blood, such as ascorbic acid and urea [68,79]. In the design of these sensors, oxygen was employed as the electron-acceptor, which can result in errors from variations in oxygen tension and limitations, known as the oxygen deficit [80]. In order to overcome these challenges, oxygen was replaced with a synthetic electron redox mediator in second generation sensors [30].

The evolution of this sensing approach also led to the development of disposable enzyme electrode strips, which were accompanied by a pocket-size blood-glucose meter [81,82]. Each strip housed miniaturized screen-printed working and reference electrodes, where the working electrode was coated with the required sensing components; glucose oxidase, an electron-shuttle redox mediator, stabilizer and crosslinking agent. Currently, the most widely used self-monitoring method is the ‘finger-pricking’ approach which involves using a test strip to sample blood from a finger via pricking, which is then analyzed via a glucometer as seen in Figure 10 [83-92]. The effectiveness of this method relies on strict compliance, which can be negatively influenced by time constraints, pain, and inconvenience [93]. It is also not a continuous monitoring approach and needs to be carried out at multiple intervals

throughout the day to help manage elevated glucose levels [88-94], especially after meals, exercise and dosing of insulin medication [94,95]. Moreover, a non-continuous method such as this can overlook periods of hyper- or hypoglycemia which occur outside of the sampling window [93]. Recent developments in implantable sensors, on the other hand, can be used to incorporate insulin pumps, which allow for instant insulin administration [92,93,95].

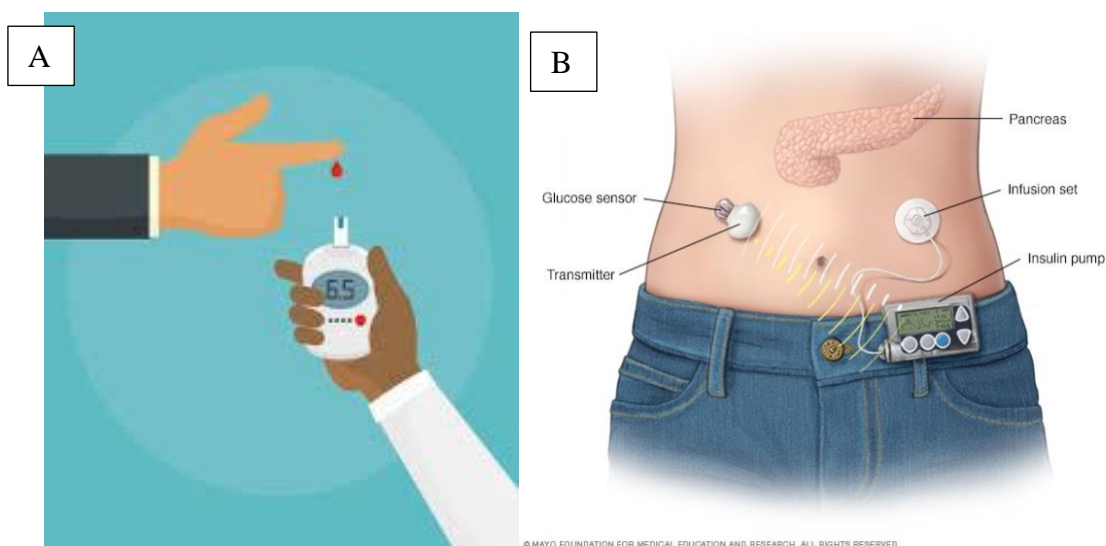


Figure 10. Illustration of a A) Glucometer [86] and B) Continuous glucose monitor (CGM). [102].

In the early 1970s, Albisser et al. and Shichiri et al. first introduced the in vivo continuous glucose monitoring system using an artificial pancreas [98,99]. The artificial pancreas design was based on continuous glucose monitoring, where the device would remove blood from the body to an external benchtop analyzer that was connected to an insulin pump. As the name suggests, the device was not implanted and therefore not portable, although it was named the ‘artificial pancreas’. This led to the development of a third generation of glucose biosensor, which was subcutaneously implanted as seen in Figure 9.

Although the device could analyze glucose concentrations in blood using GOx, this was considered an invasive method [100]. The first commercially available personalized in vivo glucose

monitor was launched by Medtronic Minimed Inc. in the 1990s [79]. Unfortunately, the device could not provide real-time information, with data being accessed by a physician every 3 days [68]. Although implantable glucose monitoring systems offer regular glucose level readings, this approach isn't recommended for all diabetics, due to its invasive nature [68] and some continuous glucose monitoring methods have been reported to show inaccuracies of up to 21% [101]. These inaccuracies are often attributed to sensor drift, caused by changes in the catalytic performance of the enzyme. This requires the device to be periodically recalibrated via the finger-pricking method [102]. Despite current commercially available glucometers, such as the Freestyle-Navigator by Abbott (Abbott Park, IL, USA), providing real-time measurements every 1–5 min, the longest working model without calibration is approximately two weeks. There is high consumer demand for a continuous glucose monitoring system which can quantify glucose concentrations without frequent calibration. Although blood remains the most studied body fluid for such measurements, other more accessible biological fluids such as interstitial fluid, ocular fluid, sweat, breath, saliva or urine have been investigated as alternative sample media for noninvasive continuous monitoring (Table 2) [66–69].

Table 2. Glucose concentration in physiological fluids for healthy and diabetic patients in mM

Physiological Fluid	Biomarker	Concentration for Healthy Patients'	Concentration for Diabetic Patients'	pH
Blood	Glucose	4.9–6.9 mM	2–40 mM	7.35–7.45
Interstitial Fluid	Glucose	3.9–6.6 mM	1.99–22.2 mM	7.2–7.4
Urine	Glucose	2.78–5.55 mM	>5.55 mM	4.5–8
Sweat	Glucose	0.06–0.11 mM	0.01–1 mM	4.5–7
Saliva	Glucose	0.23–0.38 mM	0.55–1.77 mM	6.2–7.6
Ocular Fluid	Glucose	0.05–0.5 mM	0.5–5 mM	6.5–7.6

Glucose monitoring in alternative physiological fluids

Interstitial fluid is the extracellular fluid which surrounds tissue cells. It has significant potential for medical diagnostics as it possesses a similar composition of several clinically important biomarkers to blood [103,104]. Blood and the surrounding vascularized tissue readily exchange biological analytes and small molecules by diffusion with the interstitial fluid [104]. As a result, interstitial fluid can offer valuable information about a patient's health and has been used for minimally invasive determination of inherited metabolic diseases, organ failure or drug efficacy.

Sode et al. have also developed a self-powered implantable continuous monitoring device called the BioRadioTransmitter for use in an artificial pancreas [68]. In this instance, the device is composed of a capacitor, radio transmitter and receiver. In the presence of glucose, the capacitor of the BioRadioTransmitter device discharges a radio signal, which is received and amplified by the radio receiver. The change in transmission frequency is then related to the glucose concentration [105]. Microneedles and microneedle arrays have also garnered a lot of interest over recent years for interstitial fluid sensing, since this approach can offer minimally invasive methods for biosensing. This concept was used in the development of a glucose-sensing patch by Jina et al. [106]. The device was designed in two compartments: the first containing the microneedle array and glucose biosensor with the second containing the electronics as illustrated in Figure 11.

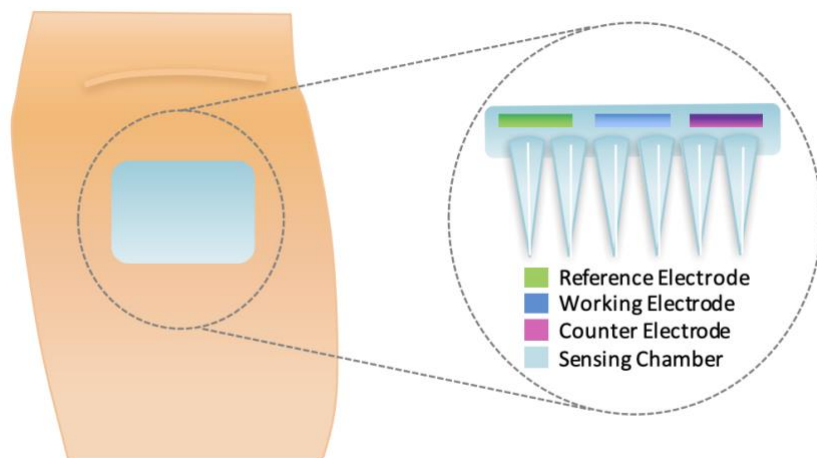


Figure 11. Schematic of the microneedle glucose-sensing patch on the forearm [69].

A microneedle patch platform allows the device to be in constant contact with the skin, providing permanent access to the interstitial fluid, and enabling this device to operate continuously [69]. In this particular case, the short length of the microneedles means that penetration is optimal for interstitial fluid sampling. Currently, the device must be recalibrated daily by the finger-prick approach [106]. Potential clogging of the microneedles and the distortion of their shape upon penetration of the skin can also affect the dynamics of sampling. Despite these shortcomings, this novel device holds great potential for non-invasive continuous glucose monitoring.

Urine has been used as a diagnostic fluid for diabetes since the 1980s due to its easy and non-invasive collection [107]. Urine is composed of metabolites, such as glucose, proteins and nitrates, as well as other dissolved salts, such as sodium and potassium. As a result, the pH of urine fluctuates between acidic pH 4.5 to basic pH 8 [108]. Due to the intermittent nature of this fluid, where collection is required for sampling, it cannot be incorporated into a continuous glucose-monitoring device.

Sweat is one of the most accessible body fluids. Eccrine glands that excrete sweat can be found all over the body [110]. Sweat has been used for the detection of disease markers such as sodium,

potassium, calcium, phosphate and glucose. The reported glucose level in sweat for healthy patients is between 0.06 and 0.11 mM and between 0.01 and 1 mM for diabetics [109]. The fluctuations in analyte concentrations result in a broad pH range of sweat, typically between pH 4.0–6.8 during exercise [111,112], which can impact the effectiveness of chemical sensing or biosensing techniques chosen for disease diagnosis or monitoring.

A non-invasive and continuous wearable glucose sweat sensing device was recently reported by Gao et al. [113]. It detects skin temperature, sodium, potassium, lactate and glucose concentrations in sweat [113]. An advantage of this approach is the use of multiple sensors which overcomes limitations of single, stand-alone sensors by providing a more comprehensive profile of sweat composition and enables data cross-comparisons. It is known that the potassium concentration in sweat is very stable during basal and exercising states. As a result, potassium levels can be used as a reference for comparing the fluctuating concentrations of other analytes, such as glucose, for performing concentration calculations. This sensor showed good correlations to the normal concentration ranges in sweat during exercise, but the drawback is that the glucose and lactate sensing units had to be changed every 2 hours to get continuous monitoring. Also, a minimum 10 μ L of sweat was required to do sweat analysis. The sensors were placed close to the skin, to allow for immediate analysis of sweat as it emerged. The illustration can be seen in Figure 12.

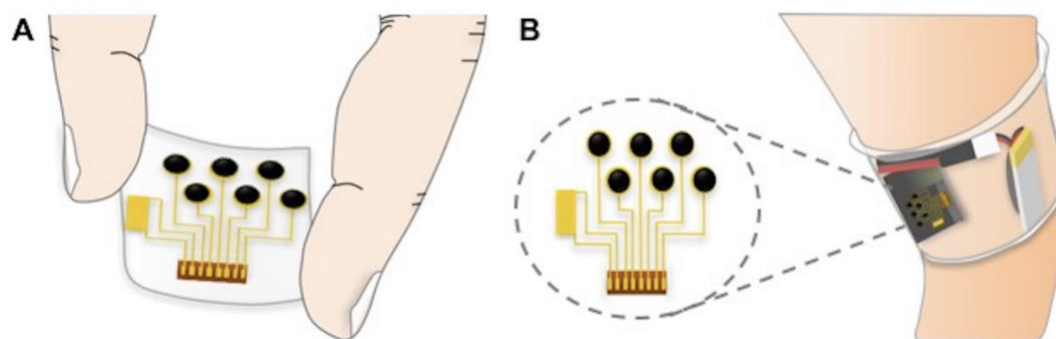


Figure 12. A) Flexible glucose sensor. B) Glucose sensor integrated into a wearable wristband for

noninvasive sensing in sweat [113].

Microsoft has collaborated with Drew Evans' group from the University of South Australia (Mawson Lakes, SA, Australia) to design hydrophilic organic electrodes that could be incorporated into flexible hydrogels, such as a contact lens [114]. In their approach, they have fabricated conductive polymeric coatings that were engineered to be biocompatible and could be grown directly on to a contact lens. The conductive polymer poly-(3,4-ethylene-dioxythiophene (PEDOT) was deposited on to the lens using oxygen plasma techniques. This lens was designed to advance the development of silicone hydrogels with technologically relevant properties, such as conductivity and pave the way for conductive hydrogel electrodes [114]. Ultimately, this lens would self-report relating optical changes to glucose concentrations. An advantage of this passive device is that no batteries or wireless connections are required to receive and transmit crucial information.

Wearable sensors have the potential to play a major role in the continuous and non-invasive monitoring of biomarkers for diabetes and other disease conditions. The interest of companies such as Google, Novartis and Microsoft suggest there is a significant market potential for new approaches to self-monitoring and disease diagnosis. Glucose biosensors are constantly evolving as per the demand and there is a need for a self-powered glucose biosensing microsystem which will eliminate the dependence of batteries as the power source, glucometers and CGM devices, thereby improving the standard of living of people suffering from diabetes.

CHAPTER 4

CHARGE PUMP CIRCUIT

Charge pump circuit

A charge pump circuit is a type of DC to DC converter that uses capacitors for energetic charge storage to raise or lower voltage [115-117]. It is a very common challenge in circuits to need to convert an available DC source to a lower or higher voltage. For AC voltages, usually a transformer is used which converts the lower voltage to higher voltages, but transformers cannot be used with a DC power source. The best approach, then, is to “chop” the low-voltage DC using an oscillator of some sort, pass the chopped AC-like waveform through a step-up transformer, and then rectify and filter it at the secondary-side output. This approach can be very successful, and enhanced versions of it are the basis for switching power supplies used to both increase (boost) and decrease (buck) the voltage between a DC source and a supply rail.

The key issue in the method mentioned above is the need for the transformer, an inductive component which is a relatively large and costly component compared to the rest of the power-conversion circuitry it supports. While some power converters prefer or even mandate a transformer due to the inherent galvanic isolation it provides, that benefit is often not needed in low-voltage circuits or localized sub-circuits [116]. A transformer-based design’s performance and cost are more suited for DC/DC converters above about 1 to 5 A output, but it is generally not an attractive solution at the low end below a few hundred mA.

To solve this problem, circuit designers have developed a topology called the charge pump, which is difficult to implement with discrete components, but is very integrated circuit (IC) friendly. The charge pump uses capacitors as the energy-storage element. In this power-conversion technique,

current (charge) is alternately switched and directed between two capacitors arranged so the circuit output is twice the input and thus functioning as a voltage-doubling boost converter. For these reasons, the charge-pump converter is also known as a switched-capacitor design.

The charge pump circuit works on the fundamental principle of physics: charge flowing back and forth in a closed circuit is not lost but instead can be transferred via switching between charge-storage elements [115-117]. In a charge-pump concept, diodes can be used to control the flow of current; in actual practice, the switches are usually switched metal–oxide–semiconductor field-effect transistors (MOSFETs), and the capacitors are external ceramic or electrolytic devices depending on the amount of capacitance needed.

Figure 13 illustrates a two-step charge-discharge cycle where capacitor C1 charges, then discharges into C2. First, the clock drives the output of inverter 1 low, so D1 is forward-biased, thus charging capacitor C1 to the supply voltage +Vdc, where D2 is off.

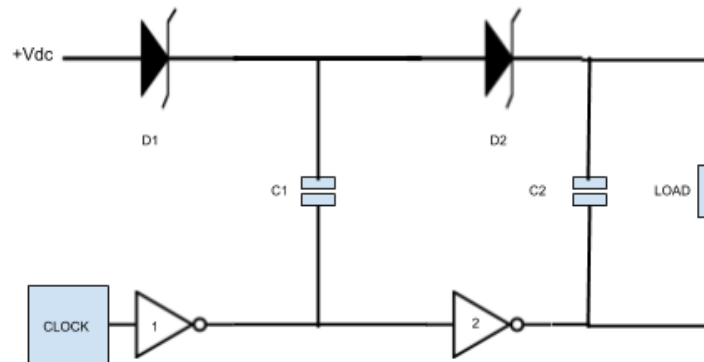


Figure 13. Two-step charge discharge cycle

Next, the clock drives the output of inverter 1 high, and the charge on C1 is now in series with +Vdc from inverter 1. As the output of inverter 2 is low, D2 becomes forward-biased and C2 charges to twice Vdc. The voltage thus seen across the load is $2 \times V_{dc}$, minus the diode forward-voltage drops and

any losses in the inverters. In practical designs using discrete components, Schottky diodes are usually used instead of conventional diodes because of their lower forward-voltage drop. However, IC-based charge pumps do not use diodes; instead, they use MOSFET switches with low on-resistance $R_{DS(ON)}$. Charge pump efficiency is high, in the range of 90 to 95% [117]. When MOSFET switches are used, the capacitor is sometimes called a “flying capacitor.” This is a designation which is a holdover from early days of electronics when a similar arrangement was used to sample a sensor voltage. The sensor output would charge a capacitor, and then the capacitor would be disconnected from the sensor and switched to a voltage-reading circuit. In effect, the capacitor would “fly” between the sensor and electronics, but there was no electrical path between the two sides. These capacitors can be small-value ceramic devices, or larger electrolytic ones, depending on the amount of current, the energy-storage needed, and the switching speed. The interplay among these parameters is also determined by the amount of output current to be charged into, and discharged from, the capacitors.

While the basic arrangement for charge pump provides voltage doubling, it is possible to instead convert a positive voltage to a negative one, or vice versa, by clever rearrangement of the components, as seen in Figure 14. Further, if more switch and capacitor segments are added, the output voltage can be triple or quadruple the input (and go even higher). For this reason, charge pumps are sometimes called voltage multipliers [116,117]. Charge pumps can double voltages, triple voltages, halve voltages, invert voltages, fractionally multiply or scale voltages and generate arbitrary voltages by quickly alternating between modes, depending on the controller and circuit topology. A simulation of an ideal charge pump can be found in Appendix A.

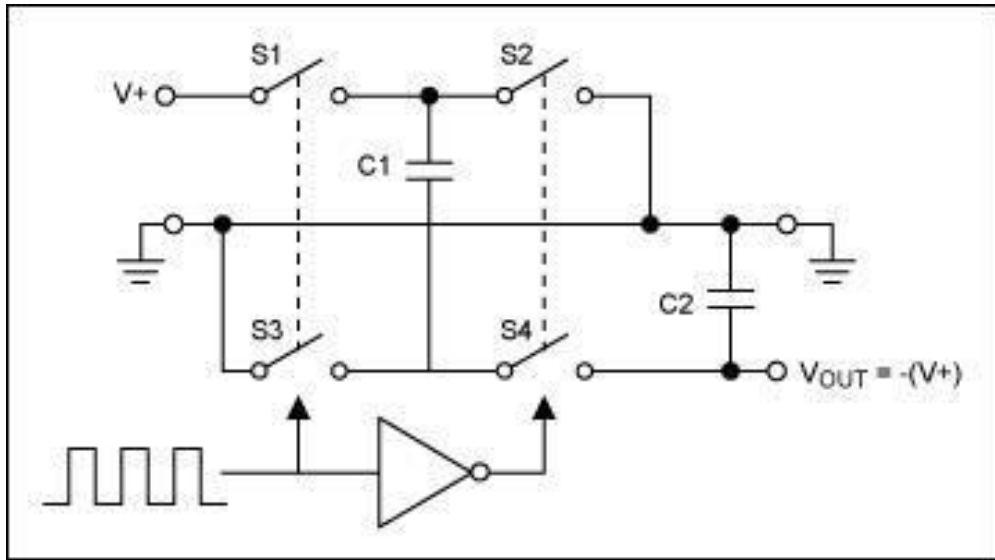


Figure 14. Reconfiguring of the basic boost-converter charge pump results in a circuit which converts a positive rail to a negative one needed for biasing or providing an offset voltage [116].

The charge-pump clock generally operates in the 10-kHz to 2-MHz range with some clocks now reaching 4 MHz. The use of a higher frequency minimizes the amount of capacitance required, as less charge needs to be stored and then dumped due to a shorter time cycle. However, there are higher losses and other negatives associated with switching at higher frequency. Some charge pumps use a clock with low or moderate accuracy and stability (e.g. 555 timer) and yield looser regulation specifications; while others use a more precise, fully controllable clock for more consistent performance and other benefits. Charge pumps are available with no need for an external clock – the user supplies it – as well as with embedded clocks for lowest parts count. The choice is made based on output regulation needs, system-level tradeoffs, bill of materials (BOM) concerns, and cost.

The pulsing nature of the higher-voltage output is smoothed by adding an output capacitor plus other components, in a standard filtering approach. Their output voltage is load dependent, where higher loads result in lower average voltages. The charge-pump regulates the pulsing by adjusting the duty cycle of the clock thus; the ratio of the two parts of the charge/discharge cycle and the output voltage

can be closely regulated. This clock adjustment is dynamically controlled by a feedback loop from the output. A well-designed charge-pump with clock control can maintain regulation to within about 1%, which is more than sufficient for most applications. Charge pumps with tighter regulation can also be available with some additional design techniques.

Charge pumps are very effective solutions for lower-current ranges of under about 100 to 500 mA, and they are best when the design needs just a small amount of current at a voltage that is not already available or locally regulated rail is needed for best performance. However, they are not a good choice at higher current levels. With some additional circuitry, switches, and more-involved architecture, they can implement a merged buck/boost regulator design with seamless transition between modes. For example, this boost/buck mode is needed where output of a Li-ion battery can range from 3.6 V when fully charged, down to 1.5 V when drained, yet the output must be maintained at 3.0 V. The combined buck boost converter starts in buck mode, then transitions to boost mode as the battery drops below the 3.0 V level; all the while, the converter output is a steady, glitch-free rail.

Charge-pump designs are available as standalone ICs which can be used to provide power rails for ICs, or just to develop low-current bias voltages for displays, among other applications. Charge-pump functionality can also be embedded within ICs or be offered as separate devices.

For example, an RS-232 IC may need only a low voltage such as 3 V or 5 V for its internal functions, but also needs a higher DC voltage of 12 V to meet the interface standard's requirements. Rather than supplying two distinct rails to the RS-232 IC, a single low-voltage rail is used, and it is boosted by an internal charge pump within the RS-232 IC to the higher voltage for the I/O interface. The same technique is used in many large-scale digital ICs, which use a low voltage internally, but need a higher voltage for their many interface and I/O pins.

They are commonly used in low-power electronics (such as mobile phones) to raise and lower voltages for different parts of the circuitry - minimizing power consumption by controlling supply

voltages carefully.

Charge pumps are used in H-bridges in high-side drivers for gate-driving high-side n-channel power MOSFETs and insulated-gate bipolar transistors (IGBTs) [115,117]. When the center of a half bridge goes low, the capacitor is charged through a diode, and this charge is used to later drive the gate of the high-side FET a few volts above the source voltage so as to switch it on. This strategy works well, provided the bridge is regularly switched and avoids the complexity of having to run a separate power supply and permits the more efficient n-channel devices to be used for both switches. This circuit (requiring the periodic switching of the high-side FET) may also be called a "bootstrap" circuit.

S882Z charge pump IC

The S-882Z Series is a charge pump IC for step-up DC-DC converter startup, which differs from conventional charge pump ICs, in that it uses fully depleted SOI (Silicon on Insulator) technology to enable ultra-low voltage operation [118]. The IC is capable of stepping up an extremely low input voltage of 0.3 V. This series enables the efficient use of very low energy levels. The stepped-up electric power is stored in a startup capacitor, and it is discharged as the startup power of the step-up DC-DC converter when the startup capacitor reaches the discharge start voltage level. Moreover, a built-in shutdown function is also provided, so that when the output voltage of the connected step-up DC-DC converter rises above a given value, the operation is stopped, thereby achieving significant power saving and battery life extension. The S-882Z Series chips come in a small SOT-23-5 package, allowing high-density mounting. The S-882Z has the following features:

- Operating input voltage 0.3 to 0.35 V
- Current consumption during operation: 0.5 mA max. (at $V_{IN} = 0.3$ V)
- Current consumption during shutdown: 0.6 μ A max. (at $V_{IN} = 0.3$ V)
- Discharge start voltage 1.8 to 2.4 V (selectable in 0.2 V steps)

- Shutdown voltage Discharge start voltage + 0.1 V (fixed)
- Oscillation frequency 350 kHz (at VIN = 0.3 V)
- External component Startup capacitor (CCPOUT), 1 unit*₁

The S-882Z has a variety of applications, where it is capable of stepping up low-voltage power supply such as solar cells and fuel cells, stepping up internal power supply voltage of RF tag, and providing intermittent power supply to an intermittently operating system. A schematic of the fabricated charge pump circuit with S-882Z IC is shown in Figure 15.

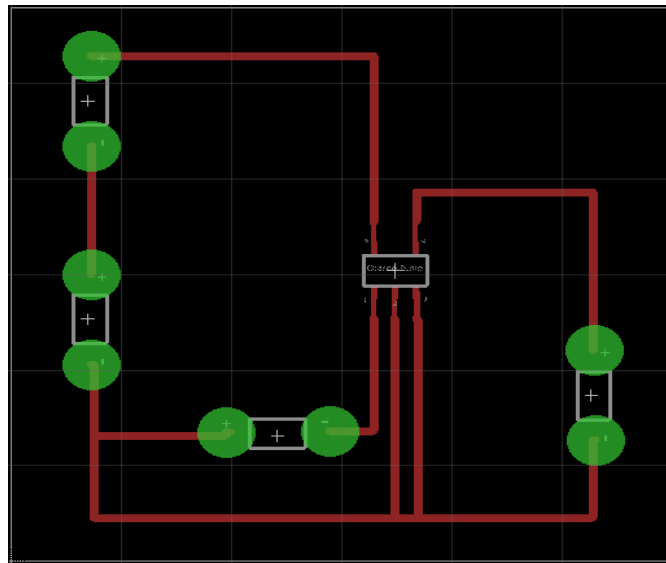


Figure 15. Schematic of charge pump circuit designed in Eagle

The S-882Z Series operate when a voltage of 0.3 V or higher is input to the VIN pin; the oscillation circuit starts operation and the CLK signal is output from the oscillation circuit as shown in Figure 16. This causes the charge pump circuit to be driven by this CLK signal, and the power of the VIN pin is converted to the stepped-up electric power in the charge pump circuit. The stepped-up electric power output from the charge pump circuit is then gradually charged to the startup capacitor (CCPOUT)

connected to the CPOUT pin and the voltage of the CPOUT pin gradually rises. When the CPOUT pin voltage (V_{CPOUT}) reaches or exceeds the discharge start voltage (V_{CPOUT1}), the output signal of the comparator (COMP1) changes from high level to low. As a result, the discharge control switch (M1), which was off, turns on. At this point, the step up electric power charged to CCPOUT is discharged from the OUT pin and the V_{CPOUT} declines to the level of the discharge stop voltage (V_{CPOUT2}). As the result of the discharge, M1 switches off, and the discharge is stopped. When the VM pin voltage (V_{VM}) reaches or exceeds the shutdown voltage (V_{OFF}), the output signal (EN^-) of the comparator (COMP2) changes from low level to high. As a result, the oscillation circuit stops operation, and the shutdown state is entered. Additionally, when V_{VM} does not reach V_{OFF} or more, the stepped-up electric power from the charge pump circuit is recharged to CCPOUT and the cycle repeats.

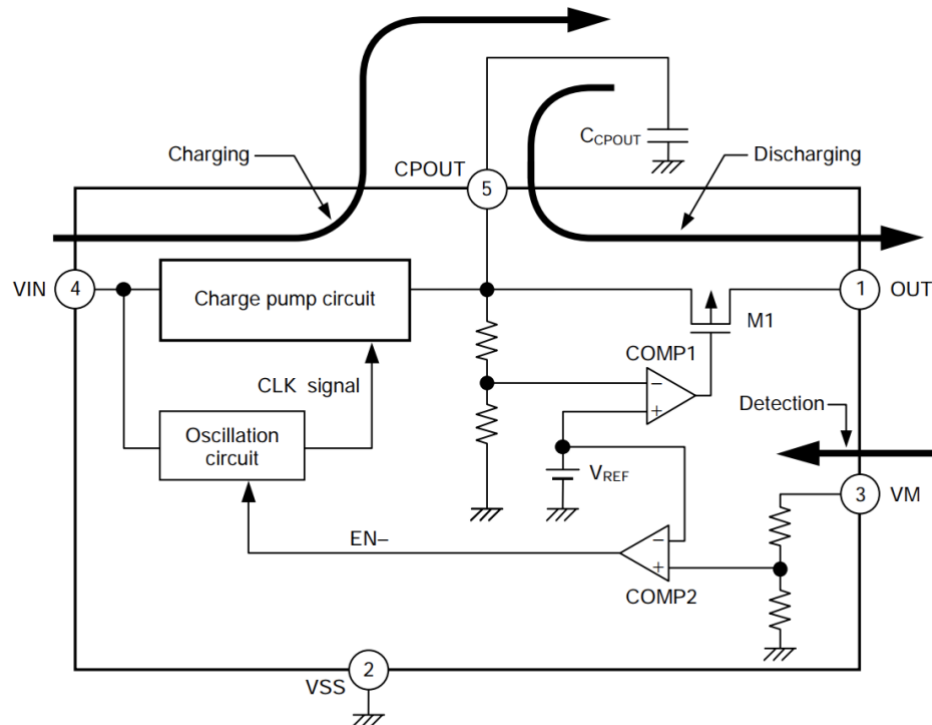


Figure 16. Internal operation of charge pump IC

CHAPTER 5

ELECTROCHEMICAL CHARACTERIZATION

Cyclic voltammetry

Cyclic Voltammetry (CV) is an electrochemical technique that measures the current that develops in an electrochemical cell under conditions where voltage is more than that predicted by the Nernst equation. A CV system consists of an electrolysis cell, a potentiostat, a current-to-voltage converter, and a data acquisition system. The electrolysis cell consists of a working electrode, counter electrode, reference electrode, and electrolytic solution. The working electrode's potential is varied linearly with time, while the reference electrode maintains a constant potential. The counter electrode conducts electricity from the signal source to the working electrode. The purpose of the electrolytic solution is to provide ions to the electrodes during oxidation and reduction. The potentiostat is an electronic device that uses a dc power source to produce a potential that can be maintained and accurately determined, while allowing small currents to be drawn into the system without changing the voltage. The current-to-voltage converter measures the resulting current, and the data acquisition system produces the resulting voltammogram.

CV is performed by cycling the potential of a working electrode and measuring the resulting current [128]. The potential of the working electrode is measured against a reference electrode which maintains a constant potential, and the resulting applied potential produces an excitation signal such as that of Figure 19. In the forward scan of Figure 19, the potential first scans negatively, starting from a greater potential (a) and ending at a lower potential (d). The potential extrema (d) is called the switching potential and is the point where the voltage is sufficient enough to have caused an oxidation or reduction of an analyte. The reverse scan occurs from (d) to (g) and is where the potential scans

positively. Figure 17 shows a typical reduction occurring from (a) to (d) and an oxidation occurring from (d) to (g). It is important to note that some analytes undergo oxidation first, in which case the potential would first scan positively. This cycle can be repeated, and the scan rate can be varied. The slope of the excitation signal gives the scan rate used.

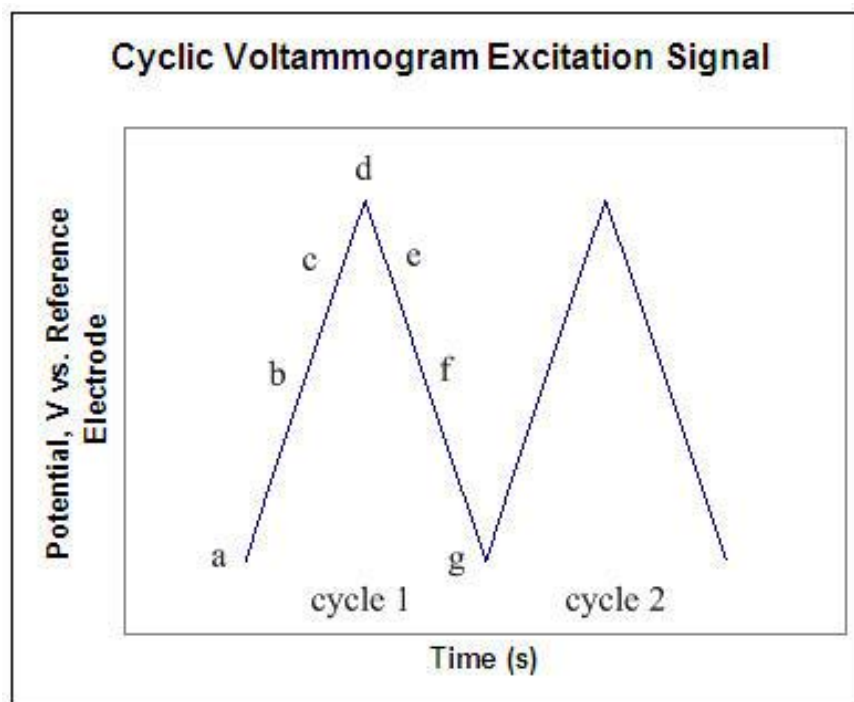
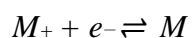


Figure 17. CV excitation signal showing a typical reduction occurring from (a) to (d) and an oxidation occurring from (d) to (g).

Figure 18 shows a cyclic voltammogram resulting from a single electron reduction and oxidation. Considering the following reversible reaction:



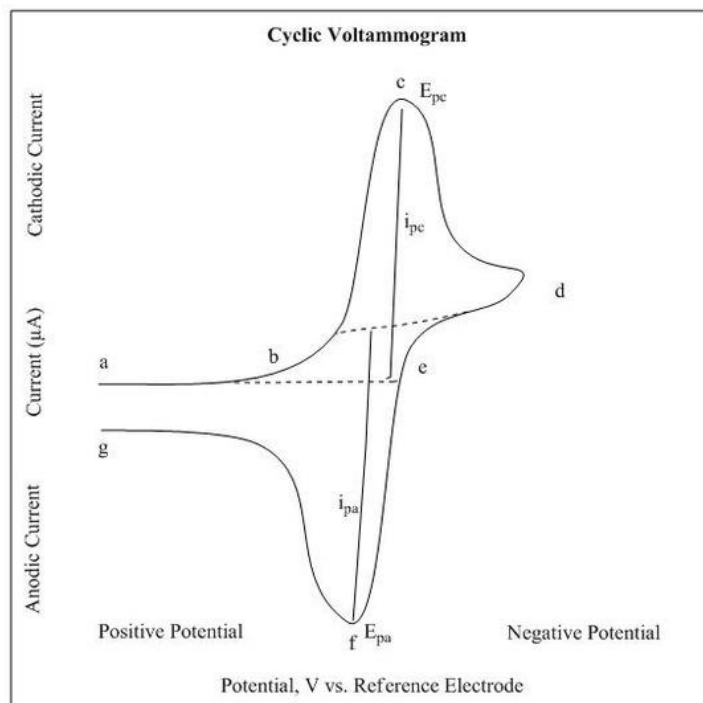


Figure 18. Voltammogram of a single electron oxidation-reduction

In an unstirred solution, mass transport of the analyte to the electrode surface occurs by diffusion alone. Fick's Law for mass transfer diffusion relates the distance from the electrode (x), time (t), and the reactant concentration (CA) to the diffusion coefficient (DA).

$$(\partial cA / \partial t) = DA (\partial^2 cA / \partial x^2) \quad (2)$$

During a reduction, current increases until it reaches a peak: when all M^+ exposed to the surface of an electrode has been reduced to M . At this point additional M^+ to be reduced can travel by diffusion alone to the surface of the electrode, and as the concentration of M increases, the distance M^+ must travel also increases [129]. During this process, the current which has peaked, begins to decline as smaller and smaller amounts of M^+ approach the electrode. It is not practical to obtain limiting currents I_{pa} and I_{pc} in a system in which the electrode has not been stirred because the currents continually decrease with time.

In a stirred solution, a Nernst diffusion layer $\sim 10^{-2}$ cm thick, lies adjacent to the electrode surface. Beyond this region is a laminar flow region, followed by a turbulent flow region that contains the bulk solution. Because diffusion is limited to the narrow Nernst diffusion region, the reacting analytes cannot diffuse into the bulk solution; therefore, Nernstian equilibrium is maintained, and diffusion-controlled currents can be obtained [129]. In this case, Fick's Law for mass transfer diffusion can be simplified to give the peak current

$$i_p = (2.69 \times 10^5) n^{3/2} S D_{A1/2} v^{1/2} C_A^* \quad (3)$$

Here, (n) is equal to the number of electrons gained in the reduction, (S) is the surface area of the working electrode in cm^2 , (D_A) is the diffusion coefficient, (v) is the sweep rate, and (CA) is the molar concentration of A in the bulk solution [128,129].

Figure 20 shows that the reduction process occurs from (a) the initial potential to (d) the switching potential. In this region, the potential is scanned negatively to cause a reduction. The resulting current is called cathodic current (i_{pc}). The corresponding peak potential occurs at (c) and is called the cathodic peak potential (E_{pc}). The E_{pc} is reached when all the substrate at the surface of the electrode has been reduced. After the switching potential has been reached (d), the potential scans positively from (d) to (g). This results in anodic current (I_{pa}) and oxidation. The peak potential at (f) is called the anodic peak potential (E_{pa}) and is reached when all the substrate at the surface of the electrode has been oxidized.

Cyclic Voltammetry can be used to study qualitative information about electrochemical processes under various conditions, such as the presence of intermediates in oxidation-reduction reactions, the reversibility of a reaction. CV can also be used to determine the electron stoichiometry of a system, the diffusion coefficient of an analyte, and the formal reduction potential, which can be used as an identification tool. In addition, because concentration is proportional to current in a

reversible, Nernstian system, concentration of an unknown solution can be determined by generating a calibration curve of current vs. concentration.

Chronoamperometry

Chronoamperometry is an electrochemical technique in which the potential of the working electrode is stepped and the resulting current from faradaic processes occurring at the electrode (caused by the potential step) is monitored as a function of time [130]. Chronoamperometry is used to study the kinetics of chemical reactions, diffusion processes, and adsorption. In this technique, a potential step is applied to the electrode and the resulting current vs. time is observed [131]. The functional relationship between current response and time is measured after applying single or double potential step to the working electrode of the electrochemical system. Limited information about the identity of the electrolyzed species can be obtained from the ratio of the peak oxidation current versus the peak reduction current. However, as with all pulsed techniques, chronoamperometry generates high charging currents, which decay exponentially with time as any resistor-capacitor (RC) circuit. The Faradaic current, which is due to electron transfer events and is most often the current component of interest decays as described in the Cottrell equation:

$$i_t = n F A C_0 D_0^{1/2} / \pi^{1/2} t^{1/2} \quad (4)$$

where,

n = stoichiometric number of electrons involved in the reaction; F = Faraday's constant (96,485 C/equivalent), A = electrode area (cm^2), C_0 = concentration of electroactive species (mol/cm^3), and D_0 = diffusion constant for electroactive species (cm^2/s).

In most electrochemical cells, this decay is much slower than the charging decay-cells with no supporting electrolyte and are notable exceptions. Most commonly a three-electrode system is

used. Since the current is integrated over relatively longer time intervals, chronoamperometry gives a better signal to noise ratio in comparison to other amperometric techniques.

Chronoamperometry experiments are most commonly either *single potential step*, in which only the current resulting from the forward step is recorded, or *double potential step*, in which the potential is returned to a final value (E_f) following a time period, usually designated as τ , at the step potential (E_s). The most useful equation in chronoamperometry is the Cottrell equation, which describes the observed current (planar electrode) at any time following a large forward potential step in a reversible redox reaction (or to large overpotential) as a function of $t^{-1/2}$. The current due to double layer charging also contributes to the total current seen following a potential step. By nature, however, this capacitive current, i_c that decays as a function of $1/t$ and is only significant during the initial period (generally a few ms) following the step. It can be easily recorded by performing the experiment in a cell containing only electrolyte and digitally subtracted. Usually it can be avoided altogether by only considering $i-t$ data taken during the last 90% of the step time.

Chronoamperometry lends itself well to the accurate measurement of electrode area (A) by use of a well-defined redox couple (known n , C_0 , and D_0). With a known electrode area, measurement of either n or D_0 for an electroactive species is easily accomplished. The double potential step method is often applied in the measurement of rate constants for chemical reactions (including product adsorption) occurring following the forward potential step.

Current-Voltage characteristics

The Current-Voltage (I-V) characteristic curves of an electrical device or component are a set of graphical curves used to define its operation within an electrical circuit. As its name suggests, I-V characteristic curves show the relationship between the current flowing through an electronic device and the applied voltage across its terminals. I-V characteristic curves are generally used as a tool to determine and understand the basic parameters of a component or device and which can also be used to mathematically model its behavior within an electronic circuit as with most electronic devices, however there are an infinite number of I-V characteristic curves representing the various inputs or parameters and as such we can display a family or group of curves on the same graph to represent the various values. For example, the “current-voltage characteristics” of a bipolar transistor can be shown with various amounts of base drive or the I-V characteristic curves of a diode operating in both its forward and reverse regions.

The static current–voltage characteristics of a component or device need not be a straight line, though take for example the characteristics of a fixed value resistor; it is expected to be reasonably straight and constant within certain ranges of current, voltage and power as it is a linear or ohmic device. There are, however, other resistive elements such as light dependent resistors (LDR’s), thermistors, varistor’s, and even the light bulb, whose I-V characteristic curves are not straight or linear lines but instead are curved or shaped and are therefore called non-linear devices because their resistances are non-linear resistances. If the electrical supply voltage, V , applied to the terminals of the resistive element R was varied, and the resulting current, I , was measured, this current would be characterized as: $I = V/R$, being one of Ohm’s Law equations. From Ohm’s Law, the voltage across the resistor increases as does the current flowing through it. Thereby, it would be possible to construct a graph to show the relationship between the voltage and current as shown with the graph representing

the volt-ampere characteristics (i-v characteristic curves) of the resistive element. Consider the circuit shown in Figure 19.

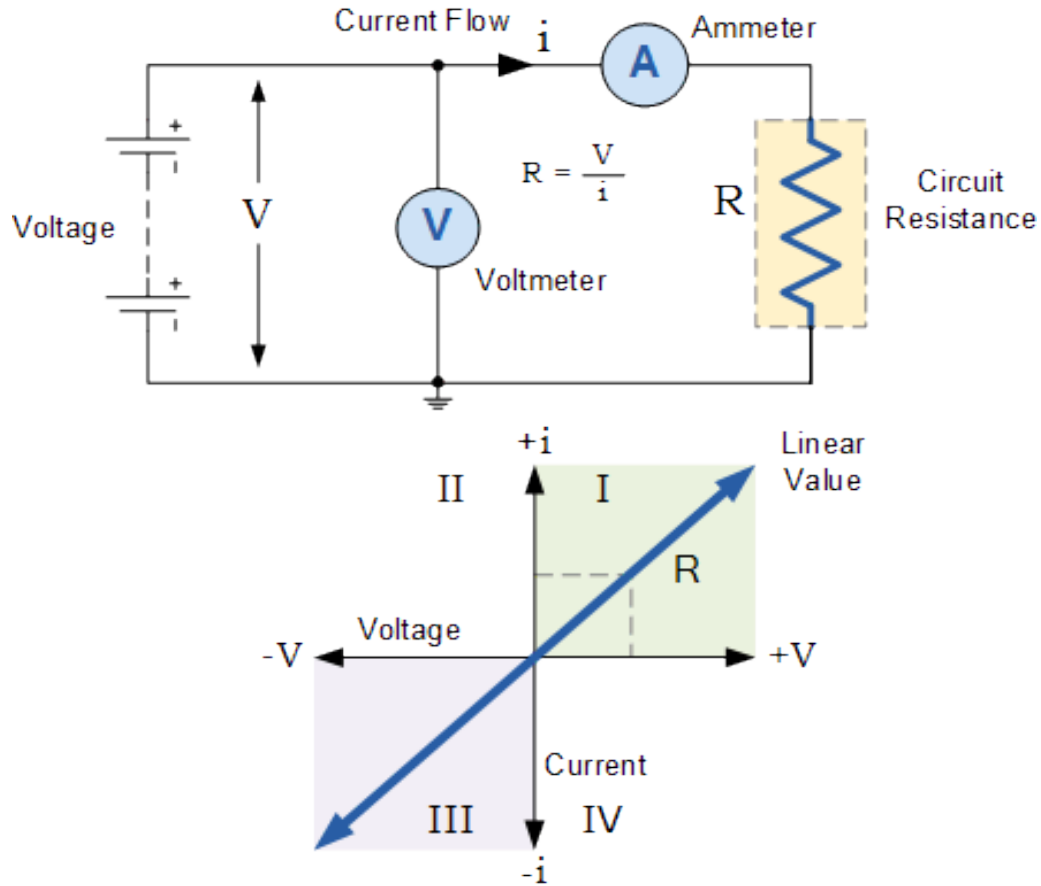


Figure 19. Resistor i-v characteristic curve

The above i-v characteristic curve defines the resistive element. If any voltage value is applied to the resistive element, the resulting current is directly obtainable from the I-V characteristics. As a result, the power dissipated (or generated) by the resistive element can also be determined from the I-V curve. If the voltage and current are positive in nature, then the I-V characteristic curves will be positive in quadrant I. If the voltage and the current are negative in nature, then the curve will be displayed in quadrant III as shown. In a pure resistance condition, the relationship between voltage

and current is linear and constant at a constant temperature, such that the current (i) is proportional to the potential difference V times the constant of proportionality $1/R$ giving $i = (1/R) \times V$. Then the current through the resistor is a function of the applied voltage and can be demonstrated visually using an I-V characteristics curve.

In this example, the current I , against the potential difference V , is a straight line with constant slope $1/R$ as the relation is linear and ohmic. However, practical resistors may exhibit non-linear behavior under certain conditions as for example, when exposed to high temperatures. Many electronic components and devices have non-linear characteristics, that is their V/I ratio is not constant.

In the case of a biofuel cell, the I-V characteristics follow the same pattern as for an ideal electronic circuit component, i.e. it follows Ohm's law. When we look into any electrochemical system, however more losses like kinetic loss (charge-transfer), activation loss, mass transport loss (concentration) and ohmic loss (ion and electron transport) are introduced. These losses affect the I-V characteristics curve because the V/I ratio is not always constant. This can be seen in the simulations performed in Appendix B.

pH and temperature characteristics

pH is a scale used to specify the acidity or basicity of a water-based solution. Acidic solutions have a lower pH, while basic solutions have a higher pH. At room temperature (25°C or 77°F), pure water is neither acidic nor basic and has a pH of 7. The pH scale is logarithmic and inversely indicates the concentration of hydrogen ions in the solution (a lower pH indicates a higher concentration of hydrogen ions). This is because the formula used to calculate pH approximates the negative of the base 10 logarithm of the molar concentration $[a]$ of hydrogen ions in the solution. More precisely, pH is the negative of the base 10 logarithm of the activity of the hydrogen ion. The neutral value of the

pH depends on the temperature, being lower than 7 if the temperature increases. The pH value can be less than 0 for very strong acids, or greater than 14 for very strong bases.

The glucose biosensor in this work was developed to be implanted and work in the human body. The normal pH of human blood lies between 7.35 – 7.48. So it is important to check the characteristics of the developed glucose biosensor at those pH levels as well as at both extreme ends of the scale to verify whether it will work in the physiological conditions.

The temperature characteristic study includes observation of the sensor behavior at different temperatures. Usually the sensor characteristics are observed by keeping all other parameters constant and just varying the temperature and measuring the current and voltage of the sensor. In this work, the biosensor was developed to work at physiological conditions. The average normal body temperature is generally accepted as 98.6°F (37°C). Some studies have shown that the "normal" body temperature can have a wide range, from 97°F (36.1°C) to 99°F (37.2°C). A temperature over 100.4°F (38°C) most often means you have a fever caused by an infection or illness. For the sensor data to be robust and reliable, it is necessary to observe its behavior at different temperatures and make sure that it doesn't give false results at both low and high extremities. To become an implantable biosensor, the sensor has to perform optimally between the temperature of 97°F (36.1°C) to 100.4°F (38°C).

CHAPTER 6

MATERIALS AND METHODS

Materials

The gas diffusion electrodes (GDE) obtained from the Fuel Cell Store (College Station, TX, USA). Gold microwire ($\phi = 250 \mu\text{m}$), isopropyl alcohol (IPA), D (+) glucose, potassium phosphate monobasic, glycol-chitosan, bilirubin oxidase (BOD) were obtained from Sigma-Aldrich. Buckypaper, a compressed network of multi-walled carbon nanotubes (MWCNTs) was purchased from Nanotech Labs (Yadkinville, NC). The platinizing solution was purchased from YSI Inc. (Yellow Springs, USA). All the solutions were prepared with $18.2 \text{ M}\Omega \text{ cm}$ Milli-Q water. The Platinum counter electrode and Ag/AgCl reference electrode were obtained from BASI Inc. PalmSense4 was used to perform the characterization study of the biofuel cell. The S882Z charge pump IC was obtained from Seiko electronics. The developed android application was installed on one Google Pixel 2XL mobile phone for sensing.

Electrode fabrication

A 3 cm long ($\phi = 250 \mu\text{m}$) gold microwire was used as the electrode material for fabrication of the anode. The gold microwire was folded in half and twisted. The electrode was then cleaned with IPA for 5 minutes and dried with nitrogen gas to remove any impurities from the surface. The gold microwire was coated with colloidal platinum using a three-electrode configuration consisting of the clean twisted gold microwire working electrode, platinum counter electrode, and Ag/AgCl reference electrode. These electrodes were then immersed in a platinizing solution, and colloidal platinum was electrodeposited on the gold microwire surface at an applied potential of -225 mV vs. Ag/AgCl for

1500 s. The electrode was then washed with DI water and dried at 260 °C for 5 minutes, followed by cooling in ambient air.

The cathode was prepared using a gas diffusion electrode (GDE) with a platinum catalyst. The GDE was first cut into a size of 0.5 cm X 0.3 cm. Then a tungsten wire was attached to the edge of the GDE electrode using polyamide to have an external connection point. This enabled easy handling and connections to the measurement devices. The electrode with the wire was then left in the desiccator to dry for 24 hrs. The electrode was then washed with IPA and then with 10 mM PBS for 10 minutes each. Figure. 20 shows the fabricated anode and cathode.

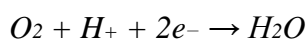


Figure 20. Fabricated Au-co-Pt anode on left and GDE cathode on the right.

The oxidation of glucose occurs in the presence of colloidal platinum (Au-co-Pt), a non-enzymatic catalyst, to result in the production of adsorbed hydrogen [132]. Au-co-Pt anode acts as the dehydrogenation site wherein the Au surface facilitates the regeneration of colloidal Pt from poisoning due to adsorbed intermediates from the oxidation of glucose. The reaction mechanism is provided below:



where glucose is oxidized to produce gluconolactone and release electrons. At the cathode, oxygen in the solution moves across the hydrophobic gas diffusion layer of the GDE towards the platinum catalytic layer. On the opposite side of the GDE, hydrogen ions released from the oxidation of glucose move across a hydrophilic layer towards the catalytic layer [133-140]. At the catalytic layer gas and liquid reactants can interact. In the presence of the platinum catalyst, oxygen is reduced with the free electrons oxidized from glucose and bonds with hydrogen to form H₂O as a byproduct. The reaction mechanism is described by the chemical equation below:



The electrochemical measurements were performed using Palmsense4 electrochemical workstation using a three-electrode configuration at room temperature.

Charge pump circuit fabrication

The anode and cathode were assembled together to realize a biofuel cell. The electrical voltage produced by this single biofuel cell was supplied as the input voltage for the charge pump integrated circuit (IC). The circuit was etched on a copper coated PCB using AZ440K developer and ferric chloride etchant. The circuit design was first printed on a transparency sheet and then placed on the photosensitive PCB surface. The PCB was then kept under ultraviolet (UV) light for 8 seconds. The PCB was then washed with a 3:1 AZ400K solution till the time the etched pattern appears. The PCB was then placed into a ferric chloride bath and etched until only the printed circuit remains. The PCB was then wiped with a concentrated AZ400K solution and then dipped in DI water followed by air drying. The S882Z charge pump IC, LED and capacitor were soldered on the etched PCB. The S882Z IC starts operation at 280 mV. The nominal input voltage as low as 300 mV provided by the biofuel cell was excited up to 1.8 V via the capacitor functioning as the transducing element. The

charging/discharging frequency of the capacitor is correlated to the changes in glucose concentration. By monitoring the capacitor frequency, the exact concentration of the analyte can be deduced.

The analyte concentration data that was retrieved from the charge pump circuit in the form of a sawtooth waveform frequency as seen in Figure 21 is the result of the capacitor charge/ discharge of the capacitor. This capacitor output is used to drive the LED circuit turning the LED ON and generating a blinking frequency that correlates to the capacitor charge/ discharge frequency.

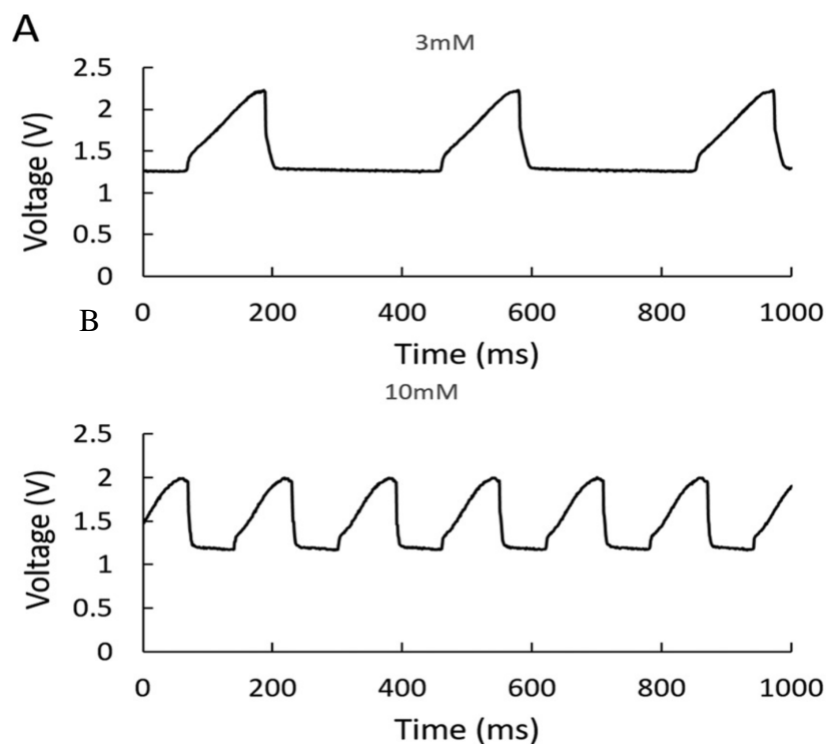


Figure 21. Sawtooth frequency obtained from charge pump circuit in A) 3mM glucose concentration B) 10mM glucose concentration

This sawtooth waveform is the charging and discharging frequency of the capacitor in the charge pump circuit which is directly proportional to the concentration. If the concentration of analyte

increases, the charging and discharging frequency of the capacitor also increases. As seen in Figure 20A, for a glucose concentration of 3 mM, the number of peaks obtained in a window of 1000 ms are 3. This is because there is less glucose available for the entire surface area of anode to oxidize, hence electrons are released which in turn charges the capacitor in the charge pump circuit slowly. In the case of Figure 20B, 10mM glucose concentration, more raw glucose is available as fuel for the anode to oxidize, resulting in more electrons being released. This charges the capacitor faster; therefore, we have a higher number of peaks. In this way, the change in concentration can be correlated with a change in capacitor frequency.

ESP8266 microcontroller

Traditional oscilloscopes display the change of an electrical signal over time, with voltage and time as the y- and x-axes, respectively on a calibrated scale. The waveform can then be analyzed for properties such as amplitude frequency, rise time, time interval, distortion among other parameters [119]. In the development of this self-powered glucose biosensor, an oscilloscope is needed to monitor the charging/ discharging frequency of the capacitor in the charge pump circuit which in turn correlates to the concentration of glucose employed as fuel in the biofuel cell [120-124].

The current limitations of the conventional and handheld oscilloscopes are price, size, and accessibility [119, 125-126]. Additionally, handheld oscilloscopes have features than their conventional counterparts. In order to monitor sensed glucose readings remotely, an ESP8266 microcontroller is coded to function as an electronic oscilloscope (e-oscilloscope). The complete e-oscilloscope costs less than \$10 and enables data to be accessed either by connecting it to a computer or through a server. As the e-oscilloscope is programmable, it can be easily customized by programming it to extract the data from the biosensing system, process the frequency readings and correlate the frequency readings to glucose concentrations.



Figure 22 . An ESP8266 Wi-Fi module

The ESP8266 Wi-Fi Module is a self-contained SOC with an integrated TCP/IP protocol stack that can give any microcontroller access to a Wi-Fi network as seen in Figure 22. The ESP8266 is capable of either hosting an application or offloading all Wi-Fi networking functions from another application processor. The ESP8266 module is an extremely cost-effective board that can be easily configured to meet the desired needs. It has the capability of acting as a standalone device. It is coded using Arduino IDE software which is a cross-platform application (for Windows, macOS, Linux) that is written in Java. The Arduino IDE employs the program *avrdude* to convert the executable code into a text file in hexadecimal encoding that is loaded into the board by a loader program in the board's firmware. Sample code is shown in Figure 23 below. The code converts the analog values received by ESP8266 from the charge pump circuit and plots it by converting it to a digital value.

```
int sensor =A0;

void setup ( )

{
```

```
Serial.begin (115200);

delay (10);

pinMode (sensor, INPUT);

Serial.println ("E-oscilloscope");

}

uint32_t x = 0;

void loop ( )

{

int f_value = analogRead (sensor);

delay (2000);

Serial.println (f_value);

}
```

Figure 23. Sample code for ESP8266 programming which takes the analog values coming from charge pump and plots it versus time.

Android application and MATLAB

Android is a mobile operating system based on a modified version of the Linux kernel and other open source software, designed primarily for touchscreen mobile devices such as smartphones and tablets. Android is developed by a consortium of developers known as the Open Handset Alliance, with the main contributor and commercial marketer being Google [127].

The core Android source code is known as Android Open Source Project (AOSP), which is primarily licensed under the Apache License. This has allowed variants of Android to be developed on a range of other electronics, such as game consoles, digital cameras, personal computers (PCs)

and others, each with a specialized user interface. Some well-known derivatives include the Android TV for televisions and Wear OS for wearables, both developed by Google.

Android's source code has been used as the basis of different ecosystems, most notably that of Google, which is associated with a suite of proprietary software called Google Mobile Services (GMS) [127] that frequently comes pre-installed on said devices. This includes core apps such as Gmail, the digital distribution platform Google Play, the associated Google Play Services development platform, and apps such as the Google Chrome web browser. These apps are licensed by manufacturers of Android devices certified under standards imposed by Google. Other competing Android ecosystems include Amazon.com's Fire OS or LineageOS. Software distribution is generally offered through proprietary application stores like the Google Play Store or the Samsung Galaxy Store, and open source platforms like Aptoide, or F-Droid, which use software packages in the application package (APK) format.

Applications ("apps"), which extend the functionality of devices, are written using the Android software development kit (SDK) and, often, the Java programming language. Java may be combined with C/C++ together with a choice of non-default runtimes that allow better C++ support. The SDK includes a comprehensive set of development tools, including a debugger, software libraries, a handset emulator based on QEMU, documentation, sample code, and tutorials. Initially, Google's supported integrated development environment (IDE) was Eclipse using the Android Development Tools (ADT) plugin. In December 2014, Google released Android Studio, based on IntelliJ IDEA as its primary IDE for Android application development.

Due to the open nature of Android, a number of third-party application marketplaces also exist for Android, either to provide a substitute for devices that are not allowed to ship with the Google Play Store, provide applications that cannot be offered on the Google Play Store due to policy violations, or for other reasons. Examples of these third-party stores have included the Amazon

Appstore, GetJar, and SlideMe. F-Droid, another alternative marketplace, seeks to only provide applications that are distributed under free and open source licenses. This allows for any person with the source code to edit the code and use it according to their need.

MATLAB (matrix laboratory) is a multi-paradigm numerical computing environment and proprietary programming language developed by MathWorks. MATLAB allows matrix manipulations, plotting of functions and data, implementation of algorithms, creation of user interfaces, and interfacing with programs written in other languages. Although MATLAB is intended primarily for numerical computing, an optional toolbox uses the MuPAD symbolic engine allowing access to symbolic computing abilities.

CHAPTER 7

RESULTS AND DISCUSSION

The non-enzymatic biofuel cell was constructed from Au-co-Pt anode and GDE cathode, as illustrated in Figure 24.

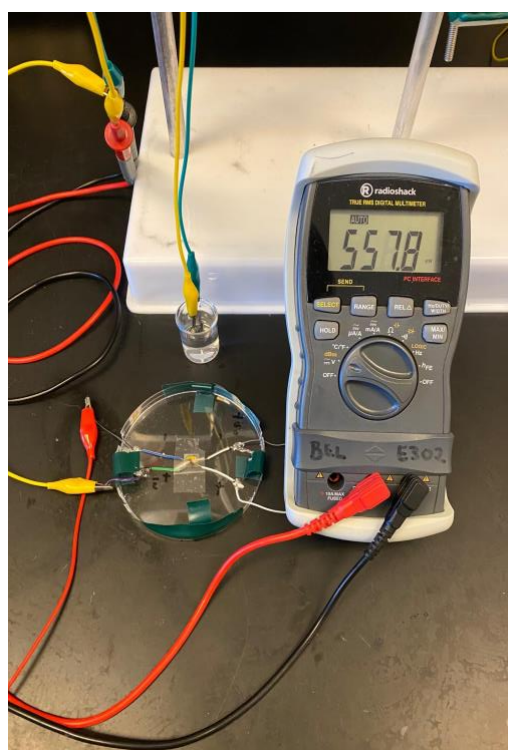


Figure 24. Assembled biofuel cell setup with voltage measurement.

The oxidation of glucose to gluconolactone by the colloidal platinum (Pt) was observed to occur at an open circuit potential of 500 mV as observed from Figure 26, where the Pt-OH surface species form and oxidize the poisoning intermediates derived from the electro-absorption of glucose, thereby exposing free Pt active sites for the direct oxidation of glucose. This further indicates the

strong catalysis of colloidal Pt on the direct oxidation of glucose [141]. In comparison, the bare braided gold microwire exhibited no electrocatalytic activity in response to glucose, and this is attributed to the fact that gold microwire surfaces do not facilitate hydrogen adsorption [142]. Therefore, the modification of colloidal Pt on the surface of gold microwire significantly improved the electrocatalytic activity towards the oxidation of glucose. The SEM image of the bare and platinum coated gold electrode is shown in Figure 25 below.

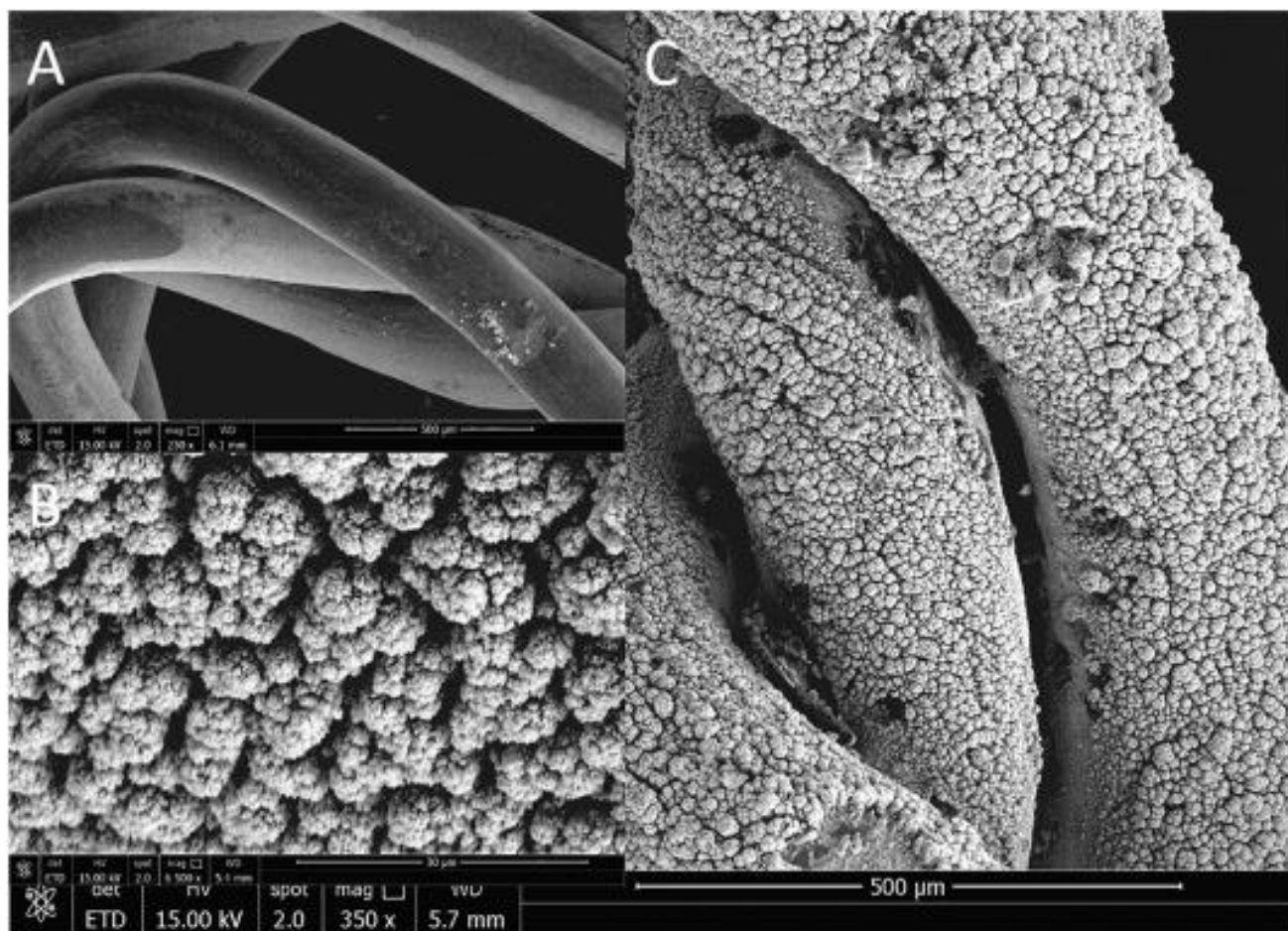


Figure 25. Scanning electron microscopy (SEM) images of (A) Braided Au microwire, (B) high-resolution SEM image of Au-co-Pt abiotic anode and (C) Au-co-Pt abiotic anode.

Electrodeposition of colloidal Pt on braided gold microwire takes advantage of the electrocatalytic activity and high surface area of colloidal Pt and provides a straightforward way to prepare nanostructured-based electrodes. The electrons generated from the oxidation reaction travel through the external circuitry whilst the cations travel through the electrolyte containing glucose and recombine at the cathode to reduce molecular oxygen to water, thereby producing a stable electrical current.

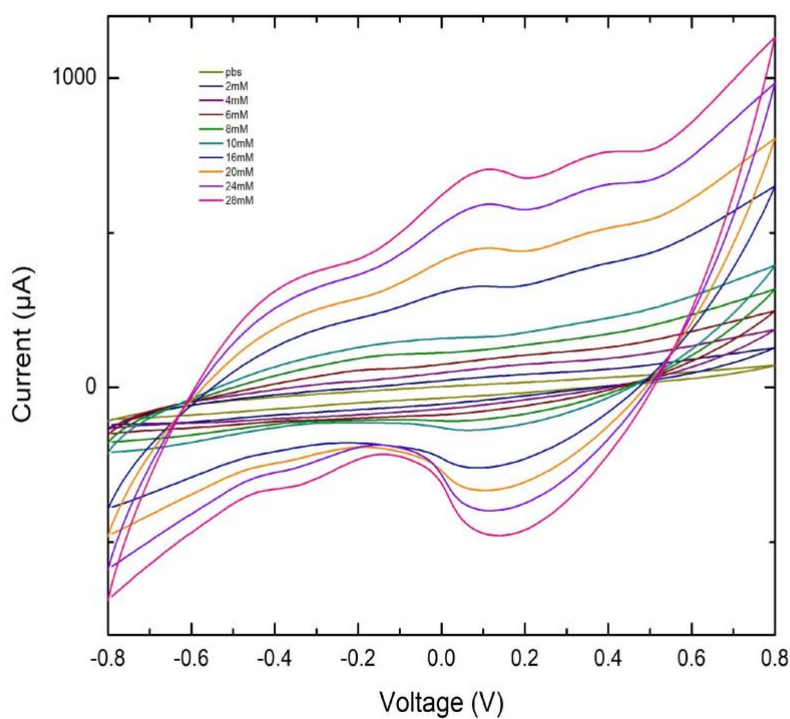


Figure 26. Cyclic voltammetry performed on the Au-co-Pt showing linear increase in current with increase in glucose concentration.

To further evaluate the electrocatalytic activity of the anode, cyclic voltammetry (CV) was performed on the Au-co-Pt anode under different glucose concentration levels. According to the

measurements acquired in Figure 26, the intensity in the reaction peak increased in the presence of increasing glucose concentrations from 1 mM to 28 mM at an oxidation onset potential of 0.5 V vs. Ag/AgCl. This showed that oxidation of glucose was happening at the anode resulting in the generation of electrons which then flows through the external circuit to the cathode forming water.

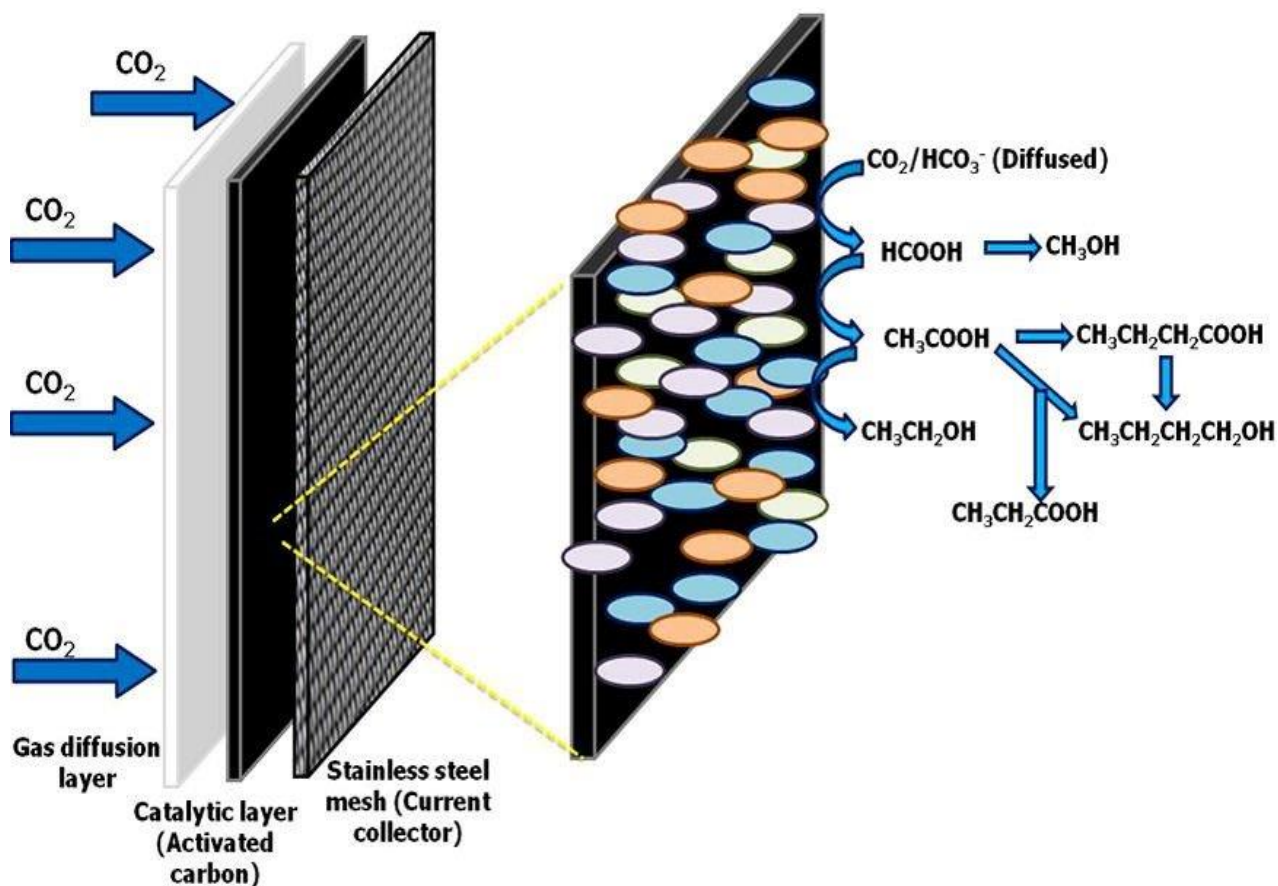


Figure 27. Internal layers of GDE electrode

To evaluate the electrocatalytic activity of the GDE cathode, cyclic voltammetry (CV) curves were measured under different levels of purged oxygen as shown in Figure 28. It was observed that the cathodic current increased with an increase in the amount of purged oxygen.

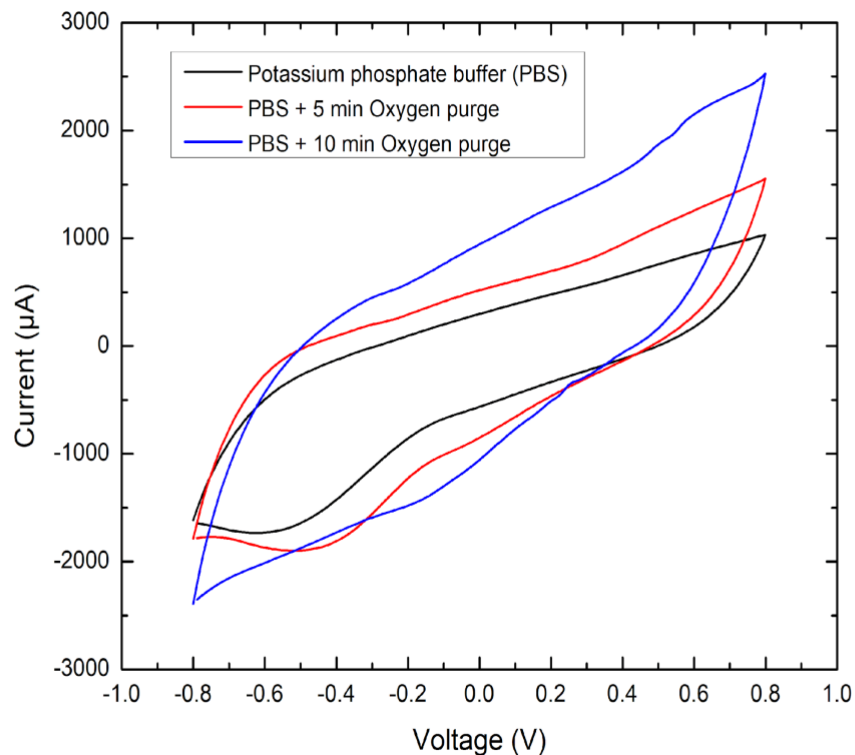


Figure 28. Cyclic voltammetry performed on the GDE cathode showing linear increase in current with increase in purged oxygen.

IV test was performed on the non-enzymatic biofuel cell to determine the power characteristics of the biofuel cell (BFC). Voltage and current measurements were taken at different resistances ranging from 1K Ohm to 1M Ohm. The resistance at which the BFC is most efficient to generate maximum power can be obtained from the IV curves. A circuit can be designed to have the same internal resistance, thus getting the most power output from the BFC. The IV and power curves for the non-enzymatic glucose biofuel cell are depicted in Figures 29 and 30. The non-enzymatic glucose biofuel cell produced maximum open circuit voltage of 0.54 V and delivered and the highest short circuit current density of 1.6 mA/cm² with a peak power density of 0.226 mW/cm² at a

concentration of 1 M glucose and an open circuit voltage of 0.38 V and delivered a short circuit current density of 0.225 mA/cm² with a peak power density of 0.022 mW/cm² at a concentration of 5mM glucose.

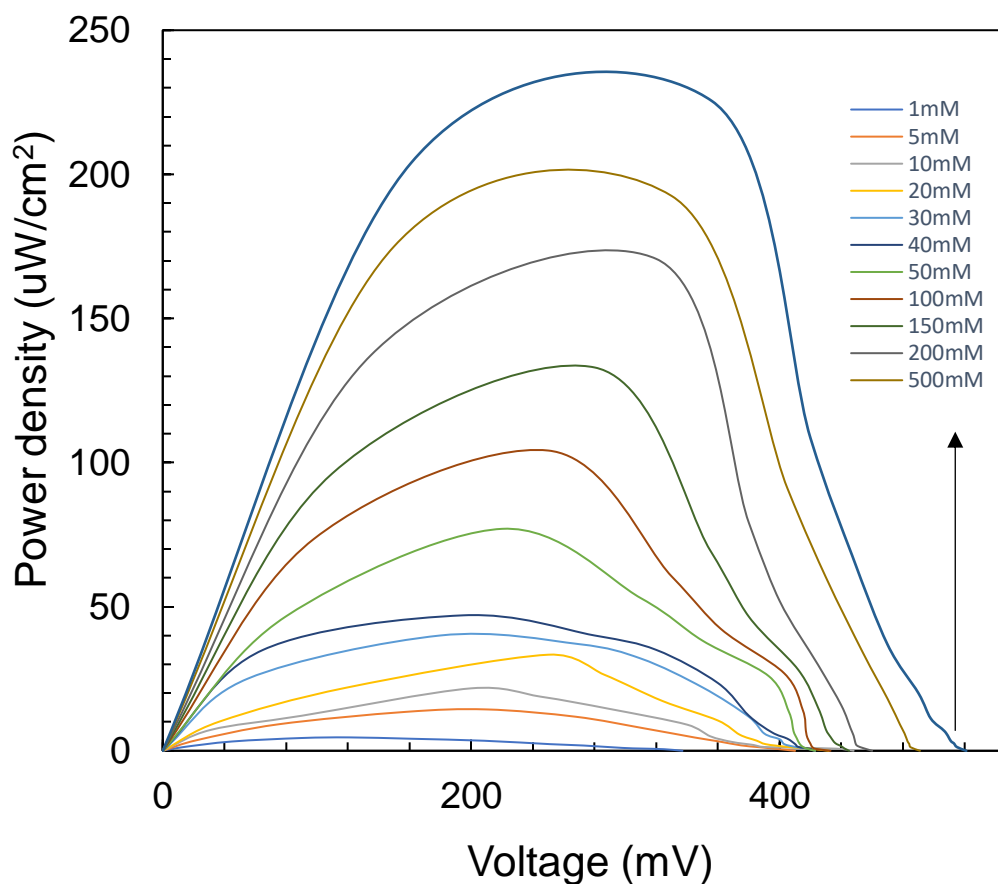


Figure 29. Polarization curve obtained from the non-enzymatic biofuel cell from glucose concentration of 1mM to 1M.

Furthermore, the peak power was observed to be directly proportional to glucose concentration as shown in Figure 29. further depicting the behavior of the oxidation reaction of an adsorbed glucose layer upon the formation of the hydrogen adsorption layer. These results suggested

that the non-enzymatic cell exhibited a linear peak power-concentration relationship at the concentration ranging from 1mM to 50 mM with a linear coefficient of 0.991 as shown in Figure 31.

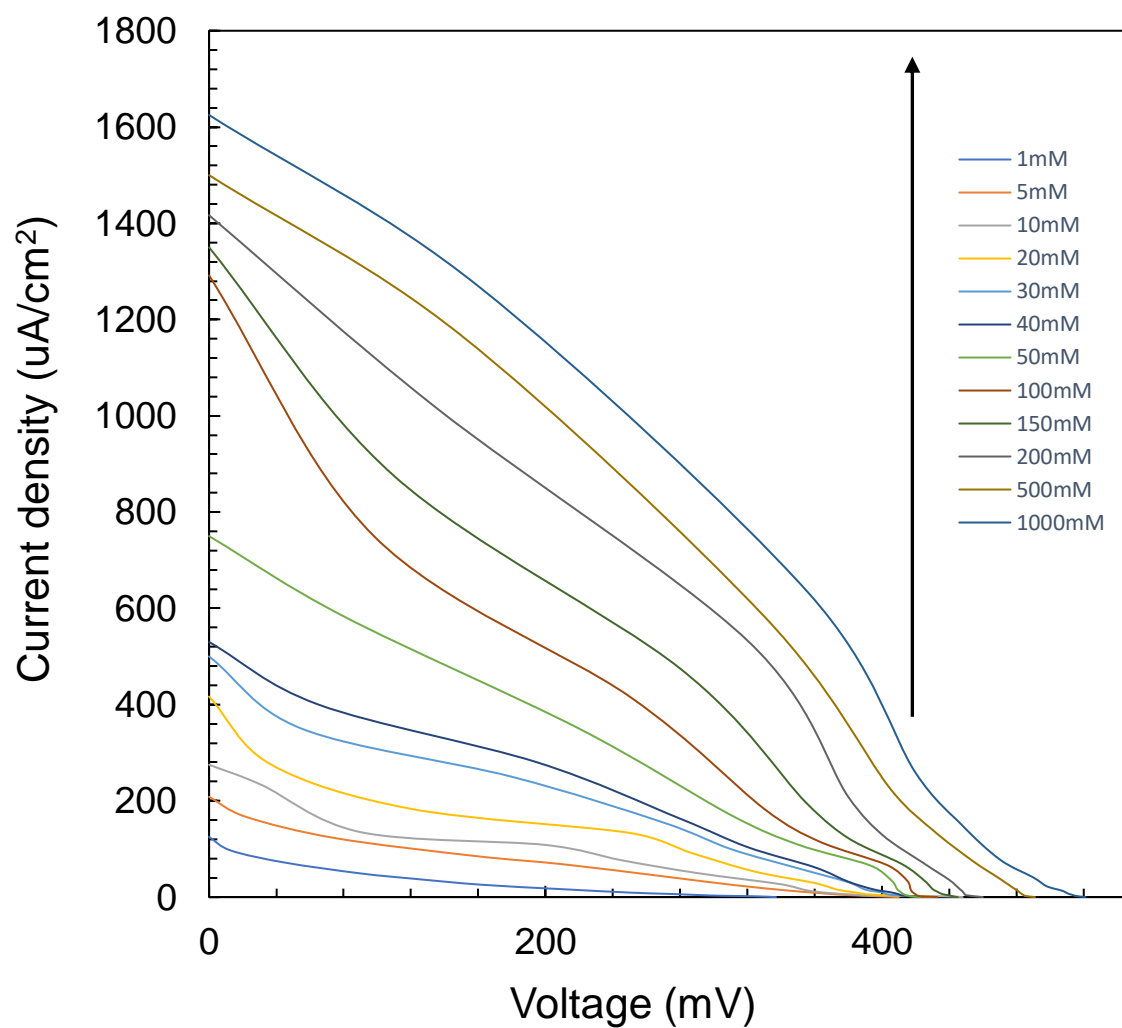


Figure 30. Power curve obtained from the non-enzymatic biofuel cell from glucose concentration of 1mM to 1M.

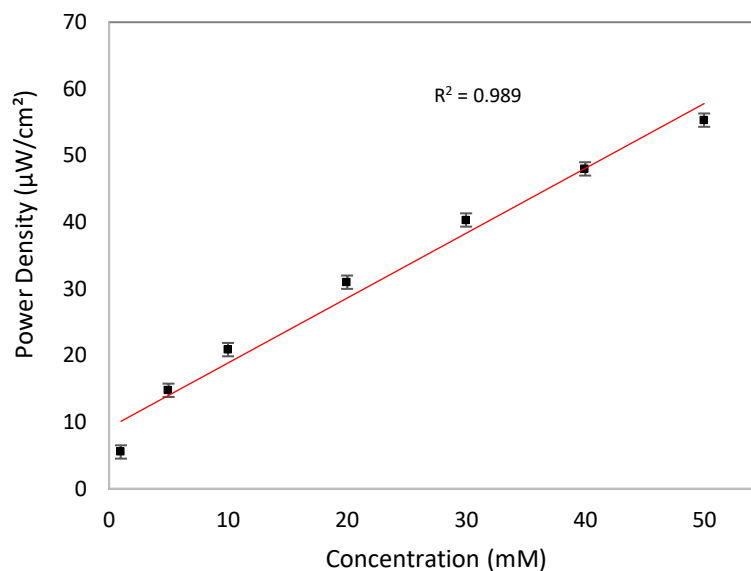


Figure 31. Power-concentration curve from 1mM to 50mM glucose. Error bars = \pm standard deviation of triplicate measurements.

The non-enzymatic glucose biofuel cell was examined under different temperatures and pH conditions in order to obtain the optimal operating conditions. The power output of the non-enzymatic glucose biofuel cell was measured at each point under no load condition. The output of the non-enzymatic glucose biofuel cell was directly connected to a multimeter to measure voltage and current. For evaluating the performance of the non-enzymatic biofuel cell at different temperatures, power output was measured in a standard glucose solution (5 mM, pH 7.4) as the temperature was increased from 20 °C - 50 °C by an increment of 5 °C. Similarly, for testing the performance under different pH from 4.7 to 10, the temperature of the 5 mM standard glucose solution was maintained at 37 °C. As shown in Figure 32 and Figure 33, the non-enzymatic biofuel cell exhibited an optimal performance at a neutral pH of 7.0 and showed an increase in power output with an increase in temperature.

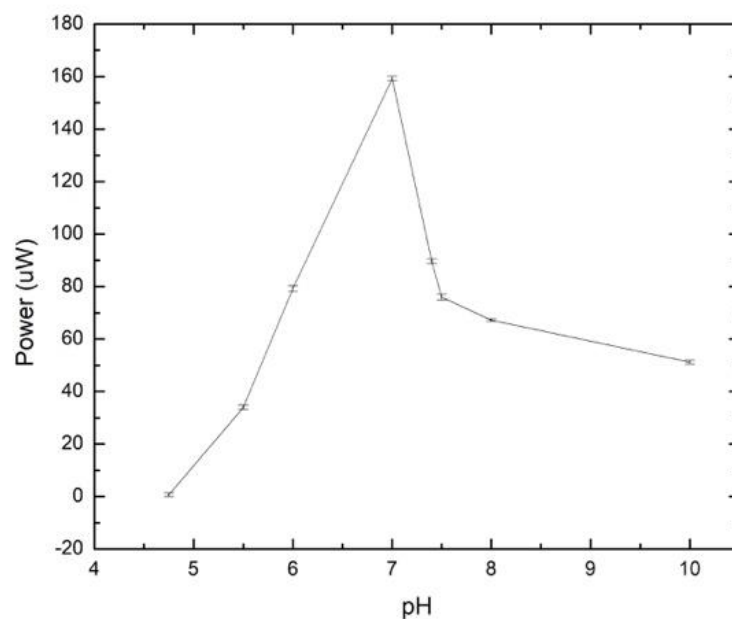


Figure 32. Effect of pH on the frequency of the non-enzymatic glucose biosensing system operating in 5 mM glucose at 37 °C.

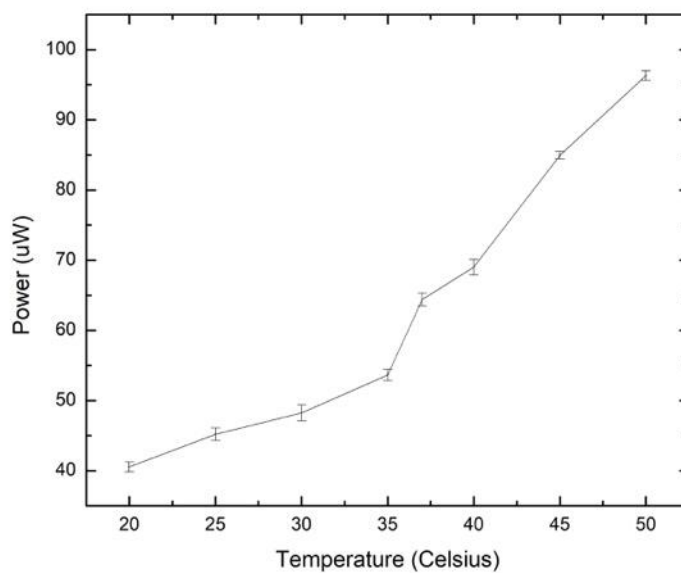


Figure 33. Effect of temperature on the frequency of the non-enzymatic glucose biosensing system operating on 5 mM glucose at a pH of 7.4.

Glucose sensing application

For the amperometry sensing application, the Au-co-Pt electrode was evaluated by measuring current response at a fixed potential with sequential addition of the glucose analyte. Figure 34 displays the amperometry response of the Au-co-Pt electrode to successive addition of 2 mM glucose in a 0.1 M PBS solution after every 50 seconds at a fixed potential of 0.5 V.

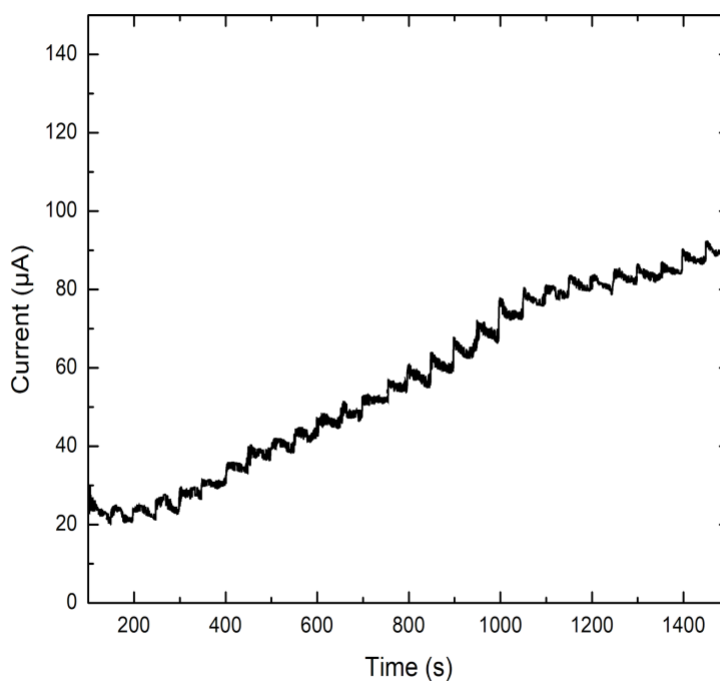


Figure 34. Amperometry response of the Au-co-Pt electrode to successive addition of 2 mM glucose in 0.1 M PBS solution after every 50 seconds interval.

As expected, the bare braided gold microwire electrode exhibited no response to the addition of glucose (not shown). In contrast, the Au-co-Pt electrode showed an enhanced linear response to the changes of glucose concentration, producing steady-state oxidation current signals as illustrated in Figure 32. The Au-co-Pt electrode gives a linear dependence with a correlation coefficient of

0.9953 in the glucose concentration range of 2 mM to 50 mM with a sensitivity of $0.616 \mu\text{A mM}^{-1}$, as depicted in Figure 35, which was in agreement with previously reported work [154-163].

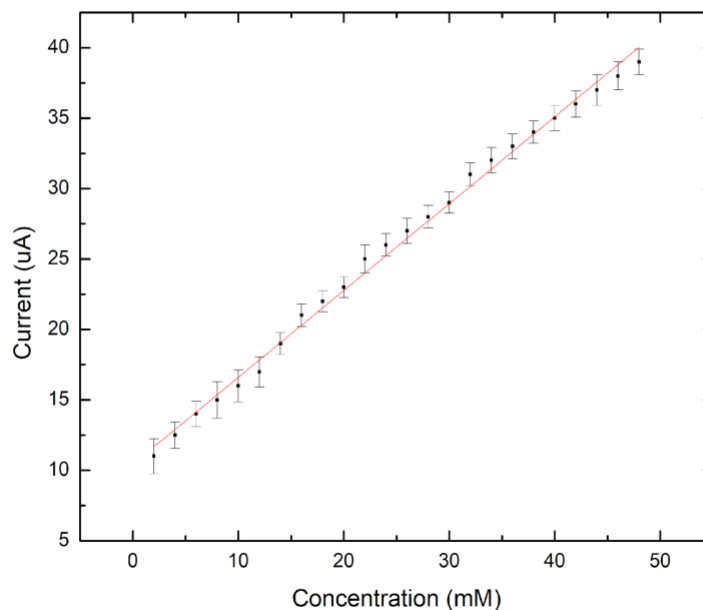


Figure 35. Calibration curve derived from the linear response of the sensor to change in glucose concentration.

Sensing the change in glucose concentration only represents part of the process of making a biosensing system as another critical task involves the correct measurement of the glucose concentration values along with continuous monitoring of the glucose concentration level and communication of the sensed glucose readings to the user, treating specialists and/or caregivers. In the literature, Ali. et al. [164] reported a prototype wireless system using an existing General Packet Radio Service (GPRS)/Global System for Mobile Communications (GSM) network and a communication protocol that facilitates remote data collection using Short Message Service (SMS) for monitoring glucose using a Programmable Interface Controllers (PIC) microcontroller directly

connected to a mobile phone, thereby rendering the entire system bulky. Soni et al. [165] developed a non-invasive optical glucose biosensor using saliva samples and a smartphone. The strip changes color upon reaction with glucose present in saliva, and the color changes were detected using a smartphone camera through red, green, blue (RGB) profiling but it still was not a continuous glucose monitoring system. As a solution to this continuous glucose monitoring problem, we employed the non-enzymatic biofuel cell as a power source as well as a glucose sensing element along with a charge pump circuit with an LED acting as a transducer and an android application to read and convey the data to the end user and treating specialists and/ or caregivers, making an integrated self-powered continuous glucose monitoring system.

The Au-co-Pt anode and the GDE cathode were assembled to realize a biofuel cell. The electrical voltage produced by this single biofuel cell was supplied as the input voltage for the charge pump integrated circuit (IC). The entire system can be seen in Figure 36. The fabricated biofuel cell generated voltage in the range of 300- 600 mV.

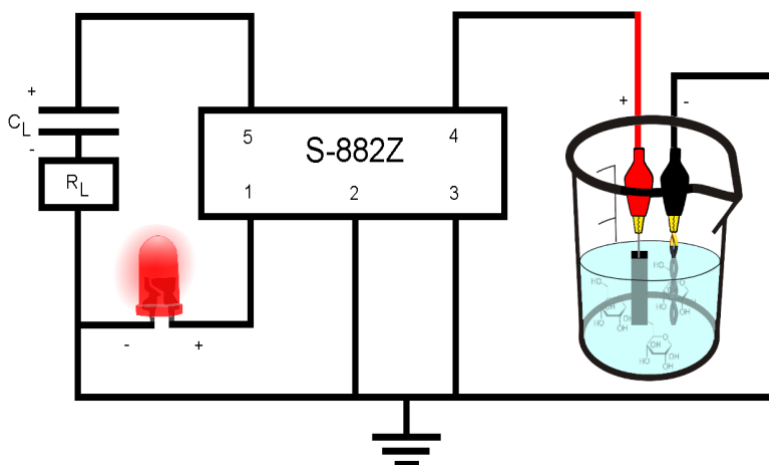


Figure 36. IC circuit with glucose biofuel cell as power source

The circuit consists of three main parts: (1) S882Z charge pump IC (2) A 10 nF capacitor (3) An ultra-low powered LED. The S882Z IC was obtained from Seiko electronics. This IC can work at a nominal input of 300 mV and amplify the input voltage up to 1.8 V. The IC is constructed from multiple stages of capacitors and switches, and the output voltage is governed by the following equation:

$$V_{OUT}=N(V_{IP}). \quad (5)$$

where N is the number of stages and VIP represents the input voltage.

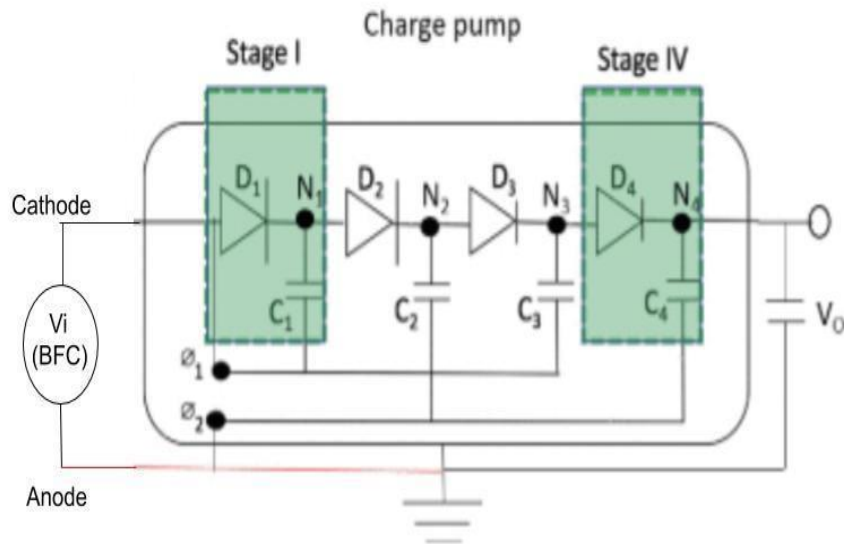


Figure 37. The construction of the self-powered glucose biosensor via a charge pump integrated circuit and a capacitor functioning as a transducer.

The input voltage, V_i , generated by the biofuel cell was applied to the first stage of the charge pump, where ' ϕ_1 ' and ' ϕ_2 ' are the clock cycles, which are complementary to each other and have the same amplitude as the input voltage as seen from Figure 37. When ϕ_1 is ON, odd number stages operate, and the capacitor ' C_1 ' gradually charges. At this time instant, clock ϕ_2 is in the OFF state and the charge accumulates at node ' N_1 '. When ϕ_2 switches ON, even numbered stages are active,

carrying the built-up voltage at stage 1 to stage 2. At this time instant, the clock signal from ϕ_1 is OFF, and the charge accumulates at node 'N₂'. This charge is carried towards the output capacitor which results in the amplified output voltage as observed from equation 5.

The capacitor functions as a transducing element, where the charging/ discharging frequency of the capacitor is directly correlated to the changes in glucose concentration. By monitoring the capacitor frequency, the exact concentration of the analyte can be deduced. This use of frequency to calculate concentration in biosensors was first presented by Slaughter et al. [166] and then further characterized by Kulkarni et al. [167].

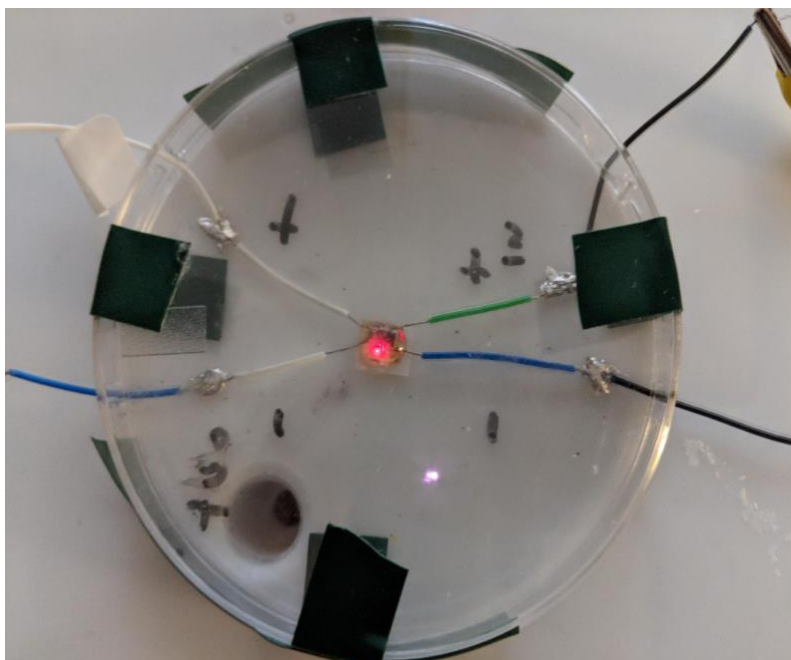


Figure 38. Charge pump circuit with LED blinking.

The capacitor in the designed charge pump circuit discharges through the LED turning it on as seen in Figure 38. It was observed that the LED blinking frequency is directly proportional to the capacitor charging/discharging frequency. The LED blinking can be considered as a visual representation of the glucose concentration and can be used to calculate the concentration using image

processing. Thus, in this work, we developed an android mobile application that uses a mobile camera to monitor and calculate the LED blinking frequency and then sends the data wirelessly to a MATLAB station where the blinking frequency is converted to glucose concentration and a message containing the current glucose level is received by the user.

A representation of the entire biosensing system consisting of the non-enzymatic biofuel cell and the charge pump circuit along with mobile glucose sensing is shown in Figure 39.

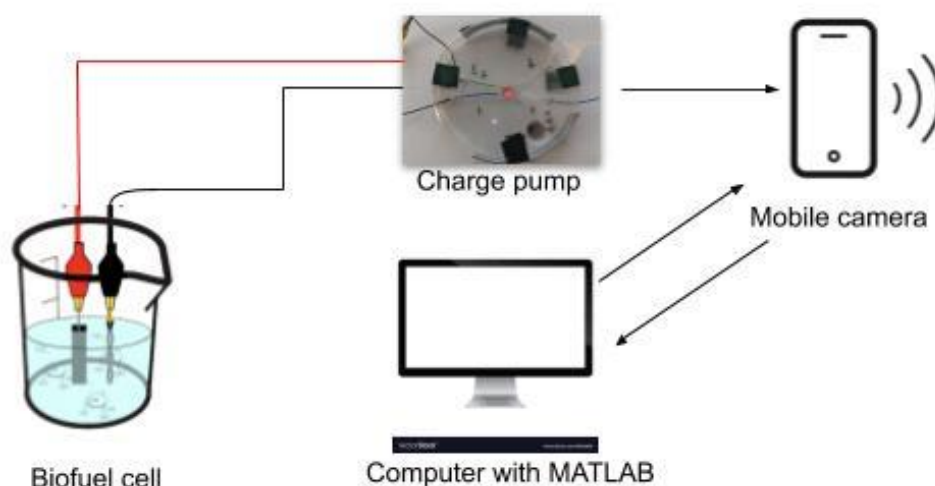
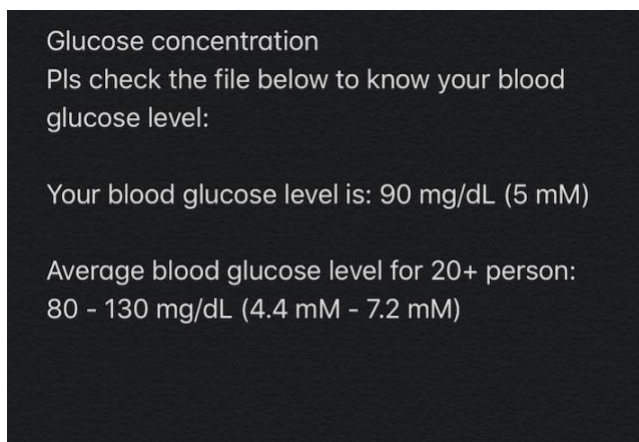


Figure 39. A model of a novel self-powered glucose monitoring biosystem with data acquisition using mobile camera.

The android application was developed based on OpenCV with Android Studio which uses the mobile camera to recognize the blinking LED and converts the observed blinking frequency into glucose concentration readings using MATLAB. The live video feed from the android application was wirelessly accessed in MATLAB using a custom MATLAB script which did continuous image processing on the video feed. The script works by first converting the live video into 100 image frames. Then each frame is analyzed individually. At first, the image is converted into a grayscale

image. Then the red component of the image is deleted from the grayscale. This is done to find out for how many frames the LED was turned ON. Then a median filter is used to reduce the noise. After all the frames are analyzed, the total number of red pixels is calculated. The total number of red pixels gives direct correlation to the LED blinking frequency. This frequency is then converted into the corresponding glucose concentration using a calibration curve.

After the glucose concentration is calculated, the MATLAB script then sends a text message and an email to the user with the present glucose level as seen in Figure 40. This message can be sent to any healthcare provider, doctor, or a user's family free of cost. It just requires a basic internet connection to work.



```
Glucose concentration
Pls check the file below to know your blood
glucose level:

Your blood glucose level is: 90 mg/dL (5 mM)

Average blood glucose level for 20+ person:
80 - 130 mg/dL (4.4 mM - 7.2 mM)
```

Figure 40. Received text message and email by the user containing information about their blood glucose level.

The waveform obtained from the capacitor output of the charge pump circuit can also be analyzed for properties such as amplitude frequency, rise time, time interval, and distortion among other parameters [168]. In the development of this self-powered glucose biosensor, a portable oscilloscope can be used to monitor the charging/ discharging frequency of the capacitor in the charge

pump circuit which in turn correlates to the concentration of glucose employed as fuel in the biofuel cell [169,170]. For this application, an ESP8266 microcontroller was employed.

The non-enzymatic biofuel cell was connected to the charge pump as illustrated in Figure 39, wherein the output from the charge pump is connected to the ADC input of the ESP8266. The ESP is then connected to the computer/laptop via a cable as shown in Figure 41.

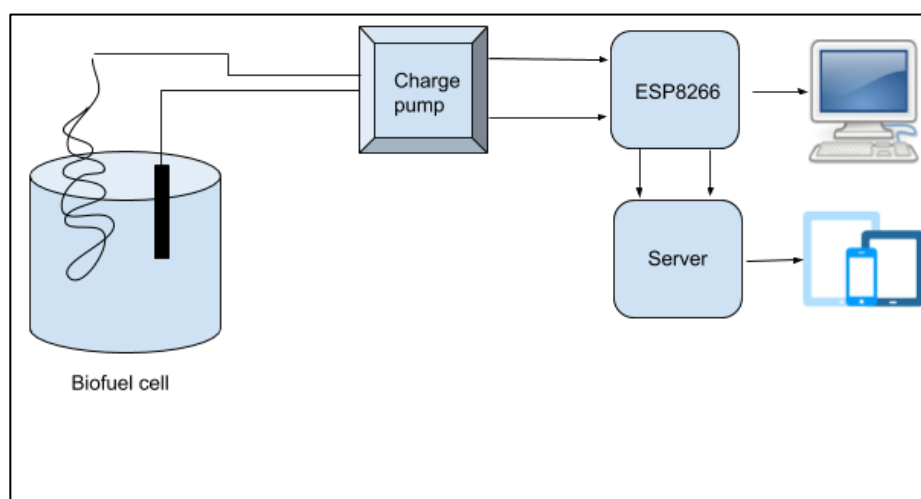


Figure 41. A model of miniaturized continuous glucose monitoring system with remote access and monitoring using E-oscilloscope (ESP8266)

The data obtained from the ESP can be viewed in the custom program called ‘e-oscilloscope’ which converts the data and plots it continuously as shown in Figure 42.

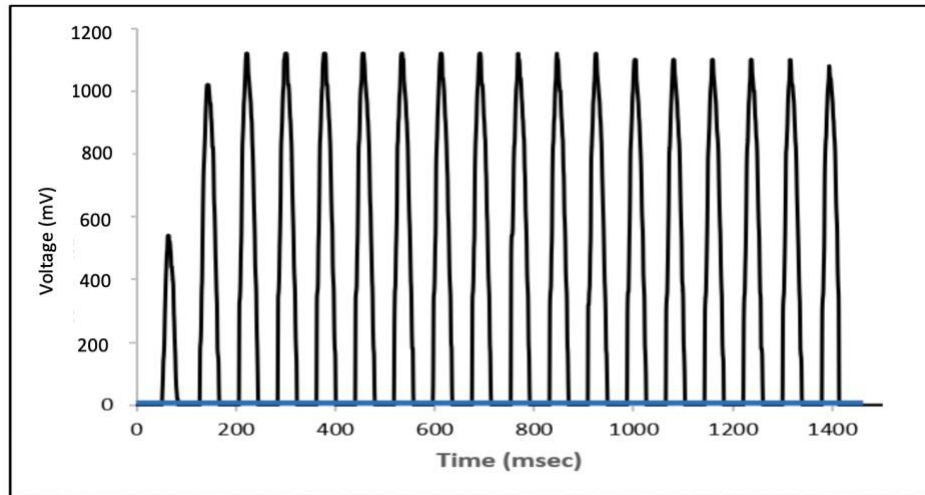


Figure 42. Capacitor charge/discharge rate obtained from glucose biosensing system operating in the absence (blue curve) and in the presence of 5 mM glucose (black curve) using the e-oscilloscope program.

For remote access of the biosensor data, a server was employed from io.adafruit.com. The microcontroller was programmed using Arduino IDE to convert the incoming data from the biosensor into waveform and then send waveform using Wi-Fi or ethernet to the server with a delay of 1500 ms. The server was then accessed remotely via computer, iPad or mobile phones. The live data feed is shown in Figure 43. The current limitation on the system is the data rate. Currently, the adafruit server allows just 30 data points per minute. This results in the generation of a rough waveform when compared to the one obtained from the wired e-oscilloscope. However, the use of an ESP module is a cost-effective approach that enables caregivers to have remote access to the sensed glucose data caregiver to monitor changes in glucose levels.

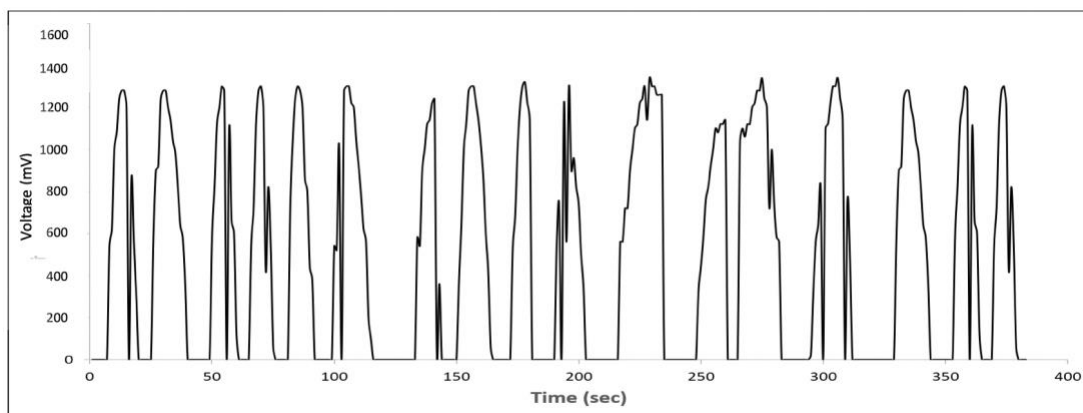


Figure 43. Adafruit live feed of the capacitor charge/discharge rate obtained from glucose biosensing system operating in the presence of 5 mM glucose using the e-oscilloscope program.

Figure 44 provides the calibration plot obtained for operating the self-powered glucose biosensors in various concentrations of glucose. A linear dynamic range of 1 mM – 25 mM was observed. As illustrated, the output frequency of the biosensor increased with increasing glucose concentrations, with a correlation coefficient, $r_2 = 0.9939$ and a sensitivity of 1.18 Hz/mM cm^2 , which were in agreement with previously reported work [171-172, 178].

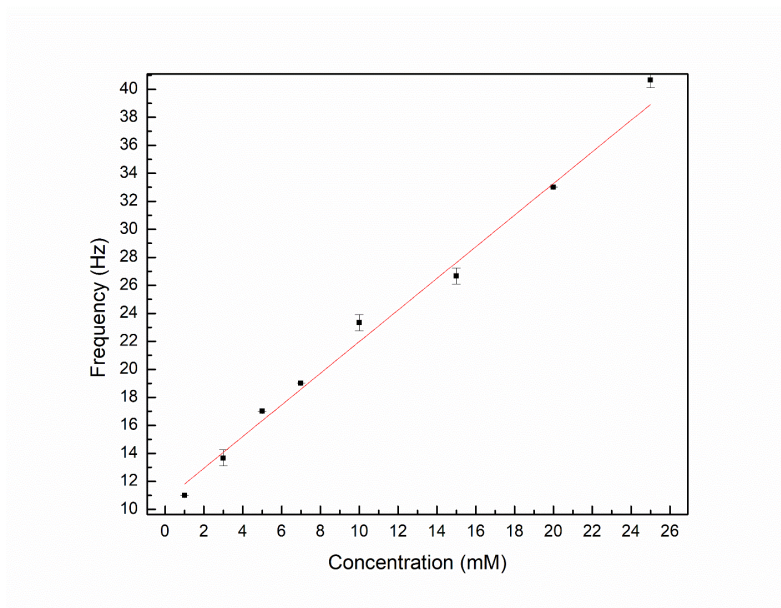


Figure 44. Calibration curve of hybrid glucose biosensing system operating in various glucose concentration using the e-oscilloscope. Error bars = \pm standard deviation of triplicate measurements.

To further determine the selectivity of the self-powered glucose biosensing system, it was characterized in the presence of various interfering species such as ascorbic acid and uric acid along with competing analytes such as fructose, maltose, and galactose. The performance of the glucose biosensor was found to determine the impact of these interfering species and competing analytes [143-146] on the biosensing system. Various semipermeable membranes such as glycol-chitosan, nafion and p-hydroxyethyl methacrylate (p-HEMA) have been employed to coat the active regions of the bioelectrodes, which in turn improves the performance of the bioelectrodes [147-149] by selectively screening against these species and extending the lifetime of the bioelectrodes by minimizing the leeching out of enzymes [150].

Two sets of experiments were performed to determine the performance of our self-powered glucose biosensing system in the presence of interfering analytes at their physiological concentration (≤ 0.42 mM) [151]. The first experiment was conducted by observing the charge/discharge frequency of the capacitor when operating in the presence of 5 mM glucose and 5 mM glucose + 0.3 mM interfering analytes (maltose (Mal), fructose (Fru), galactose (Gal), ascorbic acid (AA), uric Acid (UA)). Figure 45, shows the charge/discharge frequency of the capacitor in the presence of 5 mM glucose plus the respective 0.3 mM interfering analyte. The observed frequency was 17 Hz in the presence of 5 mM glucose. No significant change in the charge/discharge frequency was observed upon introducing 5 mM glucose plus the respective 0.3 mM interfering analyte.

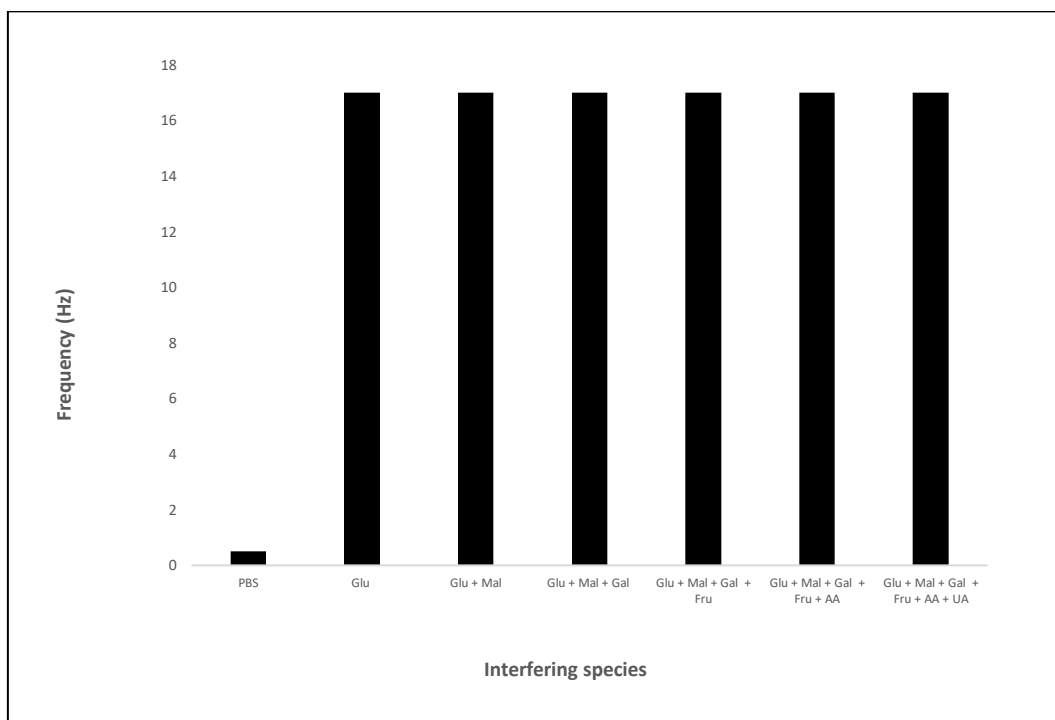


Figure 45. The charge/discharge frequency of the capacitor in the presence of 5 mM glucose and 0.3 mM interfering species

The second set of experiments focused on monitoring the charge/discharge frequency of the capacitor in the presence of the respective interfering analyte independent of glucose. As shown in Figure 46, the interfering analytes resulted in no electrical power generation; hence, no charge/discharge frequency was observed. 5 mM glucose was introduced in between each interfering analyte trial to show that the system was only selective towards glucose and the rest of the interference species had not impact on the charge/discharge frequency obtained from the self-powered glucose biosensor.

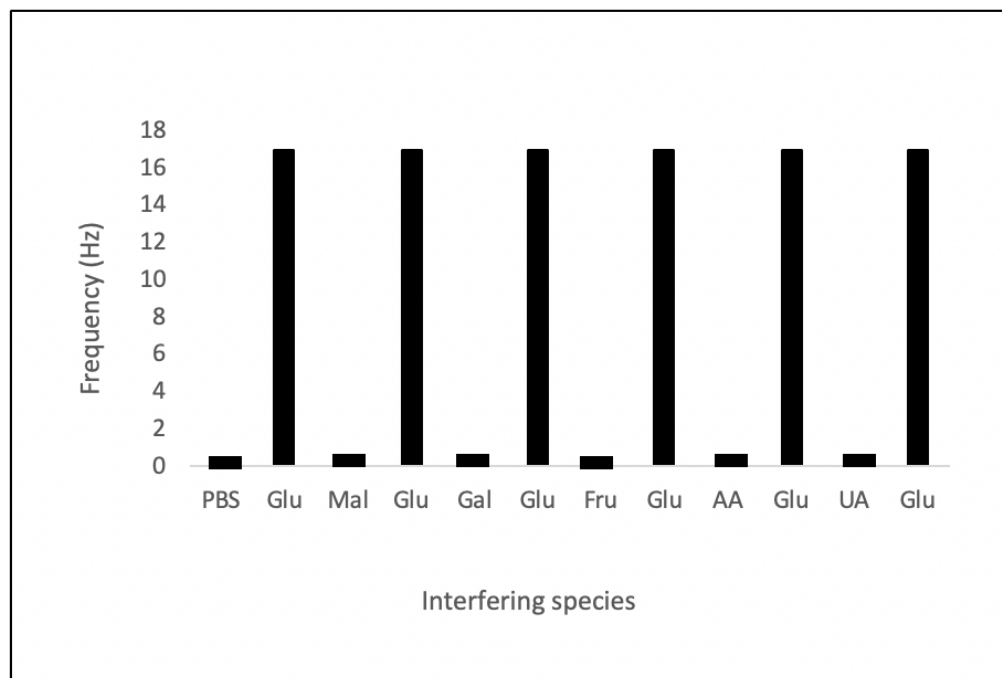


Figure 46. The charge/discharge frequency of the capacitor in the presence of the respective interfering analyte independent of glucose

As demonstrated, the self-powered glucose biosensor's performance remains unaffected by the introduction of interfering species such as ascorbic acid and uric acid because these interfering species often interfere at a potential of +0.6 to +0.7 V against Ag/AgCl reference electrode [152]. However, the biofuel cell used to construct the self-powered glucose biosensor does not generate voltage in that range, which is necessary to decompose ascorbic acid and uric acid, thereby causing these two non-competing analytes to have no effect on the performance of self-powered glucose biosensor. Additionally, glycol-chitosan was used to coat the surface of the bioelectrodes due to its ability to selectively screen against interfering species [153]. The competing analytes at their physiological concentration were also found to be ineffective at producing the minimum voltage of 0.3 V required to drive the energy amplification circuit, thereby having no effect on the overall performance of the self-powered glucose biosensor.

For the stability study of the designed biosensor, the sensors power output was observed daily for a period of 20 days. The power was measured at a glucose concentration of 10 mM. It was observed that the power output remained constant in the range of 22 -24 $\mu\text{W}/\text{cm}^2$ for 20 days as seen in Figure 47.

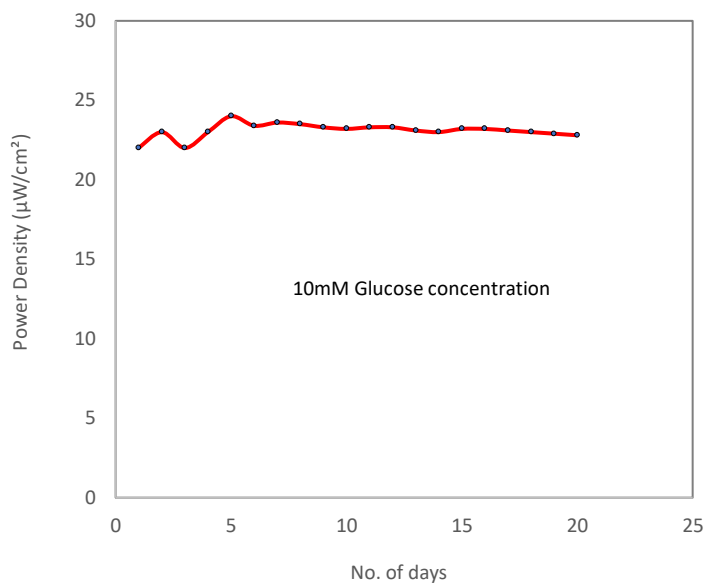


Figure 47. Stability study performed for 20 days at 10 mM glucose concentration.

CHAPTER 8

CONCLUSION

In conclusion, we demonstrated a non-enzymatic glucose biofuel cell with glucose sensing and data acquisition using mobile android application and MATLAB. The non-enzymatic glucose biofuel cell system consists of Au-co-Pt anode and GDE cathode, a charge pump circuit as voltage amplifier and with an LED, which acted as a visual representation of glucose concentration. A linear dynamic range of 1 mM – 54 mM glucose with a sensitivity of $0.616 \mu\text{A mM}^{-1}$ was observed. The Android application used a mobile camera to determine the LED blinking frequency and send the live video feed to the MATLAB workstation. The custom MATLAB script then converted the frequency to the exact glucose concentration using image processing. After the calculation performed, the script sent out a text message to the user. The text message contains details about the user's glucose concentration level. The glucose concentration could also be monitored using the ESP8266 microcontroller as a portable oscilloscope as well as from remote locations using the adafruit server. The non-enzymatic biofuel cell was also tested under different pH and temperature values to find the most favorable operating conditions. It was observed that the non-enzymatic biofuel cell performs best at a neutral pH of 7.0 and generates more power output at higher temperatures. The designed system was also tested in the presence of different interfering and competitive species. The results showed that the performance of the biofuel cell was not affected by the presence of these interfering and competitive species.

In future, the system can be tested in real world environments through animal testing to observe the biocompatibility of the sensor. More focus can be given to the development of flexible circuits and sensors that could be placed on the skin instead of implanting in the body. More work

can be done to improve the stability of these biosensors. A lot of research has been focused on designing a wireless system using near field communication (NFC). As NFC is a passive system; it does not need power from the biofuel cell and can be powered using mobile phones in the vicinity. This can open new ventures in the biosensing field.

In conclusion, this developed non-enzymatic glucose biofuel cell and sensing system can provide a cost-effective and easy to use power source for small electronic devices and medical implants and can also be used as glucose concentration measuring tool.

REFERENCES

- [1] “What Is Diabetes?” *National Institute of Diabetes and Digestive and Kidney Diseases*, U.S. Department of Health and Human Services, 1 Dec. 2016, www.niddk.nih.gov/health-information/diabetes/overview/what-is-diabetes.
- [2] Rachel Nall, RN. “Diabetes: Symptoms, Treatment, and Early Diagnosis.” *Medical News Today*, MediLexicon International, 9 Jan. 2020, www.medicalnewstoday.com/articles/323627.
- [3] “Diabetes Overview.” *Diabetes Overview - Symptoms, Causes, Treatment*, www.diabetes.org/diabetes.
- [4] “Diabetes.” *Mayo Clinic*, Mayo Foundation for Medical Education and Research, 8 Aug. 2018, www.mayoclinic.org/diseases-conditions/diabetes/symptoms-causes/syc-20371444.
- [5] Watson, Stephanie. “Everything You Need to Know About Diabetes.” <https://www.healthline.com/Health/Diabetes>, 4 Oct. 2018, www.healthline.com/health/diabetes.
- [6] Centers for Disease Control and Prevention. "National diabetes statistics report: estimates of diabetes and its burden in the United States, 2014." *Atlanta, GA: US Department of Health and Human Services* (2014).
- [7] Dansinger, Michael. “Glucometer Types, Features, Guidelines, Results.” *WebMD*, WebMD, 18 Apr. 2018, www.webmd.com/diabetes/glucometers-features-guidelines.
- [8] “Glucose Meter, Blood Glucose Meters - IHealth.” *IHealth® Official Site for Personal Health Management*, 25 Jan. 2019, ihealthlabs.com/glucometer/wireless-smart-gluco-monitoring-system/.
- [9] Manzella, Debra. “10 Steps for Using a Glucometer.” *Verywell Health*, Verywell Health, 12 Oct. 2019, www.verywellhealth.com/how-to-use-a-glucometer-1087304.
- [10] “Continuous Glucose Monitoring System.” *Continuous Glucose Monitoring System*, www.freestylelibre.us/.
- [11] “Continuous Glucose Monitoring.” *National Institute of Diabetes and Digestive and Kidney Diseases*, U.S. Department of Health and Human Services, 1 June 2017, www.niddk.nih.gov/health-information/diabetes/overview/managing-diabetes/continuous-glucose-monitoring.
- [12] Dansinger, Michael. “Continuous Glucose Monitoring for Diabetes.” *WebMD*, WebMD, 1 Dec. 2019, www.webmd.com/diabetes/guide/continuous-glucose-monitoring.

- [13] Zak.huber. "Continuous Glucose Monitoring (CGM): 24 Hour Glucose Monitor." *Dexcom*, 1 Aug. 2019, www.dexcom.com/continuous-glucose-monitoring.
- [14] "Rechargeable Battery Market: Global Industry Trends, Share, Size, Growth, Opportunity and Forecast 2019-2024", *Researchandmarkets.com*, 2019. [Online]. Available: <https://www.researchandmarkets.com/reports/4775741/rechargeable-battery-market-global-industry>.
- [15] B. Schweber, "Lithium Batteries: The Pros and Cons", *Electronics360*, 2015. [Online]. Available: <https://electronics360.globalspec.com/article/5555/lithium-batteries-the-pros-and-cons>.
- [16] Andújar JM, F Segura (2009) Fuel cells: History and updating, a walk along two centuries. *Renewable and sustainable energy reviews* 13: 2309-2322.
- [17] G. Slaughter and T. Kulkarni, "Enzymatic glucose biofuel cell and its application", *Biochip and Tissue chip*, 2015.
- [18] Hoff AJ, Deisenhofer J (1997) Photophysics of photosynthesis, Structure and spectroscopy of reaction centers of purple bacteria. *Physics reports* 287: 1-247.
- [19] S.S. Mahshid, S. Camire, F. Ricci, A. Vallee-Belisle, "A highly selective electrochemical DNA-based sensor that employs steric hindrance effects to detect proteins directly in whole blood", *J. Am. Chem. Soc.*, 137, pp. 15596-15599, 2015.
- [20] S. Jeong, J. Park, D. Pathania, C.M. Castro, R. Weissleder, H. Lee, "Integrated magneto-electrochemical sensor for exosome analysis", *ACS Nano*, 10, pp. 1802-1809, 2016.
- [21] G. Slaughter, "Current Advances in biosensor design and fabrication", R.A. Meyers (Ed.), *Encyclopedia of Analytical Chemistry*, John Wiley, Chichester (June 14 2018),
- [22] J.S. Narayanan, G. Slaughter, "The preparation of AuNPs-HRP needle-type biosensor for ultrasensitive detection of hydrogen peroxide *Med. Devices Sens.*, 1 (2018), pp. 1-9
- [23] E. Bakker, "Electrochemical sensors", *Anal. Chem.*, 76 (2004), pp. 3285-3298
- [24] D. Chen, H.B. Feng, J.H. Li, "Graphene oxide: preparation, functionalization, and electrochemical applications *Chem. Rev.*, 112 (2012), pp. 6027-6053
- [25] H.B. Wang, H.D. Zhang, Y. Chen, Y. Li, T. Gan, "H₂O₂-mediated fluorescence quenching of double stranded DNA templated copper nanoparticles for label-free and sensitive detection of glucose, *RSC Adv.*, 5 (2015), pp. 77906-77912

- [26] L. Wang, J. Zheng, Y. Li, S. Yang, C. Liu, Y. Xiao, J. Li, Z. Cao, R. Yang, "AgNP-DNA@GQDs hybrid: new approach for sensitive detection of H₂O₂ and glucose via simultaneous AgNP etching and DNA cleavage", *Anal. Chem.*, 86 (2014), pp. 12348-12354
- [27] G. Slaughter, "Fabrication of Nano-indented-electrodes for glucose detection", *J. Diab. Sci. Technol.*, 4 (2) (2010), pp. 320-327
- [28] D. Ivnitski, K. Artyushkova, P. Atanassov, "Surface characterization and direct electrochemistry of redox copper centers of bilirubin oxidase from fungi *Myrothecium verrucaria*", *Bioelectrochemistry*, 74 (2008), pp. 101-110
- [29] B. Haghghi, B. Karimi, M. Tavahodi, H. Behzadnia, "Electrochemical behavior of glucose oxidase immobilized on Pd-nanoparticles decorated ionic liquid derived fibrillated mesoporous carbon", *Electroanal.*, 26 (2014), pp. 2010-2016
- [30] G. Slaughter, J. Sunday, "Fabrication of enzymatic glucose hydrogel biosensor based on hydrothermally grown ZnO nanoclusters", *IEEE Sensors J.*, 14 (2014), pp. 1573-1576
- [31] Z. Wang, S. Liu, P. Wu, C. Cai, "Detection of glucose based on direct electron transfer reaction of glucose oxidase immobilized on highly ordered polyaniline nanotubes", *Anal. Chem.*, 81 (2009), pp. 1638-1645
- [32] C.X. Guo, C.M. Li, "Direct electron transfer of glucose oxidase and biosensing of glucose on hollow sphere-nanostructured conducting polymer/metal oxide composite", *Physical. Chem. Chem. Phys.*, 12 (2010), pp. 12153-12159
- [33] S.I. Brahim, G. Slaughter, A. Guiseppi-Elie, "Electrical and electrochemical characterization of electroconductive PPy-p(HEMA) composite hydrogels", *Smart Struct. Mat.*, 5053 (2003), pp. 1-12
- [34] B. Liang, L. Fang, G. Yang, Y. Hu, X. Guo, X. Ye, "Direct electron transfer glucose biosensor based on glucose oxidase self-assembled on electrochemically reduced carboxyl graphene", *Biosens. Bioelectron.*, 43 (2013), pp. 131-136
- [35] P. Yang, L. Wang, Q. Wu, Z. Chen, X. Lin, "A method for determination of glucose by an amperometric bienzyme biosensor based on silver nanocubes modified Au electrode", *Sensors Actuators B Chem.*, 194 (2014), pp. 71-78
- [36] X. Che, R. Yuan, Y. Chai, J. Li, Z. Song, W. Li, X. Zhong, "A glucose biosensor based on chitosan-Prussian blue-multiwall carbon nanotubes-hollow PtCo nanochains formed by one-step electrodeposition", *Colloids Surf. B: Biointerfaces*, 84 (2011), pp. 454-461

- [37] Md.Q. Hasan, R. Kuis, J. Shankara Narayanan, G. Slaughter, "Fabrication of highly effective hybrid biofuel cell based on integral colloidal platinum and bilirubin oxidase on gold support", *Nat. Sci. Rep.*, 8 (2018), Article 16351
- [38] J. Russell and R. Cohn, "Gas diffusion electrode", *JBookvika publications.*, 638 (2012), pp. 196
- [39] G. Slaughter, T. Kulkarni, "Fabrication of palladium nanowire array electrode for biofuel cell application", *Microelectron. Eng.*, 149 (2016), pp. 92-96
- [40] N. Furuya, "A technique is described for production of a gas diffusion electrode by electrophoresis". *Journal of Solid State Electrochemistry*. **8**: 48–50, 2003.
- [41] S. Ernst, "The electrooxidation of glucose in phosphate buffer solutions Part I. Reactivity and kinetics below 350 mV/RHE", *Journal of Electroanalytical Chemistry*, vol. 100, no. 1, pp. 173-183, 1979. Available: 10.1016/0368-1874(79)85110-2.
- [42] F. Kubanek, T. Turek and U. Krewer, "Modeling Oxygen Gas Diffusion Electrodes for Various Technical Applications", *Chemie Ingenieur Technik*, vol. 91, no. 6, pp. 720-733, 2019. Available: 10.1002/cite.201800181
- [43] "Fuel Cells." *SpringerLink*, Springer, London, 1 Jan. 1970, link.springer.com/chapter/10.1007%2F978-1-84882-511-6_7.
- [44] Spiridigliozzi, Luca. "Fuel Cells." *SpringerLink*, Springer, Cham, 1 Jan. 1970, link.springer.com/chapter/10.1007/978-3-319-99395-9_2.
- [45] "Types of Fuel Cells." *Energy.gov*, Department of Energy, www.energy.gov/eere/fuelcells/types-fuel-cells.
- [46] Davis, Frank. "Biofuel Cells—Recent Advances and Applications." *Researchgate*, Biosensor and Bioelectronics, Mar. 2007, www.researchgate.net/publication/7001687_Biofuel_Cells-Recent_Advances_and_Applications.
- [47] Service, Robert F. "Biofuel Cells." *Science*, American Association for the Advancement of Science, 17 May 2002, science.sciencemag.org/content/296/5571/1223.
- [48] Yadav, Mukesh, and Ram Singh. "Biofuel Cells: Concepts and Perspectives for Implantable Devices." *ResearchGate*, CRC Press, Jan. 2017, www.researchgate.net/publication/311576436_Biofuel_Cells_Concepts_and_Perspectives_for_Implantable_Devices.
- [49] Moehlenbrock, M. J.; Minter, S. D. *Chem. Soc. Rev.* 2008, 37, 1188-1196.
- [50] Aulenta, F.; Tocca, L.; Verdini, R.; Reale, P.; Majone, M. *Envir. Sci. Tech.* 2011, 45, 8444-8451.

- [51] Zhang, F.; Ge, Z.; Grimaud, J.; Hurst, J.; He, Z. *Envir. Sci. Tech.* 2013, 47, 4941-4948.
- [52] Arechederra, R.; Minteer, S. D. *Electrochim. Acta* 2008, 53, 6698-6703.
- [53] Atanassov, Palamev, and Scott Bantta. "Enzymatic Biofuel Cells." *Researchgate, Electrochemical Society Interface*, June 2007, www.researchgate.net/publication/260192029_Enzymatic_Biofuel_Cells.
- [54] Barton, Scott, and Josh Gallaway. "Enzymatic Biofuel Cells for Implantable and Microscale Devices." *Enzymatic Biofuel Cells for Implantable and Microscale Devices / Chemical Reviews*, Chem. Rev, Sept. 2004, pubs.acs.org/doi/10.1021/cr020719k.
- [55] Bullen, R.A, and F.C Walsh. "Biofuel Cells and Their Development." *Biosensors and Bioelectronics*, Elsevier, Jan. 2006, blogs.epfl.ch/biofuelcells/documents/Biofuel%20cells%20and%20their%20development.pdf.
- [56] Yu, Ellen, and Scoot Keith. "Enzymatic Biofuel Cells—Fabrication of Enzyme Electrodes." *Research Gate, Energies*, Mar. 2010, www.researchgate.net/publication/41163156_Enzymatic_Biofuel_Cells-Fabrication_of_Enzyme_Electrodes.
- [57] Chen, Yun, et al. "Design of an Enzymatic Biofuel Cell with Large Power Output." *Journal of Materials Chemistry A*, The Royal Society of Chemistry, 20 Apr. 2015, pubs.rsc.org/en/content/articlelanding/2015/ta/c5ta01432h#!divAbstract.
- [58] Sidney, Aquino, and De Andrade. "New Energy Sources: the Enzymatic Biofuel Cell." *Journal of the Brazilian Chemical Society*, Brazilian Chemical Society, Dec. 2013, www.scielo.br/scielo.php?script=sci_arttext&pid=S0103-50532013001200002.
- [59] Kerzenmacher, Sven, and Arne Kloke. "Biofuel Cells for Energy Supply of Distributed System: State of the Art and Application." *Researchgate, Sensoren and Messsysteme*, May 2010.
- [60] Yadav, Mukesh, et al. "Biofuel Cells: Concepts and Perspectives for Implantable Revoices." *Researchgate, CRC Press*, Jan. 2017.
- [61] Potter, M. C.; *Proceedings of the Royal Society of London. Series B, Containing Papers of a Biological Character* **1911**, 84, 260. Available in <http://m.rspb.royalsocietypublishing.org/content/84/571/260.full.pdf>, accessed in November, 2013.
- [62] Yahiro, A. T.; Lee, S. M.; Kimble, D. O.; *Biochim. Biophys. Acta (Specialized Section on Biophysical Subjects)* **1964**, 88, 375.

- [63] Bhalla, Nikhil, et al. "Introduction to Biosensors." *Essays in Biochemistry*, Portland Press Limited, 30 June 2016, www.ncbi.nlm.nih.gov/pmc/articles/PMC4986445/.
- [64] Kawamura, Akifumi, and Takashi Miyata. "Biosensors." *Biosensors - an Overview / ScienceDirect Topics*, 2016, www.sciencedirect.com/topics/engineering/biosensors.
- [65] Mehrotra, Parikha. "Biosensors and Their Applications - A Review." *Journal of Oral Biology and Craniofacial Research*, Elsevier, 2016, www.ncbi.nlm.nih.gov/pmc/articles/PMC4862100/.
- [66] Makaram, P.; Owens, D.; Aceros, J. Trends in Nanomaterial-Based Non-Invasive Diabetes Sensing Technologies. *Diagnostics* 2014, 4, 27–46, doi:10.3390/diagnostics4020027.
- [67] Do Amaral, C.E.F.; Wolf, B. Current development in non-invasive glucose monitoring. *Med. Eng. Phys.* 2008, 30, 541–549, doi:10.1016/j.medengphy.2007.06.003.
- [68] Yoo, E.H.; Lee, S.Y. Glucose biosensors: An overview of use in clinical practice. *Sensors* 2010, 10, 4558–4576, doi:10.3390/s100504558.
- [69] Coyle, S.; Curto, V.F.; Benito-Lopez, F.; Florea, L.; Diamond, D. Wearable bio and chemical sensors. In *Wearable Sensors*; Elsevier Inc.: Amsterdam, The Netherlands, 2014; pp. 65–83.
- [70] American Diabetes Association. Diagnosis and classification of diabetes mellitus. *Diabetes Care* 2004, 27, 5–10
- [71] Badugu, R.; Lakowicz, J.R.; Geddes, C.R. Ophthalmic glucose monitoring using disposable contact lenses— A review. *J. Fluoresc.* 2004, 14, 617–633, doi:10.1023/B:JOFL.0000039349.89929.da
- [72] . Badugu, R.; Lakowicz, J.R.; Geddes, C.R. Fluorescence sensors for monosaccharides based on the 6- methylquinolinium nucleus and boronic acid moiety: Potential application to ophthalmic diagnostics. *Talanta* 2005, 65, 762–768, doi:10.1016/j.talanta.2004.08.003.
- [73] Clark Jr., L.C.; Lyons, C. Electrode systems for continuous monitoring in cardiovascular surgery. *Ann. N. Y. Acad. Sci.* 1962, 102, 29–45, doi:10.1111/j.1749-6632.1962.tb13623.x.
- [74] Price, C.P. Point-of-care testing in diabetes mellitus. *Clin. Chem. Lab. Med.* 2003, 41, 1213–1219, doi:10.1515/CCLM.2003.185.
- [75] D'Costa, E.J.; Higgins, I.J.; Turner, A.P. Quinoprotein glucose dehydrogenase and its application in an amperometric glucose sensor. *Biosensors* 1986, 2, 71–87, doi:10.1016/0265-928X(86)80011-6.
- [76] Heller, A.; Feldman, B. Electrochemical glucose sensors and their applications in diabetes management. *Chem. Rev.* 2008, 108, 2482–2505, doi: 10.1021/cr068069y.

- [77] Bankar, S.B.; Bule, M.V.; Singhal, R.S.; Ananthanarayan, L. Glucose oxidase - an overview. *Biotechnol. Adv.* 2009, 27, 489–501, doi:10.1016/j.biotechadv.2009.04.003.
- [78] Guilbault, G.G.; Lubrano, G.J. An enzyme electrode for the amperometric determination of glucose. *Anal. Chim. Acta* 1973, 64, 439–455, doi:10.1016/S0003-2670(01)82476-4.
- [79] Wang, J. Glucose biosensors: 40 Years of advances and challenges. *Electroanalysis* 2001, 13, 983–988.
- [80] Clark, L.C., Jr. Monitor and control of blood and tissue oxygen tensions. *Trans. Am. Soc. Artif. Intern. Organs* 1956, 2, 41–48.
- [81] Hilditch, P.; Green, M. Disposable electrochemical biosensors. *Analyst* 1991, 116, 1217–1220.
- [82] Matthews, D.; Holman, R.; Brown, E.; Streemson, J.; Watson, A.; Hughes, S. Pen-sized digital 30-s blood glucose meter. *Lancet* 1987, 1, 778–779.
- [83] Fang, H.; Kaur, G.; Wang, B. Progress in boronic acid-based fluorescent glucose sensors, *J. Fluoresc.* 2004, 14, 481–489, doi:10.1023/B:JOFL.0000039336.51399.3b.
- [84] Pickup, J.C.; Hussain, F.; Evans, N.D.; Rolinski, O.J.; Birch, D.J.S. Fluorescence-based glucose sensors. *Biosens. Bioelectron.* 2005, 20, 2555–2565, doi:10.1016/j.bios.2004.10.002.
- [85] Wang, J. Electrochemical glucose biosensors. *Chem. Rev.* 2008, 108, 814–825, doi:10.1021/cr068123a.
- [86] Badugu, R.; Lakowicz, J.R.; Geddes, C.R. Boronic acid fluorescent sensors for monosaccharide signalling based on the 6-methoxyquinolinium heterocyclic nucleus: Progress toward noninvasive and continuous glucose monitoring. *Bioorgan. Med. Chem.* 2005, 13, 113–119, doi:10.1016/j.bmc.2004.09.058.
- [87] Badugu, R.; Lakowicz, J.R.; Geddes, C.R. Ophthalmic glucose sensing: A novel monosaccharide sensing disposable and colourless contact lens. *Analyst* 2004, 129, 516–521, doi:10.1039/b314463c.
- [88] Badugu, R.; Lakowicz, J.R.; Geddes, C.R. Noninvasive continuous monitoring of physiological glucose using a monosaccharide-sensing contact lens. *Anal. Chem.* 2004, 76, 610–618, doi:10.1021/ac0303721.
- [89] Badugu, R.; Lakowicz, J.R.; Geddes, C.R. A glucose sensing contact lens: A non-invasive technique for continuous physiological glucose monitoring. *J. Fluoresc.* 2003, 13, 371–374.
- [90] Moreno-Bondi, M.C.; Wolfbeis, O.S. Oxygen optrode for use in a fiber-optic glucose biosensor. *Anal. Chem.* 1990, 62, 2377–2380, doi:10.1021/ac00220a021.

- [91] Larin, K.V.; Motamedi, M.; Ashitkov, T.V.; Esenaliev, R.O. Specificity of noninvasive blood glucose sensing using optical coherence tomography technique: A pilot study, *Phys. Med. Biol.* 2003, 48, 1371–1390.
- [92] Nathan, D.M. The Diabetes Control and Complications Trial/Epidemiology of Diabetes Interventions and Complications Study at 30 years: Overview. *Diabetes Care* 2014, 37, 9–16, doi:10.2337/dc13-2112.
- [93] Clarke, A.; O’Kelly, S. Glucose Monitoring Systems. Available online: <http://www.diabetes.ie/living-withdiabetes/educational-articles/diabetes-and-research-articles/continuous-glucose-monitoring-cgmsystems/> (accessed on 8 October 2014). 4
- [94] Badugu, R.; Lakowicz J, R.; Geddes C, D. Wavelength-ratiometric and colorimetric robes for glucose determination. *Dyes and Pigments.* 2006, 68, 159-163, doi: 10.1016/j.dyepig.2004.12.020.
- [95] Badugu, R.; Lakowicz, J.R.; Geddes, C.R. A glucose-sensing contact lens: From bench top to patient. *Curr. Op. Biotechnol.* 2005, 16, 100–107, doi:10.1016/j.copbio.2004.12.007.
- [96] Newman, J.; Turner, A.P.F. Home blood glucose biosensors: A commercial perspective. *Biosens. Bioelectron.* 2005, 20, 2435–2453, doi:10.1016/j.bios.2004.11.012. 4
- [97] Boiroux, D.; Batora, V.; Hagdrup, M.; Tarnik, M.; Murgas, J.; Schmidt, S.; Norgaard, K.; Poulsen, N.K.; Madsen, H.; Jorgensen, J.B. Comparison of prediction models for a dual-hormone artificial pancreas. *IFAC PapersOnLine* 2015, 48, 7–12, doi:10.1016/j.ifacol.2015.10.106.
- [98] Nishida, K.; Shimoda, S.; Ichinose, K.; Araki, E.; Shichiri, M. What is the artificial endocrine pancreas? Mechanism and history. *World J. Gastroenterol.* 2009, 15, 4105–4110, doi:10.3748/wjg.15.4105.
- [99] Albisser, A.M.; Leibel, B.S.; Ewart, T.G.; Davidovac, Z.; Botz, C.K.; Zingg, W.; Schipper, H.; Gander, R. Clinical control of diabetes by the artificial pancreas. *Diabetes* 1974, 23, 397–404, doi:10.2337/diab.23.5.397.
- [100] Bindra, D.S.; Zhang, Y.; Wilson, G.S.; Sternberg, R; Thévenot, D.R.; Moatti, D.; Reach, G. Design and in vitro studies of a needle-type glucose sensor for subcutaneous monitoring. *Anal. Chem.* 1991, 63, 1692–1696.
- [101] McGreevy, R. Flash glucose monitoring latest concept in testing. *The Irish Times*, 22 October 2013. Available online: www.irishtimes.com (22 October 2013).

- [102] Worsley, G.J.; Tourniaire, G.A.; Medlock, K.E.S.; Sartain, F.K.; Harmer, H.E.; Thatcher, M.; Horgan, A.M.; Pritchard, J. Continuous blood glucose monitoring with a thin-film optical sensor. *Clin. Chem.* 2007, 53, 1820–1826, doi:10.1373/clinchem.2007.091629.
- [103] Corrie, S.J.; Coffey, J.W.; Islam, J.; Markey, K.A.; Kendall, M.A.F. Blood, sweat, and tears: Developing clinically relevant protein biosensors for integrated body fluid analysis. *Analyst* 2015, 140, 4350–4364, doi:10.1039/c5an00464k.
- [104] Bandodkar, A.J.; Wang, J. Non-invasive wearable electrochemical sensors: A review. *Trends Biotechnol.* 2014, 32, 363–371, doi:10.1016/j.tibiotech.2014.04.005.
- [105] Hanashi, T.; Yamazaki, T.; Tsugawa, W.; Ikebukuro, K.; Sode, K. BioRadioTransmitter: A self-powered wireless glucose-sensing system. *J. Diabetes Sci. Technol.* 2011, 5, 1030–1035
- [106] Jina, A.; Tierney, M.J.; Tamada, J.A.; McGill, S.; Desai, S.; Chua, B.; Chang, A.; Christiansen, M. Design, development, and evaluation of a novel microneedle array-based continuous glucose monitor. *J. Diabetes Sci. Technol.* 2014, 8, 483–487, doi:10.1177/1932296814526191.
- [107] Zhang, W.; Du, Y.; Wang, M.L. On-chip highly sensitive saliva glucose sensing using multilayer films composed of single-walled carbon nanotubes, gold nanoparticles, and glucose oxidase. *Sens. Bio-Sens. Res.* 2015, 4, 96–102, doi:10.1016/j.sbsr.2015.04.006.
- [108] Corrie, S.J.; Coffey, J.W.; Islam, J.; Markey, K.A.; Kendall, M.A.F. Blood, sweat, and tears: Developing clinically relevant protein biosensors for integrated body fluid analysis. *Analyst* 2015, 140, 4350–4364, doi:10.1039/c5an00464k.
- [109] Lee, H.; Song, C.; Hong, Y.S.; Kim, M.S.; Cho, H.R.; Kang, T.; Shin, K.; Choi, S.H.; Hyeon, T.; Kim, D. Wearable/disposable sweat-based glucose monitoring device with multistage transdermal drug delivery module. *Sci. Adv.* 2017, 3, e1601314, doi:10.1126/sciadv.1601314.
- [110] Heikenfeld, J. Non-invasive analyte access and sensing through eccrine sweat: Challenges and outlook circa 2016. *Electroanalysis* 2016, 28, 1242–1249, doi:10.1002/elan.201600018.
- [111] Morris, D.; Coyle, S.; Wu, Y.; Lau, K.T.; Wallace, G.; Diamond, D. Bio-sensing textile based patch with integrated optical detection system for sweat monitoring. *Sens. Actuators B Chem.* 2009, 139, 231–236, doi:10.1016/j.snb.2009.02.032.
- [112] Mitsubayashi, K.; Suzuki, M.; Tamiya, E.; Karube, I. Analysis of metabolites in sweat as a measure of physical condition. *Anal. Chim. Acta* 1994, 289, 27–34, doi:10.1016/0003-2670(94)80004-9.

- [113] Gao, W.; Emaminejad, S.; Nyein, H.Y.Y.; Challa, S.; Chen, K.; Peck, A.; Fahad, H.M.; Ota, H.; Shiraki, H.; Kiriya, D.; et al. Fully integrated wearable sensor arrays for multiplexed in situ perspiration analysis. *Nature* 2016, 529, 509–514, doi:10.1038/nature16521.
- [114] Moser, T.; Celma, C.; Lebert, A.; Charrault, E.; Brooke, R.; Murphy, P.J.; Browne, G.; Young, R.; Higgs, T.; Evans, D. Hydrophilic organic electrode on flexible hydrogels. *ACS Appl. Mater. Interfaces* 2016, 8, 974–982, doi:10.1021/acsami.5b10831.
- [115] “DC-DC Fundamentals - Charge Pump Regulator Overview.” *TI Training*, 3 Jan. 2019, training.ti.com/dc-dc-fundamentals-charge-pump-regulator-overview.
- [116] Harres, Dan. “Charge Pump Circuits.” *Charge Pump Circuits - an Overview | ScienceDirect Topics*, 2013, www.sciencedirect.com/topics/engineering/charge-pump-circuits.
- [117] Schweber, Bill, et al. “What Is a Charge Pump and Why Is It Useful? (Part 1).” *Power Electronic Tips*, www.powelectronicstips.com/faq-what-is-a-charge-pump-and-why-is-it-useful-part-1-faq/.
- [118] “S-882Z Datasheet.” *S-882Z Datasheet - Ultra-Low Voltage Operation Charge PUMP IC FOR Step-Up*, Texas Instruments, www.digchip.com/datasheets/parts/datasheet/432/S-882Z.php.
- [119] N. Kularatna, "Fundamentals of Oscilloscopes", *Digital and Analogue Instrumentation: Testing and Measurement*, Institution of Engineering and Technology, pp. 165–208, 2003.
- [120] T. Kulkarni and G. Slaughter, "Characteristics of Two Self-Powered Glucose Biosensors.", *IEEE Sensors Journal*, vol. 17, no. 12, pp. 3607-3612, 2017.
- [121] A. Baingane and G. Slaughter, "Enzyme-Free Self-Powered Glucose Sensing System.", *IEEE SENSORS*, pp.1-4, 2018.
- [122] A. Baingane, J.S. Narayanan and G. Slaughter, “Sensitive Electrochemical Detection of Glucose via a Hybrid Self-Powered Biosensing System.”, *Sensing and Bio-Sensing Research*, Elsevier, vol. 20, pp. 41-46, 2018.
- [123] G. Slaughter and T. Kulkarni, “Highly Selective and Sensitive Self-Powered Glucose Sensor Based on Capacitor Circuit.”, *Nature News*, Nature Publishing Group, vol. 7, pp. 1471, 2017.
- [124] G. Slaughter and T. Kulkarni, “A Self-Powered Glucose Biosensing System.”, *Biosensors and Bioelectronics*, Elsevier, vol. 15, no. 78, pp. 45-50, 2015.
- [125] “Home.” *ValueTronics International*, www.valuetronics.com/product/tbs1032b-tektronix-digitaloscilloscopenew?gclid=EAIaIQobChMIIsZf1auJ4QIVTFmGCh0ARwfcEAQYBSABEgJoJfD_BwE.

- [126] Banggood.com. “US\$104.00 30% Hantek 3in1 Digital Oscilloscope+Waveform Generator+Multimeter Portable USB 2 Channels 40mhz 70mhz LCD Display Test Meter
- [127] “Android (Operating System).” *Ultraverse Wiki*, ultraverse.fandom.com/wiki/Android_(operating_system).
- [128] Libretexts. “Cyclic Voltammetry.” *Chemistry LibreTexts*, Libretexts, 5 Dec. 2019, chem.libretexts.org/Bookshelves/Analytical_Chemistry/Supplemental_Modules_(Analytical_Chemistry)/Instrumental_Analysis/Cyclic_Voltammetry.
- [129] Elgrishi, Noemie, and Brian McCarthy. “A Practical Beginner’s Guide to Cyclic Voltammetry.” *Pubs.acs.org*, Journal of Chemical Education, 2018.
- [130] “Chronoamperometry Purpose.” *Chronoamperometry Purpose*, www.gamry.com/Framework%20Help/HTML5%20-%20Tripane%20-%20Audience%20A/Content/PE/Experimental_Techniques/Chronoamperometry/Purpose.htm
- [131] Libretexts. “Chronoamperometry.” *Chemistry LibreTexts*, Libretexts, 3 June 2019, chem.libretexts.org/Bookshelves/Analytical_Chemistry/Supplemental_Modules_(Analytical_Chemistry)/Analytical_Sciences_Digital_Library/JASDL/Courseware/Analytical_Electrochemistry%3A_The_Basic_Concepts/04_Voltammetric_Methods/A._Basics_of_Voltammetry/01_Potential_Step_Methods/a)_Chronoamperometry.
- [132] G. Slaughter and T. Kulkarni, “Highly Selective and Sensitive Self-Powered Glucose Sensor Based on Capacitor Circuit,” *Sci. Rep.*, vol. 7, no. 1, p. 1471, 2017.
- [133] G. Slaughter and T. Kulkarni, “A Self-Powered Glucose Biosensing System,” *Biosensors and Bioelectronics*, vol. 78, pp.45-50, 2015.
- [134] JD. Yuen, A. Baingane, Q. Hasan, LC. Shriver-Lake, SA. Walper, D Zabetakis, JC. Breger, DA. Stenger and G. Slaughter, “A Fully-Flexible Solution-Processed Autonomous Glucose Indicator,” *Sci. Rep.*, vol. 9, no. 1, p. 6931, 2019.
- [135] Roman, T., W. A. Dino, H. Nakanishi, and H. Kasai. "Amino acid adsorption on single-walled carbon nanotubes." *The European Physical Journal D-Atomic, Molecular, Optical and Plasma Physics* 38, no. 1 (2006): 117-120.

- [136] Katz, Evgeny, José M. Pingarrón, Shay Mailloux, Nataliia Guz, Maria Gamella, Galina Melman, and Artem Melman. "Substance Release Triggered by Biomolecular Signals in Bioelectronic Systems." *The journal of physical chemistry letters* 6, no. 8 (2015): 1340- 1347.
- [137] Miyake, Takeo, Syuhei Yoshino, Takeo Yamada, Kenji Hata, and Matsuhiko Nishizawa. "Self-Regulating Enzyme– Nanotube Ensemble Films and Their Application as Flexible Electrodes for Biofuel Cells." *Journal of the American Chemical Society* 133, no. 13 (2011): 5129-5134.
- [138] Katz, Evgeny, and Kevin MacVittie. "Implanted biofuel cells operating in vivo– methods, applications and perspectives–feature article." *Energy & Environmental Science* 6, no. 10 (2013): 2791-2803.
- [139] Sales, Fernanda C. P. F., Rodrigo M. Iost, Marcus V. A. Martins, Maria C. Almeida, and Frank N. Crespilho. "An Intravenous Implantable Glucose/dioxygen Biofuel Cell with Modified Flexible Carbon Fiber Electrodes." *Lab Chip* 13, no. 3 (2013): 468-74.
- [140] Rasmussen, Michelle, Roy E. Ritzmann, Irene Lee, Alan J. Pollack, and Daniel Scherson. "An Implantable Biofuel Cell for a Live Insect." *J. Am. Chem. Soc. Journal of the American Chemical Society* 134, no. 3 (2012): 1458-460.
- [141] Giroud, Fabien, Chantal Gondran, Karine Gorgy, Vincent Vivier, and Serge Cosnier. "An Enzymatic Biofuel Cell Based on Electrically Wired Polyphenol Oxidase and Glucose Oxidase Operating under Physiological Conditions." *Electrochimica Acta* 85 (2012): 278-82.
- [142] Cinquin, Philippe, Chantal Gondran, Fabien Giroud, Simon Mazabrard, Aymeric Pellissier, François Boucher, Jean-Pierre Alcaraz, Karine Gorgy, François Lenouvel, Stéphane Mathé, Paolo Porcu, and Serge Cosnier. "A Glucose BioFuel Cell Implanted in Rats." *PLoS ONE* 5, no. 5 (2010).

- [143] Barrière, Frédéric, Paul Kavanagh, and Dónal Leech. "A laccase–glucose Oxidase Biofuel Cell Prototype Operating in a Physiological Buffer." *Electrochimica Acta* 51, no. 24 (2006): 5187-192.
- [144] Yang C-Y, Tsai T-H, Chen S-M, Lou B-M, and Liu X. "Development of a Multiple Biosensor and Its Application of Biofuel Cell." *International Journal of Electrochemical Science* 10, no. 1 (2015): 579-88.
- [145] Falk, Magnus, Miguel Alcalde, Philip N. Bartlett, Antonio L. De Lacey, Lo Gorton, Cristina Gutierrez-Sanchez, Raoudha Haddad, Jeremy Kilburn, Dónal Leech, Roland Ludwig, Edmond Magner, Diana M. Mate, Peter Ó. Conghaile, Roberto Ortiz, Marcos Pita, Sascha Pöller, Tautgirdas Ruzgas, Urszula Salaj-Kosla, Wolfgang Schuhmann, Fredrik Sebelius, Minling Shao, Leonard Stoica, Cristoph Sygmund, Jonas Tilly, Miguel D. Toscano, Jeevanthi Vivekananthan, Emma Wright, and Sergey Shleev. "Self-Powered Wireless Carbohydrate/Oxygen Sensitive Biodevice Based on Radio Signal Transmission." *PLoS ONE* 9, no. 10 (2014).
- [146] Miyake, Takeo, Keigo Haneda, Nobuhiro Nagai, Yohei Yatagawa, Hideyuki Onami, Syuhei Yoshino, Toshiaki Abe, and Matsuhiko Nishizawa. "Enzymatic Biofuel Cells Designed for Direct Power Generation from Biofluids in Living Organisms." *Energy & Environmental Science Energy Environ. Sci.* 4, no. 12 (2011): 5008.
- [147] Pizzariello, A., M. Stred'ansky, and S. Miertuš. "A Glucose/hydrogen Peroxide Biofuel Cell That Uses Oxidase and Peroxidase as Catalysts by Composite Bulk-modified
- [148] Clark, Leland C., and Champ Lyons. "Electrode Systems for Continuous Monitoring In Cardiovascular Surgery." *Annals of the New York Academy of Sciences* 102, no. 1 (2006): 29-45.
- [149] Miyake, Takeo, Keigo Haneda, Syuhei Yoshino, and Matsuhiko Nishizawa. "Flexible, layered biofuel cells." *Biosensors and Bioelectronics* 40, no. 1 (2013): 45-49.
- [150] Palumbo, Gaetano, and Domenico Pappalardo. "Charge pump circuits: An overview on design strategies and topologies." *Circuits and Systems Magazine, IEEE* 10, no. 1 (2010): 31-45.

- [151] Slaughter, Gymama, and Tanmay Kulkarni. "A self-powered glucose biosensing system." *Biosensors and Bioelectronics* 78 (2016): 45-50.
- [152] Reid, Russell C., Shelley D. Minter, and Bruce K. Gale. "Contact lens biofuel cell tested in a synthetic tear solution." *Biosensors and Bioelectronics* 68 (2015): 142-148.
- [153] Kulkarni, Tanmay, and Gymama Slaughter. "Self-powered glucose biosensor operating under physiological conditions." *SENSORS, 2016 IEEE*. IEEE, 2016.
- [154] Morales, A., F. Céspedes, and S. Alegret. "Graphite–methacrylate biocomposite material with renewable sensing surface for reagentless amperometric biosensors based on glucose dehydrogenase." *Materials Science and Engineering: C* 7.2 (1999): 99-104.
- [155] Gerard, Manju, Asha Chaubey, and B. D. Malhotra. "Application of conducting polymers to biosensors." *Biosensors and Bioelectronics* 17.5 (2002): 345-359.
- [156] Kulkarni, Tanmay, and Gymama Slaughter. "Application of Semipermeable Membranes in Glucose Biosensing." *Membranes* 6.4 (2016): 55.
- [157] Lee, Seung Ho, et al. "A Simple and Facile Glucose Biosensor Based on Prussian Blue Modified Graphite String." *Journal of Sensors* 2016 (2016).
- [158] C.X. Guo, C.M. Li, "Direct electron transfer of glucose oxidase and biosensing of glucose on hollow sphere-nanostructured conducting polymer/metal oxide composite", *Physical. Chem. Chem. Phys.*, 12 (2010), pp. 12153-12159
- [159] S.I. Brahim, G. Slaughter, A. Guiseppi-Elie, "Electrical and electrochemical characterization of electroconductive PPy-p(HEMA) composite hydrogels", *Smart Struct. Mat.*, 5053 (2003), pp. 1-12
- [160] B. Liang, L. Fang, G. Yang, Y. Hu, X. Guo, X. Ye, "Direct electron transfer glucose biosensor based on glucose oxidase self-assembled on electrochemically reduced carboxyl graphene", *Biosens. Bioelectron.*, 43 (2013), pp. 131-136
- [161] P. Yang, L. Wang, Q. Wu, Z. Chen, X. Lin, "A method for determination of glucose by an amperometric bienzyme biosensor based on silver nanocubes modified Au electrode", *Sensors Actuators B Chem.*, 194 (2014), pp. 71-78
- [162] X. Che, R. Yuan, Y. Chai, J. Li, Z. Song, W. Li, X. Zhong, "A glucose biosensor based on chitosan-Prussian blue-multiwall carbon nanotubes-hollow PtCo nanochains formed by one-step electrodeposition", *Colloids Surf. B: Biointerfaces*, 84 (2011), pp. 454-461

- [163] Md.Q. Hasan, R. Kuis, J. Shankara Narayanan, G. Slaughter, "Fabrication of highly effective hybrid biofuel cell based on integral colloidal platinum and bilirubin oxidase on gold support", *Nat. Sci. Rep.*, 8 (2018), Article 16351
- [164] J. Russell and R. Cohn, "Gas diffusion electrode", JBookvika publications., 638 (2012), pp. 196
- [165] G. Slaughter, T. Kulkarni, "Fabrication of palladium nanowire array electrode for biofuel cell application", *Microelectron. Eng.*, 149 (2016), pp. 92-96
- [166] N. Furuya, "A technique is described for production of a gas diffusion electrode by electrophoresis". *Journal of Solid State Electrochemistry*. **8**: 48–50, 2003.
- [167] S. Ernst, "The electrooxidation of glucose in phosphate buffer solutions Part I. Reactivity and kinetics below 350 mV/RHE", *Journal of Electroanalytical Chemistry*, vol. 100, no. 1, pp. 173-183, 1979. Available: 10.1016/0368-1874(79)85110-2.
- [168] F. Kubanek, T. Turek and U. Krewer, "Modeling Oxygen Gas Diffusion Electrodes for Various Technical Applications", *Chemie Ingenieur Technik*, vol. 91, no. 6, pp. 720-733, 2019. Available: 10.1002/cite.201800181
- [169] S. Trasatti, "Work function, electronegativity, and electrochemical behaviour of metals: III. Electrolytic hydrogen evolution in acid solutions", *J. Electroanal. Chem. Interfacial Electrochem.*, vol. 39, p. 163, 1972.
- [170] A. Baingane and G. Slaughter, "Enzyme-Free Self-Powered Glucose Sensing System," *IEEE SENSORS*, pp.1-4, 2018.
- [171] K. M. Vittie et al., "From 'cyborg' lobsters to a pacemaker powered by implantable biofuel cells", *Biofuel Cells. Energy Environ. Sci.*, vol. 6, no. 1, pp. 81-86, Sep. 2012.
- [172] P. Pinyou et al., "Coupling of an enzymatic biofuel cell to an electrochemical cell for self-powered glucose sensing with optical readout", *Bioelectrochemistry*, vol. 106, pp. 22-27, Dec. 2015.
- [173] X. Yan, X. Ge and S. Cui, "Pt-decorated nanoporous gold for glucose electrooxidation in neutral and alkaline solutions ", *Nanosc. Res. Lett.*, vol. 6 , p. 313, 2011.
- [174] A. Baingane, J. Shankara Narayanan, and G. Slaughter, "Sensitive electrochemical detection of glucose via a hybrid self-powered biosensing system," *Sens. Bio-Sensing Res.*, vol. 20, pp. 41–46, 2018.

- [175] S.M. Usman Ali, T. Aijazi, K. Axelsson, O. Nur and M. Willander, "Wireless Remote Monitoring of Glucose Using a Functionalized ZnO Nanowire Arrays Based Sensor," *MDPI*, vol.11, no. 9, pp.8485-8496, 2011.
- [176] A. Soni and SK. Jha, "Smartphone Based Non-Invasive Salivary Glucose Biosensor," *Analytica ChimicaActa*, vol.996, pp.54-63, 2017.
- [177] G. Slaughter and T. Kulkarni, "Highly Selective and Sensitive Self-Powered Glucose Sensor Based on Capacitor Circuit," *Sci. Rep.*, vol. 7, no. 1, p. 1471, 2017.
- [178] T. Kulkarni and G. Slaughter, "Characteristics of Two Self-Powered Glucose Biosensors," in *IEEE Sensors Journal*, vol. 17, no. 12, pp. 3607-3612, 2017.

APPENDIX A

IDEAL CHARGE PUMP SIMULATION

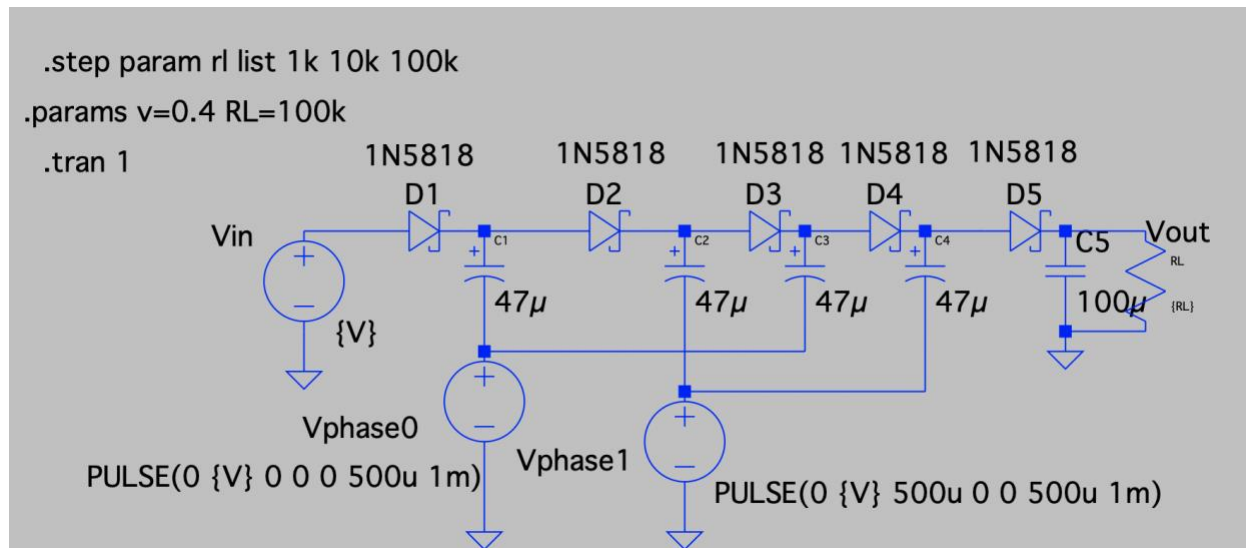


Figure 48. Ideal charge pump circuit

A simulation of an ideal multistage charge pump circuit was performed, wherein a charge pump circuit amplifies the input voltage to a level needed by the user (see Figure 48). The amplification level depends on the number of stages used in the charge pump circuit. An input voltage of 0.4 V was used to simulate the circuit under different load conditions ranging from 1 K ohm to 100 K ohm. Vphase0 and Vphase1 are two square waves that are the opposite of one another. That is, when Vphase0 is high, Vphase1 is low and vice versa. C1 to C4 are 47 μ F each.

The input voltage is applied to drive the circuit, and initially C1 is empty and Vphase0 is low. C1 will charge through D1 until it is at voltage V_{in} . Then Vphase0 goes high. The capacitor stores energy so it cannot just go to zero volts. In fact, when C1 will charge to V_{in} , the voltage across the capacitor will charge to V_{in} and since Vphase0 is now at V_{in} , the voltage across C1 is

still V_{in} and the voltage from the junction of D1, C1, and D2 will be twice V_{in} : V_{in} from V_{phase0} and another V_{in} from C1.

The process repeats with the next stage. C2 charges to $2 \times V_{in}$ while V_{phase1} is low and then jumps to $3 \times V_{in}$ when V_{phase1} goes high. In theory, multiple stages can be added to get an integer multiple of your input voltage. The final capacitor, C5, does not add any voltage because it connects to ground, but it smooths out the output.

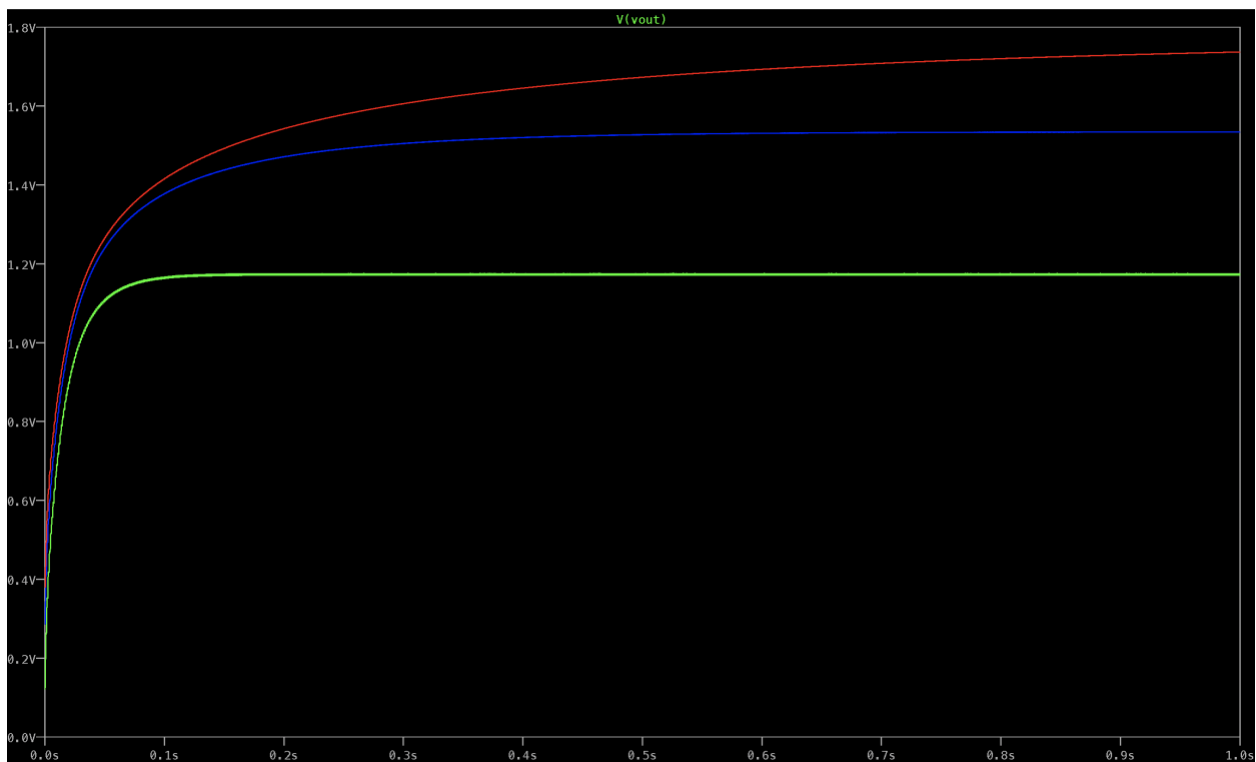


Figure 49. Output voltage across different load resistance level of 1, 10 and 100 K ohms.

In figure 49 above, the final output voltage across different load resistance levels is presented. The green curve represents 1 K ohm, the blue curve represents 10 K ohm and the red curve represents 100 K ohm load resistance. With an increase in load resistance, an increase in

output voltage is observed. The bigger C5 and the higher RL, the longer it will take to charge to the final value.

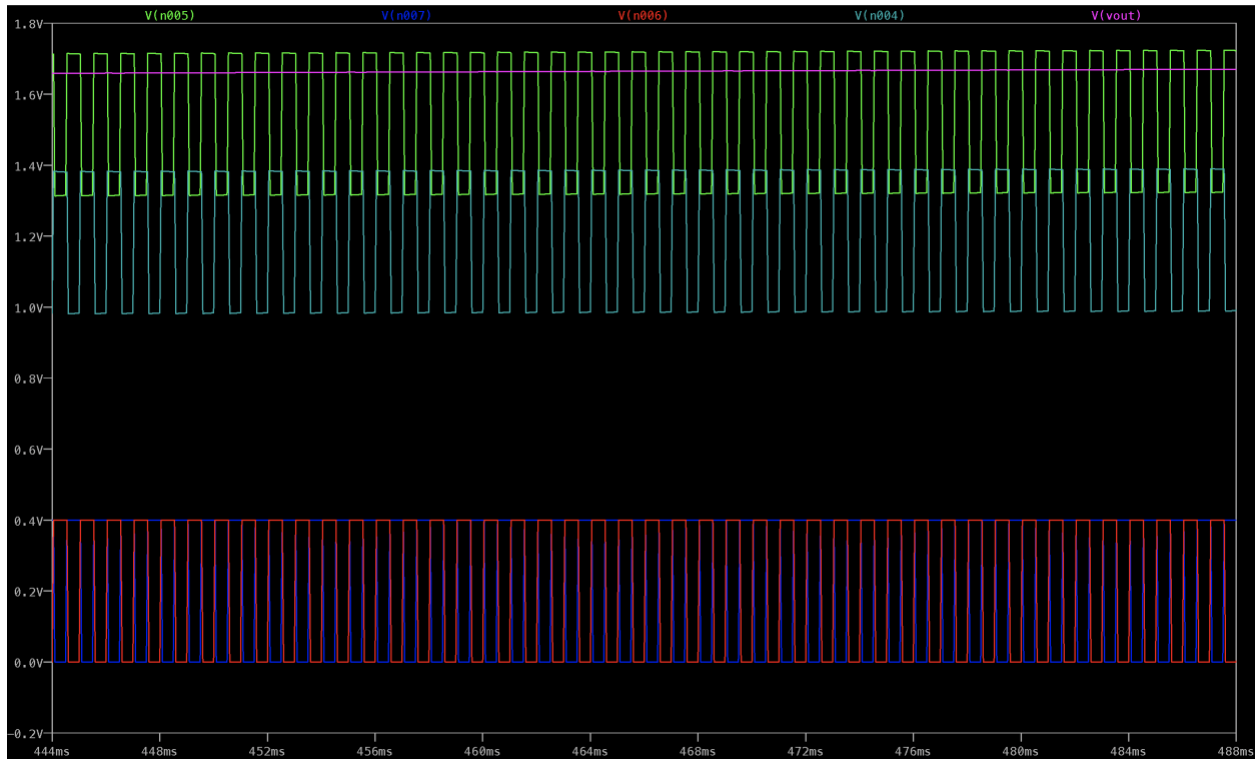


Figure 50. Output waveforms at different nodes and stages in the circuit.

Figure 50 shows the output waveforms at different nodes and stages of the circuit. $V(n004)$ and $V(n005)$ shows the stage output for 2 and 3 stages. With an increase in the number of stages, higher output voltages are attained. $V(n006)$ and $V(n007)$ show the clock input which is out of phase with each other. $V(out)$ shows the final smooth output DC voltage without any noise.

APPENDIX B

POLARIZATION AND CALIBRATION CURVE SIMULATIONS

1) IV Characteristics

```

clear
clc

%% ideal system %%

% Electrode surface area is 0.12 sq-mm
x = input (' Enter the glucose concentration in mM: ');
SA = input (' Enter the surface area of the electrode: ');

r = [1 5 15 25 50 100 200 300 500 700 1000]; % resistance values for IV

xi = []; % Initialize array/vector
for i=1:11
    xii = input('Enter the observed voltage values: ');
    if xii==1000
        break
    else
        xi(end+1)=xii;
    end
end

I = xi./r;
P = xi.*I;
PD = P/SA;
CD = I/SA;

figure (1);
plot (xi, PD, '*g')
xlabel('Output voltage in mV')
ylabel('Output power density in  $\mu$ W/sq-cm')

figure (2);
plot (xi, CD, '*g')
xlabel('Output voltage in mV')
ylabel('Output current density in  $\mu$ A/sq-cm')

```

Additionally, the IV test simulation was performed to determine the power characteristics of the biofuel cell (BFC). Voltage and current measurements were taken at different resistances ranging from 1K Ohm to 1M Ohm. Current decreases with an increase in resistance, and voltage increases with an increase in resistance. The resistance at which the BFC is most efficient to

generate maximum power can be obtained from the IV curves. The output power density versus the output voltage curve is an inverted curve, and the output current density versus output voltage results in a straight line with negative linear slope. Experimental conditions results in non-ideal curves because of the different losses in the circuit and the reactions (e.g., ohmic losses, thermodynamic loss, etc). A circuit can be designed to have the same internal resistance, thus getting the most power output from the BFC.

Code execution began with the input of the concentration values for which the IV test is performed. The power and current density depends on the surface area of the electrode. In this stimulation, a surface area of 0.12 sq-cm was employed. Different resistances ranging from 1 K ohm to 1M ohm were used. The voltage and current across each resistance was measured, and then the user entered the observed voltages. The code then calculated the output current density and power density using ohms law and then plotted the graphs.

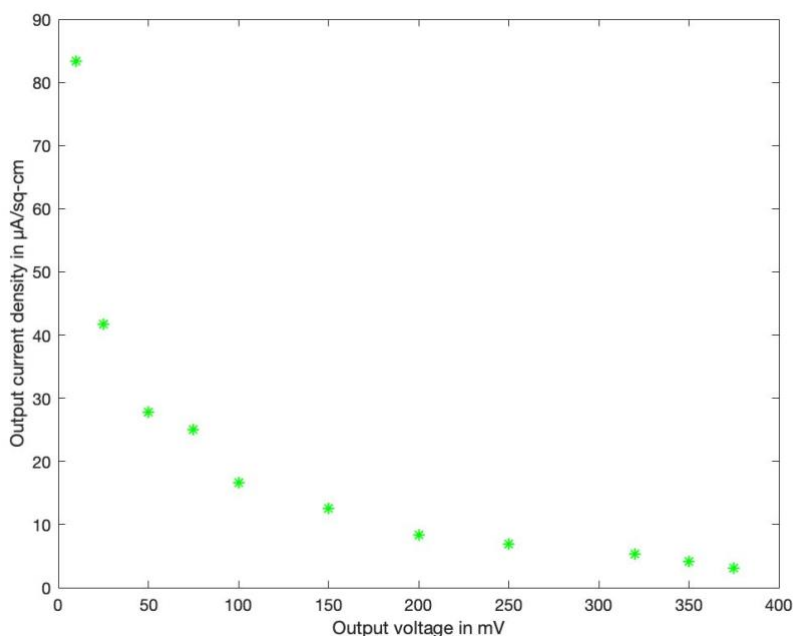


Figure 51. Power curve obtained from the simulation

Figure 51 shows the power curve obtained from the performed MATLAB simulation. A decrease in the output current value was observed with an increase in resistance and voltage.

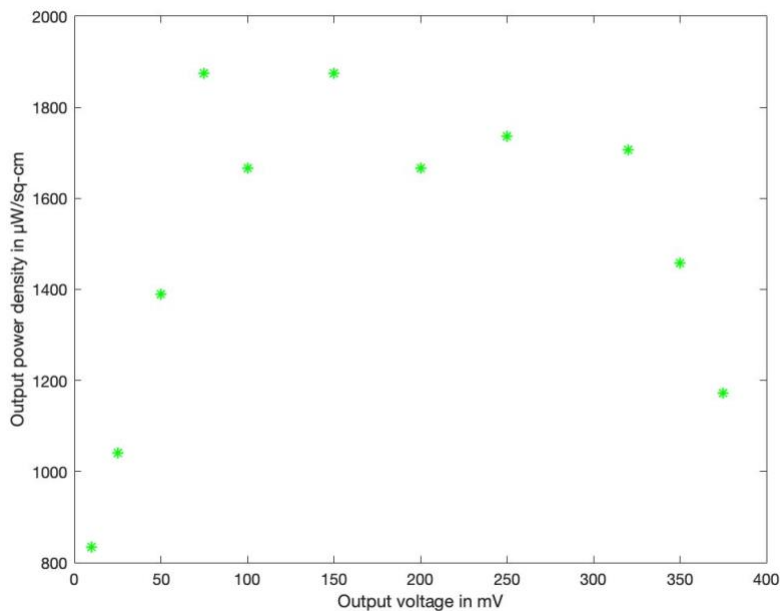


Figure 52. Polarization curve obtained from the MATLAB simulation.

Figure 52 shows the polarization curve obtained from the performed MATLAB simulation. An increase in power was observed with an increase in resistance and voltage. As shown, the power increases gradually until maximum power is attained. Afterwards the power output starts decreasing.

2) Calibration curve

```
clear
clc
% y = mx + c , equation of line
% x = glucose concentration, y = current, m = slope of the line , c =
constant
% From our results y = 0.9728x + 9.1564
% Electrode surface are 0.12 sq-mm
SA = input (' Enter the surface area of the electrode: ');
x = [1 5 10 20 30 40 50];% glucose concentration
```

```

m = 0.9728;
c = 9.1564;
P = m*x + c;
PD = P/SA;% Power density
figure (1);
plot (x, PD, 'm*')
xlabel('Glucose concentration in mM')
ylabel('Output power density in  $\mu$ W/sq-cm')

```

The above code uses the line equation of the calibration curve that was generated from the experimental data employing the biofuel cell. The equation used is $y = 0.9728x + 9.1564$. Different glucose concentrations ranging from 1 mM to 50 mM were set. First the surface area of the electrode is entered. Then the code calculates the power density and plots the results. With an increase in glucose concentration, an increase in output power density is attained.

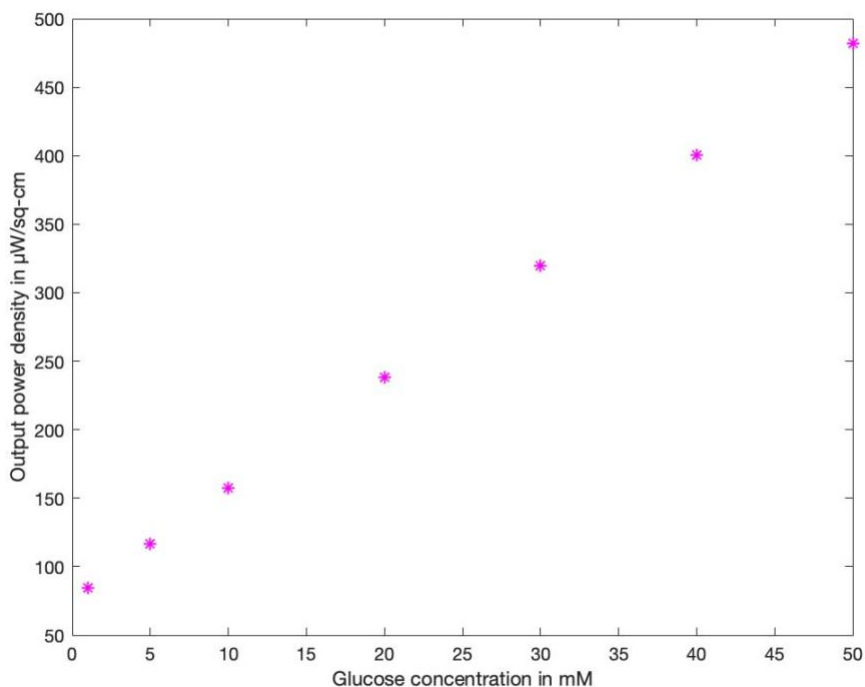


Figure 53. Calibration curve obtained from the MATLAB simulation.

Figure 53 shows the calibration curve for glucose concentration ranging from 1 mM to 50 mM. With increasing concentration there was a linear increase in power generated.

VITA

Ankit Baingane
Norfolk, VA 23508

EDUCATION

Old Dominion University, Norfolk, VA
Doctor of Philosophy in Electrical and Computer Engineering August 2020

University of Maryland, Baltimore County
Master of Science in Computer Engineering December 2017

PUBLICATION

Peer-Reviewed Journals

- Ankit Baingane and Gymama Slaughter, “A self-powered glucose monitoring system with remote data access,” IEEE Transactions on Nanobioscience, doi: 10.1109/TNB.2020.3002453, 2020.
- Jonathan D. Yuen, Ankit Baingane, Md Qumrul Hasan, Daniel Zabetakis, Joyce C. Breger, Gymama Slaughter, “A Fully-Flexible, Solution-Processed, Autonomous Glucose Indicator”, Nature Sci Rep. 9 (6931) 1-9, 2019.
- Ankit Baingane, J. Shankara Narayanan, and Gymama Slaughter, “Sensitive electrochemical detection of glucose via a hybrid self-powered biosensing system,” Sensing and Biosensing, 20, 41-46, 2018.
- Ankit Baingane and Gymama Slaughter, “Self-Powered Electrochemical Lactate Biosensing” Energies, 10, 1582, 1-9, 2017.
- Ankit Baingane, Naomi Mburu and Gymama Slaughter, “Simultaneous Monitoring of Glucose and Lactate by Self-powered Biosensor” Sensors & Transducers, 214, 7, 34 - 38, 2017.
- Ankit Baingane, Naomi Mburu and Gymama Slaughter "Developing a dual self-powered biosensor for monitoring glucose and lactate," Sensors & Transducers. 214, 7, 34 - 38 (2017).

Peer-Reviewed Conference Proceedings (appeared/ to appear)

- Ankit Baingane and Gymama Slaughter, Enzyme-free self-powered glucose sensing system, IEEE Sensors, October 27-31, 2018.
- Robinson Kuis, Md Qumrul Hasan, Ankit Baingane and Gymama Slaughter. Operation stability of chitosan and nafion-chitosan coatings on bioelectrodes in enzymatic glucose biofuel cells, IEEE NEMS, Sept. 27-30, 2020.
- Ankit Baingane and Gymama Slaughter. A wireless self-powered glucose monitoring biosystem, IEEE NEMS, Sept. 27-30, 2020.
- Dominic Nnanyelugoh, Ankit Baingane and Gymama Slaughter. Glucose abiotic biofuel cell, IEEE NEMS, Sept. 27-30, 2020.